Dissertation presented
as a partial requirement for the degree of
Master of Science

Muon Acceptances for Neutrino Charged Current Interactions at CAPTAIN-MINERνA for 2 $< E_{\nu_\mu} <$ 10 GeV

Gian Fredy Ricardo Caceres Vera

Advisor:
Hélio da Motta Filho

Centro Brasileiro de Pesquisas Físicas

Rio de Janeiro, August 2016

To my mother Elsa

Acknowledgements

I would like to express my gratitude to my advisor Dr. Helio da Motta for giving me the opportunity to work in the MINERνA collaboration, for the advices and support given, and for the trust placed in me to do this work.

To all the MINERνA collaboration, specially to Dr. Jorge Morfin for all the support on my stay at Fermilab and the guidance provided. To the spokespersons Dr. Deborah Harris and Dr. Kevin Mc Farland for the knowledge transmitted. To Dipak Rimal and Trung Lee for the patient and help to make this dissertation possible, thank you guys!

I want to thank to the proffesors at the Centro Brasileiro de Pesquisas Físicas and to CAPES for the scholarship (2014-2016).

My most profound gratitude goes to my mother Elsa and my sister Fabiola. Even though they were far away from me, they were always with me. I love you.

Abstract

CAPTAIN-MINERνA is a fusion of the CAPTAIN (Cryogenic Apparatus for Precision Tests of Argon Interactions with Neutrinos) and the MINERνA (Main Injector Experiment for ν-A) detectors at Fermilab Muon Neutrino beamline (NuMI beamline), aimed at making detailed studies of neutrino interactions with argon which will be relevant for future neutrino oscillation experiments.

In this dissertation, we present the muon acceptances for charged current interactions in CAPTAIN-MINERνA at muon neutrino energies around 6 GeV. GENIE 2.8.4 is used to generate 132,589 neutrino charged current interactions with argon in the CAPTAIN detector and GEANT4 is employed to simulate the muon trajectories. All simulations use a simple geometry of the CAPTAIN-MINERνA detector elaborated by the MINERνA collaboration. Finally, the CAPTAIN detector is divided in four sectors and the muon acceptances from each sector are calculated.

Contents

List of Figures

List of Tables

Chapter 1

Introduction

In the last decades neutrino physics has become a very active and exciting research field. Many experiments around the world are trying to figure out the diverse properties of these particles describing their oscillation and how they interact with matter. The neutrino interaction with matter is still waiting for experimental results with high statistics measurements in the energy range between 1 GeV and 20 GeV where three different processes overlap: charged current quasi-elastic, resonance pion production and deep inelastic scattering. Measuring neutrino interaction cross sections facilitates high precision neutrino oscillation measurements. Furthermore, neutrinos play a very important role in various branches of subatomic physics as well as in astrophysics and cosmology. Currently there is evidence that neutrinos have mass and can change flavor [1]. Developing an understanding of neutrinos is rightfully one of the top priorities of the particle physics community because it has the potential to reveal new physics. New experiments are been planned using liquid argon as the active target. It is of uppermost importance to understand all aspects of neutrino interaction with argon. CAPTAIN-MINERvA is a proposed experiment aimed at measuring the cross section of neutrino-argon interactions. This dissertation describes the proposed CAPTAIN-MINERνA experiment and calculates the muon acceptance for charged current neutrino interactions at E_ν around 6 GeV.

Chapter 2

Introduction to Neutrino Physics

2.1 Brief History

The study of the β decay gave the first hint of the existence of neutrinos. In the early twentieth century it was believed that the energy spectrum of the β decay was discrete. However, in 1911, Von Bayer, Otto Hahn and Lise Meitner ran an experiment that suggested that the β decay energy spectrum had a continuous instead of discrete spectrum [2] as the one observed in the alpha decay. This was contradicting the energy conservation law. In 1927, Ellis and Wooster confirmed that the β decay energy spectrum was really continuous by showing that the electron energy distribution corresponds to a three particle final state where the particles share the energy [3].

In 1930, in order to resolve this contradiction and preserve the conservation of energy principle Wolfgang Ernst Pauli proposed in his famous letter "Dear Radioactive Ladies and Gentlemen" addressed to the participants of the physics conference in Tubingen [4] the existence of a spin $\frac{1}{2}$ particle that had charge zero which he called "neutron". He was, however, skeptical about his idea saying "I have done something very bad today by proposing a particle that cannot be detected; it is something no theorist should never do".

In 1932, James Chadwick discovered a neutral particle of mass similar to that of the proton which was also named "neutron" [5]. In 1934 Enrico Fermi succeeded on developing a β decay theory integrating the particle proposed by Pauli [6]. He understood Pauli's particle should have mass of the order of the mass of an electron so he named it "neutrino" (Italian for "small neutron").

It took 22 years for the first observation of neutrinos made by Reines and Cowan [7], [8], [9], in 1956. They used the antineutrino flux of the order of $10^{12}\ cm^{-2}s^{-1}$ coming from a nuclear reactor. Antineutrinos coming from beta decays were detected via inverse beta decay,

$$\overline{\nu}_e + p \rightarrow n + e^+. \tag{2.1}$$

where positrons were detected in a tank full of liquid scintillator.

In the sixties Goldhaber measured the left helicity of neutrinos [10] and Davis was able to discriminate ν from its antiparticle $\overline{\nu}$ [11]. [12]. In 1959 Chien-Shiung Wu discovered parity violation in weak interaction [13] when a preferred direction of the produced electrons respect to the spin of the ^{60}Co nuclei was observed in the β decay of ^{60}Co.

In 1962 Schwartz, Lederman, Steinberg and colleagues published results of the first accelerator produced neutrino at Brookhaven National Laboratory. They showed that neutrinos produced by the charged pions beam interacted producing only muons[14]. This was evidence of a new kind of neutrino: the muon neutrino ν_μ.

In 1973 neutral current induced processes was announced by the Gargamelle bubble chamber collaboration at CERN [15] and later confirmed by the same collaboration in 1974.

In the seventies, studies of solar neutrinos began measuring the solar neutrino flux. In 1968 Davis' studies showed a discrepancy between the measured solar neutrino flux and the theoretical prediction [16]. This was known as the "solar neutrino problem". This discrepancy also observed in atmospheric neutrino fluxes[1] was known as the "atmospheric neutrino anomaly" and in 1988, for the first time, neutrino oscillations were suggested as the reason for this discrepancy in the results given by the Kamiokande detector [19].

In 1967, Gribov And Pontecorvo considered a scheme of neutrino mixing and oscillations [20] that explained the flux discrepancy of the solar neutrinos. Mass terms had to be included in order to explain the oscillation of neutrinos[2].

Mainly because of the τ short life time it was not until 2000 that the μ_τ could be observed at the Fermilab DONUT experiment[3] [21]. There is no doubt new surprises and discoveries are ahead. Many neutrino facilities around the world have been built to perform detailed studies of neutrinos.

Along the time, the studies of neutrino interactions with matter and oscillation phenomena have been an amazing journey on creativity and innovation of mankind willing to better understand the nature of what we are made of. A new era of physics has started looking for expanding the limits of our understanding of the universe.

[1] Measurements made in 1986 by IMB [17] and Kamiokande [18] did not have a zenith angle dependence and were not paid attention.

[2] Neutrino oscillation is not predicted by the Standard Model and it is then an indication of a physics beyond the Standard Model.

[3] Long before the discovery of the ν_{tau} the existence of just three light neutrinos was predicted at Large Electron-Positron collider (LEP) at CERN [22], [23], [24], [25].

2.2 The Standard Model

The standard model is the theory that describes the elementary building blocks of matter and how do they interact. However it is incomplete and describes just three of the four forces known in nature[4]:electromagnetic, strong and weak. The Standard Model describes nature in terms of elementary particles (quarks and leptons) and particles that mediate the interactions (bosons).

There are six quarks and six leptons (all of them fermions that have spin 1/2), that come in three generations or pairs. The first generation consists of the lightest and most stable particles whereas the heavier and less stable particles belong to the second and third generations. The quarks generations are: up(u) and down(d); strange (s) and charm (c); bottom (b) and top (t). Leptons can be charged (e, μ and τ) and neutral (ν_e, ν_μ and ν_τ).

There are four bosons have (spin 1) and mediate the forces of the Standard Model: the gluon (g) that mediates the strong force; the photon (γ) that mediates the electromagnetic force; the W^+ and Z bosons that mediate the weak force. The fifth boson, the Higgs boson (H), has spin 0 and is the responsible for giving mass to the other particles.

The 16+1 fundamental particles are summarized in Table 2.1.

2.2.1 Neutrinos in the Standard Model

Neutrinos are the only fermions in the Standard Model that interact only by means of the weak interaction. Two different processes can be observed: Neutral Current interaction (NC) mediated by the boson Z^0; and Charged Current interaction (CC) mediated by the bosons $W^\pm$. In a NC interaction the neutrino produced is the same incoming neutrino, however in a CC interaction a charged lepton is produced. In a CC interaction the interacting neutrino and the lepton produced are from the same generation, thus we know to which family the interacting neutrino belongs by the kind of lepton produced in the CC interaction.

2.2.2 Helicity

Helicity is the projection of the spin onto the direction of the momentum. The particle helicity can have two possible states: spin and momentum having same directions (positive helicity); spin and momentum having opposite directions (negative helicity). For particles having mass any of these states can be possible because the momentum depends of the relative velocity of the frame of reference.

The chirality of a particles is a more abstract concept. It is determined by whether the particle transforms into a right- or a left-handed representation of the Poincaré group. It has

[4]Gravitation is not included in the Standard Model.

QUARKS		
Quarks	Mass	Electric charge
up (u)	$2.2^{+0.6}_{-0.4}$ MeV/c^2	$+\frac{2}{3}$
down (d)	$4.7^{+0.5}_{-0.4}$ MeV/c^2	$-\frac{1}{3}$
strange (s)	96^{+8}_{-4} MeV/c^2	$-\frac{1}{3}$
charm (c)	1.275±0.03 GeV/c^2	$+\frac{2}{3}$
bottom (b)	$4.66^{0.01}_{0}$.03 GeV/c^2	$-\frac{1}{3}$
top (t)	173.21 ±0.51 ± 0.71 GeV/c^2	$+\frac{2}{3}$
LEPTONS		
Leptons	Mass	Electric charge
electron (e)	0.5109989461 ± 0.0000000031 MeV/c^2	-1
electron neutrino (ν_e)	< 2 eV/c^2	0
muon (μ)	105.6583745 ± 0.0000024 MeV/c^2	-1
muon neutrino (ν_μ)	< 0.19 MeV/c^2	0
tau (τ)	1776.86 ± 0.12 MeV/c^2	-1
tau neutrino (ν_τ)	< 18.2 MeV/c^2	0
BOSONS		
Bosons	Mass	Electric charge
photon(γ)	$< 1 \times 10^{-18}$ eV/c^2	0
$W^\pm$	80.385± 0.015 GeV/c^2	±1
Z^0	91.1876 ± 0.0021 GeV/c^2	0
gluon (g)	0	0
Higgs	125.09 ±0.21 ± 0.11 GeV/c^2	0

Table 2.1: Particles in the Standard Model [26].

two possible states: right-handed (RH) and left-handed (LH). For massless particles the the chirality and helicity are identical. In 1958 Goldhaber [10] determined that neutrinos are LH while antineutrinos are RH.

2.2.3 Neutrino Oscillation and Masses

Neutrino oscillations are possible only if neutrinos are massive. Each neutrino flavor (ν_e, ν_μ, ν_τ) is understood as a combination of three mass states[5] (ν_1,ν_2,ν_3). When a neutrino is produced with a specific flavor, its quantum state evolves to a combination of mass states with the proportions oscillating in time. The probability of detecting a specific neutrino flavor depends on the amplitude of the respective mass state.

Let's consider, for simplicity, a system consisted of two neutrino flavors, ν_α ans ν_β. Both of these states being superposition of mass eigenstates ν_1 and ν_2 with masses m_1 and m_2 respectively:

$$|\nu_\alpha\rangle = |\nu_1\rangle cos\theta + |\nu_2\rangle sin\theta, \tag{2.2}$$

$$|\nu_\beta\rangle = -|\nu_1\rangle sin\theta + |\nu_2\rangle cos\theta, \tag{2.3}$$

where θ is the neutrino mixing angle. The evolution in time of the state is dictated by the free Hamiltonian. The state at $t = 0$ is

$$|\nu_\beta(t=0)\rangle = -|\nu_1\rangle sin\theta + |\nu_2\rangle cos\theta \tag{2.4}$$

and at time t the state will be given by

$$|\nu_\beta(t)\rangle = -|\nu_1\rangle sin\theta e^{-\frac{iE_1 t}{\hbar}} + |\nu_2\rangle cos\theta e^{-\frac{iE_2 t}{\hbar}}. \tag{2.5}$$

We take $\hbar$=c=1 and consider the extreme relativistic approximation for very small neutrino masses $E_{1,2} = \sqrt{(p^2 + m_{1,2}^2)} \sim p + \frac{m_{1,2}^2}{2p}$. Then we have for the state in any time t.

$$|\nu_\beta(t)\rangle = -|\nu_1\rangle sin\theta e^{-i(p+\frac{m_1^2}{2p})t} + |\nu_2\rangle cos\theta e^{-i(p+\frac{m_2^2}{2p})t}. \tag{2.6}$$

Then using $\Delta m^2 = m_2^2 - m_1^2$ and the relativistic sustitution $p = E$, the probability of finding a different neutrino flavor is:

$$P(\nu_\beta \to \nu_\alpha, t) = |\langle\nu_\alpha|\nu_\beta(t)\rangle|^2 = sin^2(2\theta) sin^2(\frac{\Delta m^2 L}{4E}) \tag{2.7}$$

The last line is valid for highly relativistic particles with L being the distance traveled by the neutrino.

[5]This idea was first introduced by Gribov and Pontecorvo [20].

Because only mass square difference appears in this definition, measuring oscillation probabilities can only tell that at least one of the neutrinos has non-zero mass. This two flavor scheme can be easily extended to a three flavor scheme. In such a scheme the flavor eigenstates are related to the mass eigenstates by the Pontecorvo-Maki-Nakagawa-Sakata (PMNS) matrix containing three mixing angles θ_{12}, θ_{13}, θ_{23} and a phase. Further we have three squared mass differences Δm^2_{12}, Δm^2_{13}, Δm^2_{23}. Neutrinos in the Standard Model have no mass , which is why the understanding of neutrino interactions will surely reveal new physics.

2.3 Neutrino Interactions

In the neutrino energy region of a few GeV a neutrino scatters off a nucleon or an entire nucleus via Charged Current (CC) or Neutral Current (NC) interaction. CC and NC interactions are mediated by $W^{\pm}$ and Z^0 bosons respectively. In this section the processes: Elastic and Quasielastic, Single Resonant Meson production via Baryon Resonances Coherent Pion Production, Deep Inelastic Scattering (DIS) are presented. The Feynman diagrams for these processes are shown in Figure 2.2.

2.3.1 Elastic and Quasielastic scattering

In both of these scatterings the neutrino scatters off an entire nucleon. In the case of a Charged Current interaction the process is called "Quasielastic scattering" and in the case of a Neutral Current interaction it is called "Elastic scattering". These interactions for neutrinos are as follows:

$$(CC)\ \nu_l + n \rightarrow l^- + p \tag{2.8}$$

$$(NC)\ \nu_l + N \rightarrow \nu_l + N. \tag{2.9}$$

Where l^- refers to any of the charged leptons e^-, μ^-, τ^- and N to a nucleon. The Charged Current Quasielastic interaction is the more predominant for $E_\nu < 2$ GeV. The CC antineutrino interaction produce the respective positive lepton, while the NC (neutrino and anitneutrino) interactions are not that easily identified. Data for neutrino and antineutrino CC Cross Sections are shown in Figure 2.1.

2.3.2 Single Resonant Meson production via Baryon Resonances

Neutrino-nucleus interaction can excite baryon resonances which decay into a nucleon and a meson in the final state. In the few GeV energy range the intermediate state is dominated

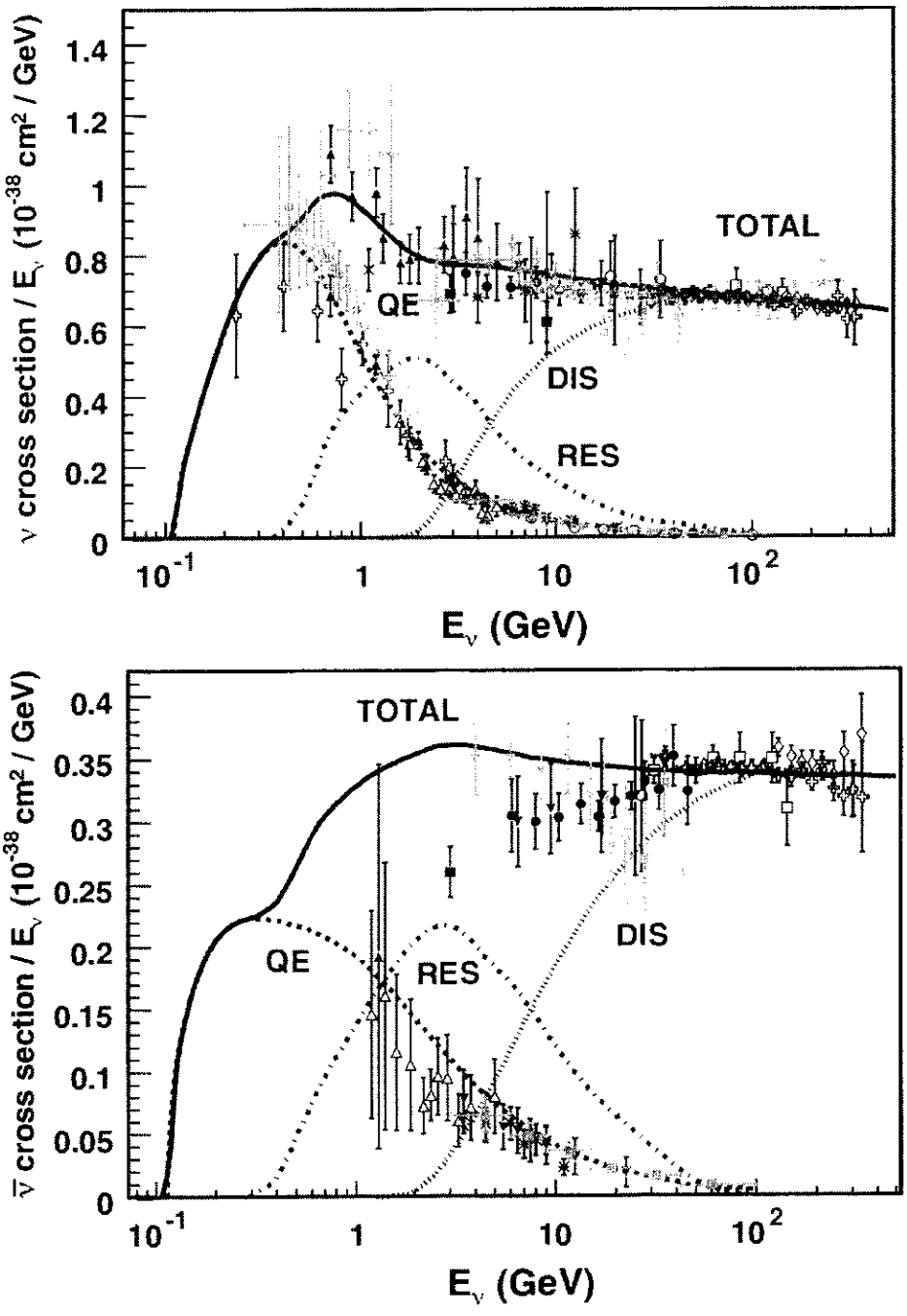

Figure 2.1: Existing measurements for total neutrino and antineutrino per nucleon CC cross sections (for an isoscalar target) and additional CC inclusive data for lower energy as a function of energy are shown [27]. Contributions from quasielastic scattering (dashed), resonance production (dot-dashed), and deep inelastic scattering (dotted) predicted by the NUANCE generator [28] are also shown.

by the $\Delta(1232)$ resonance which mainly decays into a nucleon and a pion. The CC and NC neutrino interactions are as follows:

$$(CC)\ \nu_l - N \rightarrow l^- + \Delta \rightarrow l^- + N^\circ + \pi^+ \tag{2.10}$$

$$(NC)\ \nu_l - N \rightarrow \nu_l + \Delta \rightarrow \nu_l + N^\circ + \pi^+. \tag{2.11}$$

Here N° refers to a nucleon different to the original N. A variety of final states can exist and the π^+ produced could be π^-, π^0 or π^+. These two types of interactions are known as CC1π and NC1π interactions.

2.3.3 Coherent Pion Production

Another interaction that produces Pions is that of the neutrino interacting coherently with an entire nucleus which remains unchanged in its ground state after the interaction. The momentum transfered to the nucleus is kept small and no nuclear breakup occurs. However the nucleus is excited, decaying and coming back to its ground state by emitting a Pion. The outgoing pion and lepton tend to go in the same direction as the incoming neutrino. The CC and NC neutrino interactions are as follows:

$$(CC)\ \nu_l + A \rightarrow l^- + A + \pi^+ \tag{2.12}$$

$$(NC)\ \nu_l + A \rightarrow \nu_l + A + \pi^0. \tag{2.13}$$

Where A is the nucleus in its ground state.

2.3.4 Deep Inelastic Scattering (DIS)

In the high energy region $E_\nu > 5$ GeV, the neutrino scatters off a quark inside the nucleon. The high momentum transfer breaks the nucleon containing the struck quark producing hadrons in the final state. The CC and NC neutrino interactions are as follows:

$$\nu_l + N \rightarrow l^- + N^\circ + hadrons \tag{2.14}$$

$$\nu_l + N \rightarrow \nu_l + N^\circ + hadrons. \tag{2.15}$$

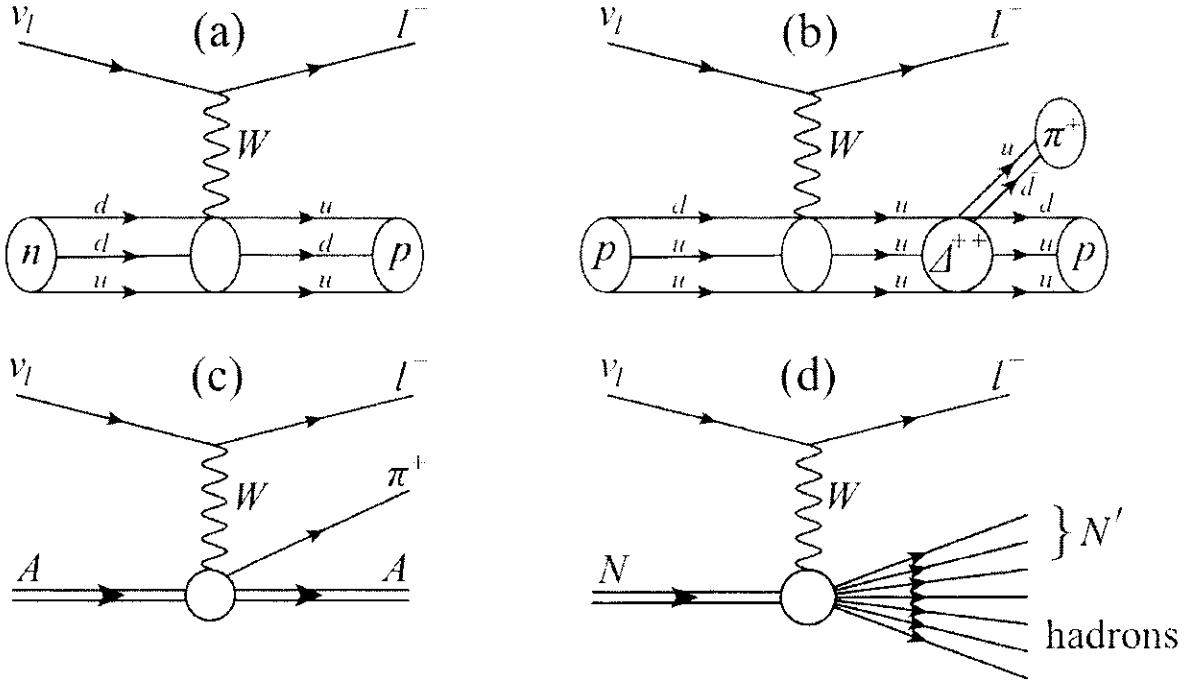

Figure 2.2: Feynman diagrams for CC neutrino interactions. (a)Charged Current Quasielastic (b)Resonant production (c)Coherent Pion production (d)Deep Inelastic Scattering.

2.4 Neutrino Oscillation Experiments

In this section some important results are mentioned and a summary of oscillation experiments with neutrinos from accelerators is presented.

2.4.1 Solar Neutrinos

The first hint of neutrino oscillations came from the Homestake experiment headed by Raymond Davis. The Homestake Solar Neutrino detector was designed to be sensitive to the electron neutrino via $\nu_e + {}^{37}Cl \rightarrow e^- + {}^{37}Ar$, where radioactive isotopes of Argon-37 were identified and counted to detect the electron neutrino [16]. The experiment collected data from the late 1960s to 1996. The final results for the production of Argon atoms was [29] $2.56 \pm 0.16(stat) \pm 0.16(syst)$ SNU[6]. Prediction of the Standard Solar Model (model BP04) is $8.5^{+1.8}_{-1.8}$ SNU [30]. This discrepancy, as mentioned before, was called the "solar neutrino problem".

The solar neutrino experiment Sudbury Neutrino Observatory (SNO) started observations in 1999 and completed in 2006. The SNO was a water-Cherenkov detector that used ultra-pure heavy water (D_2O) as neutrino target. This experiment was sensitive to three reactions:

[6] 1 SNU = 1 Solar Neutrino Unit = $10^{-36} captures \times s^{-1}$ *per atom.*

$$\nu_x + e^- \rightarrow \nu_x + e^- \ (elastic\ scattering). \tag{2.16}$$

$$\nu_e + d \rightarrow e^- + p + p \ (\nu_e\ charged - current). \tag{2.17}$$

$$\nu_x + d \rightarrow \nu_x + p + n \ (neutral\ current). \tag{2.18}$$

The CC reaction is only sensitive to electron neutrino and the NC reaction is equally sensitive to all neutrino flavors. The ES reaction is sensitive to all neutrino flavors but less sensitive to ν_τ and ν_μ. In 2001 a first measurement of ^8B flux deduced from ES $[\phi^{ES}(\nu_x)]$ and CC $[\phi^{CC}(\nu_e)]$ reactions showed that $\phi^{CC}(\nu_e) < \phi^{ES}(\nu_x)$ suggesting electron neutrinos change into other active flavor [31]. In 2002 these fluxes were updated and the 8^B flux deduced from the NC reaction was measured [32]. These results in $10^6\ cm^{-2}sec^{-1}$ were:

$$\phi_{CC}^{SNO} = 1.76^{+0.06}_{-0.05}(stat)^{+0.09}_{-0.09}(syst). \tag{2.19}$$

$$\phi_{ES}^{SNO} = 2.39^{+0.24}_{-0.23}(stat)^{+0.12}_{-0.12}(syst). \tag{2.20}$$

$$\phi_{NC}^{SNO} = 5.09^{+0.44}_{-0.43}(stat)^{+0.46}_{-0.43}(syst). \tag{2.21}$$

The measurement of the total flux ϕ_{NC}^{SNO} confirmed that ν_e indeed oscillated to other neutrino flavors.

The Super-Kamiokande detector holds 50.000 tons of water and detects charged particles via Cherenkov radiation. Here, solar neutrinos interactions are detected via the elastic scattering reaction. The neutral current reaction can measure interaction rate of any neutrino flavor.

$$\nu_x + e^- \rightarrow \nu_x + e^-(via\ neutral - current). \tag{2.22}$$

However the sensitivity to ν_e neutral current interaction,

$$\nu_e + e^- \rightarrow \nu_e + e^- \tag{2.23}$$

is higher relative to ν_τ and ν_μ neutral current interactions, because it is enhanced by the ν_e charged current interactions measured. For events over the 5 MeV threshold in Super-Kamiokande the ^8B flux measured was $(2.35 \pm 0.02(stat.) \pm 0.08(syst.))10^6 cm^{-2}sec^{-1}$ [33] and the computed theoretical flux was $(5.69 \pm 1.0)10^6 cm^{-2}sec^{-1}$ [34]. This discrepancy agrees with results from other experiments.

2.4.2 Neutrinos from Nuclear Reactors

In 2002 the Kamioka Liquid-scintillator Anti-Neutrino Detector's (KamLAND) results gave the first remarkable evidence on neutrino oscillation coming from nuclear reactors [35]. The detector detects electron anti-neutrinos via inverse β decay:

$$\overline{\nu_e} + p \rightarrow e^+ + n. \tag{2.24}$$

The produced positron is detected in a scintillator and approximately 200 μs later the neutron captures a proton producing a photon via

$$n - p \rightarrow d + \gamma \ (2.2\ MeV). \tag{2.25}$$

This time delay between the initial scintillating light produced by the positron and the latter photon is a robust signature of electron anti-neutrino detection. The ratio of the observed to the expected energy spectra for the electron anti-neutrino events are shown in figure 2.3. The electron anti-neutrinos for KamLAND come from comercial nuclear reactors in Japan and the average distance from the reactors to the detector is about 180 km [36].

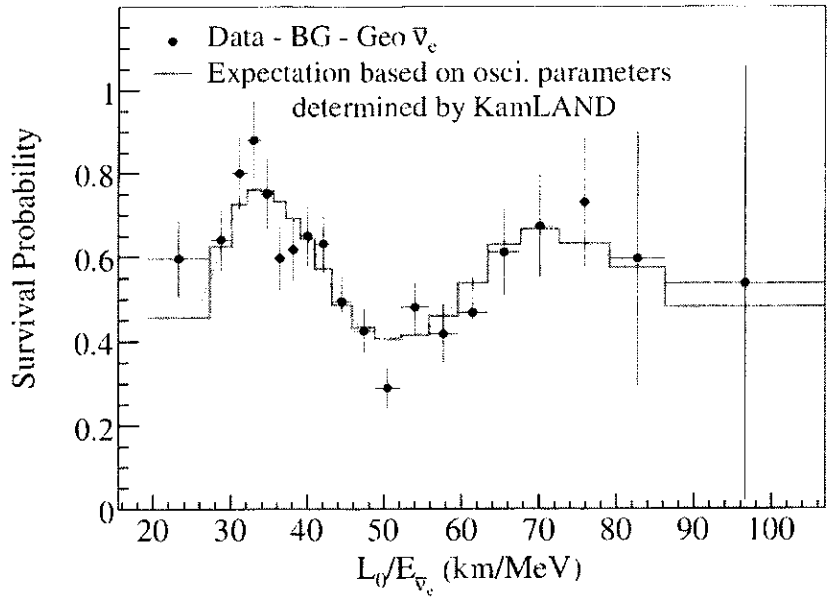

Figure 2.3: KamLAND ratio of the observed to the no-oscillation expected events for the electron anti-neutrino events as a function of $\frac{L_0}{E_{\overline{\nu}_e}}$ where $L_0 = 180km$.

CHOOZ [37] and Palo Verde [38] were two first-generation kilometer-baseline reactor experiments located in France and United States, respectively. The objective of these experiments was to measure the θ_{13} oscillation parameter. CHOOZ could measure an upper limit of

$sin^2(\theta_{13}) < 0.10$ at 90% confidence level. Baseline reactor experiments as Double CHOOZ [39], [40] in France, RENO [41] in Korea and Daya Bay [42], [43] in China are aimed to get better measurements of this parameter.

2.4.3 Atmospheric Neutrinos

Atmospheric neutrinos are produced by decays of kaons and pions produced by interactions of cosmic rays with nuclei in the Earth's atmosphere. At these high energy interactions, many Pions and less abundant Kaons decay via:

$$\pi^{\pm}(K^{\pm}) \rightarrow \mu^{\pm} + \nu_{\mu}(\overline{\nu}_{\mu}) \tag{2.26}$$

$$\mu^{\pm} \rightarrow e^{\pm} + \nu_{e}(\overline{\nu}_{e}) + \overline{\nu}_{\mu}(\nu_{\mu}). \tag{2.27}$$

However Kaons are responsible for higher energy neutrinos than those produced by Pion decays [44]. This reaction chain produces approximately two muon neutrinos per one electron neutrino.

The Super-Kamiokande experiment confirmed Muon neutrino disappearance due to neutrino oscillations. Despite a decrease in the events ratio $\frac{\nu_{\mu}}{\nu_{e}}$ relative to the predicted events was observed, the strong argument for Muon neutrino oscillations came from the distribution of events as a function of the zenith angle [45], as shown in Figure 2.4. The decrease in the upward-going μ-like events suggested μ neutrinos oscillated when traveling through the earth towards the detector. The electron neutrinos distribution was as predicted. Comparison with Kamiokande data confirmed this decrease was due to the oscillation $\nu_{\mu} \rightarrow \nu_{\tau}$. Subsequent data from Super-Kamiokande SK-I, SK-II, SK-III upgrades provided more statistics and confirmed this result.

At the time the Super-Kamiokande's data confirmed neutrino oscillations, two other experiments that measured atmospheric neutrinos, Soudan-2 [46], [47] and MACRO [48], [49] showed also in their data a ν_{μ} deficit dependent of the zenith angle.

2.4.4 Neutrinos from Accelerators

Accelerator long-baseline neutrino experiments consist of two detectors separated a long distance one from each other aligned on- or off-axis aligned with the neutrino beam produced in the accelerator. Man-made neutrino beams have the chief advantage on reducing systematics errors of measurements of neutrino oscillation parameters. However, high neutrino beams

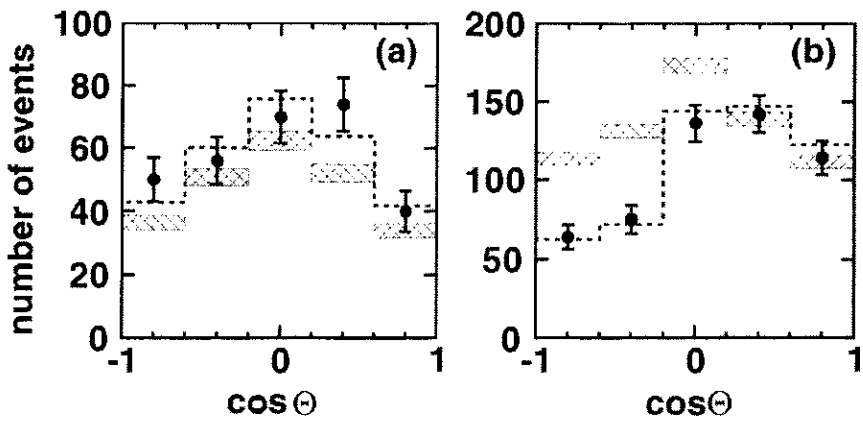

Figure 2.4: Zenith angle distributions for atmospheric neutrinos events. The left and right panel shows the distributions for e-like and μ-like events, respectively. Θ is the zenith angle, and $cos\Theta = 1$ and $cos\Theta = -1$ is vertically downward-going and upward-going, respectively.

present serious experimental challenges for neutrino oscillation experiments[7].

T2K (Tokai to Kamioka) is a neutrino oscillation experiment [50] that uses the muon neutrino beam produced at J-PARC facility and the Super-Kamiokande detector located 295 km away to study mainly oscillations $\nu_\mu \rightarrow \nu_e$. T2K is the successor of the K2K (KEK to Kamioka) experiment [51] wich was a neutrino experiment that operated from 1999 to 2004 and used the KEK 12 GeV proton synchrotron (average muon neutrino energy $\approx$1.3 GeV) and the Super-Kamiokande detector located 250 km away. One of the goals of K2K was the verificarion of the Super-Kamiokande's measurements on atmospheric neutrino oscillations presented in 1998.

The NuMI beam is a muon neutrino beam of a few GeV energy (from 2 to 10 GeV) produced at Fermilab, USA. The Near Detectors of MINOS (Main Injector Neutrino Oscillation Search) [52] and NOνA (NuMI Off-Axis ν_e Appearance) [53].[54].[55] experiments are located at Fermilab. MINOS experiment has its Far Detector 735 km away at the Soudan Underground Laboratory in Minnesota and uses the NuMI beam to study disappearance of muon neutrinos. NOνA experiment has its Far Detector 810 km away from Fermilab and its main goal is the measurement of electron neutrino appearance applying an "off-axis" technique that provides a narrow peak in the energy spectrum.

The CNGS beam is a muon neutrino beam produced at CERN. At the Gran Sasso Laboratory located in Italy, 730 km away, are located the OPERA (Oscillation Project with Emulsion-tRacking Apparatus) and ICARUS (Imaging Cosmic And Rare Underground Signals) experiments. Both OPERA and ICARUS have as main goal studying the ν_τ appearance.

[7]It must, for instance, be able to produce a sufficient number of interactions a few hundreds kilometers away from the source.

Chapter 3

MINERνA Experiment

3.1 The NuMI Beamline

The Neutrinos at Main Injector facility (NuMI) constructed at Fermilab provides a high intensity on-axis ν_μ or $\overline{\nu}_\mu$ beam of 2-20 GeV variable energy to the MINERνA , MINOS and NOνA experiments. At the time of this writing the neutrino beam had an energy peak of 6 GeV. The neutrino beam results from the decays of pions and kaons produced by collisions of 120 GeV protons in a graphite target. Two magnetic "horns" focus the positive (negative) mesons that produce a ν_μ ($\overline{\nu}_\mu$) beam [56],[57] upon decaying.

Fermilab uses a series of accelerators to create the energetic protons required to produce the neutrino beam. The creation process begins with the acceleration of hydrogen negative ions in a Linear Accelerator (LINAC) to about 400 MeV. The accelerated hydrogen ions are then send to the Booster where a carbon foil removes electrons from the ions to obtain just protons which are then accelerated to 8 GeV. Then, the protons are sent to the Main Injector where they are accelerated to 120 GeV. At every 1.9 s a 8.4 μs spill with 3.5×10^{13} protons are extracted and sent towards the 0.95 m long segmented water cooled graphite target, called the NuMI target [58]. Protons are extracted with a 58 $mrad$ (3.323 $^\circ$) angle towards Sudan [59].

Two horns steer pions and kaons towards the proton beam path. For this purpose they operate by a pulsed +(-) 185 kA current[1] [57]. The relative placement of the two horns and the NuMI target optimizes the momentum spectra of the focused particles resulting in different neutrino energy spectra [59]. The target is assembled on a system of rails that make posible moving the target along the beamline. Figure 3.1 shows the different spectra of neutrino energies produced by different configurations.

The constituent parts of the NuMI beamline are shown schematically in figure 3.2. The

[1]This current can be set to different values in order to make special studies and characterization of the beamline

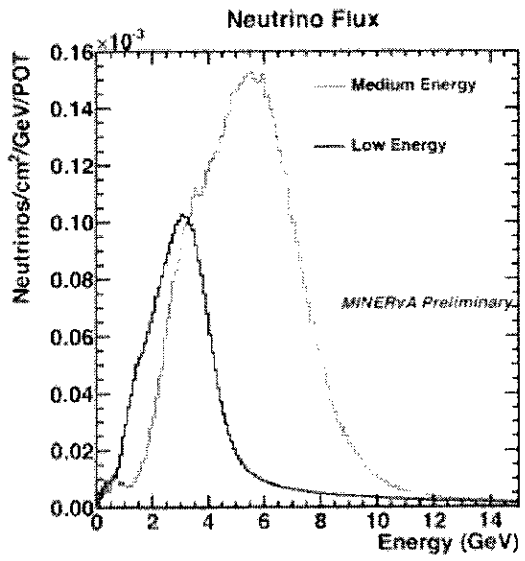

Figure 3.1: NuMI configurations. Low Energy and Medium Energy. (Flux estimation using a GEANT4 based simulation of the NuMI beam line).

pions and kaons are left to decay in a 657 m long and 2 m base steel pipe kept at a constant presion of 1 $Torr$ [59]. The hadron absorber removes all the remaining hadrons coming out the decay volume. The secondary and tertiary particle beams are monitored by an hadron monitor and three muon monitors located next to the absorber, as shown in figure 3.3. The dolomite rock between the monitors remove most of muons leaving neutrinos in the beam. The resulting neutrino beam consists of 97.8 % ν_μ and few $\bar{\nu}_\mu$ (1.8 %) and ν_e (0.4 %)[2]. The resulting NuMI neutrino beam is delivered to the MINERνA detector that is located 100 m underground, just upstream of the MINOS near detector [60].

3.2 The MINERνA detector

The MINERνA detector employs polystyrene scintillator to track particles and two types of calorimeters to contain showers produced by neutrino interactions. The MINERνA detector is provided of targets of a wide range of nucleon numbers to enable studies of nuclear dependence in neutrino interactions, measure form factors and measure cross-sections in this nuclei number variety to improve the systematic uncertainties in future neutrino oscillation experiments [61].

The MINERνA detector consists of a veto wall, a cryogenic liquid helium target and a 5 m length hexagonal prism with 4.10 m diagonal length called MINERνA main detector, as is shown schematically in figure 3.4 and figure 3.5.

[2] ν_e are the result of decay of muons.

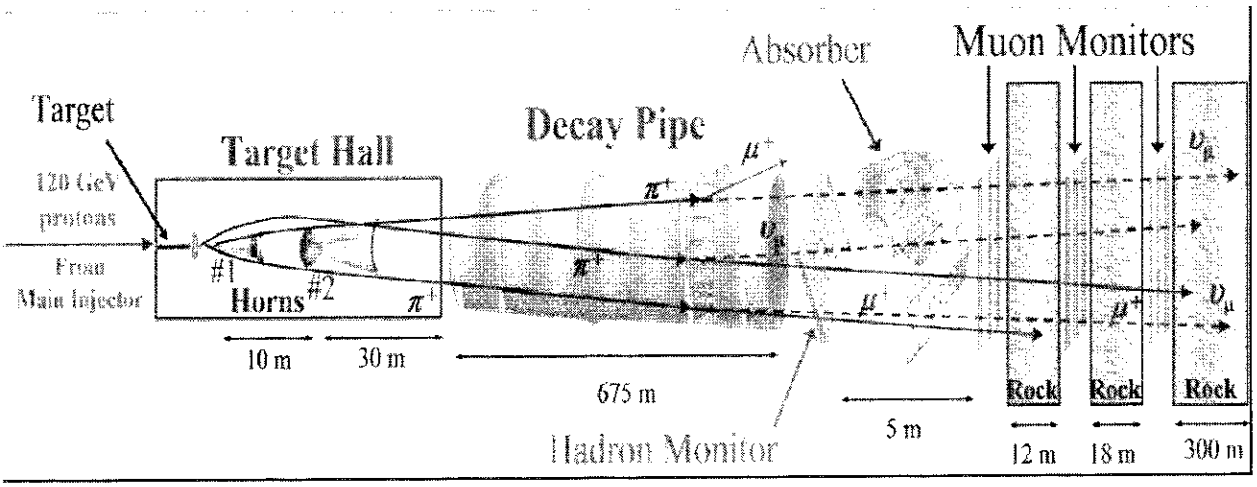

Figure 3.2: Schematic view of the NuMI beamline.

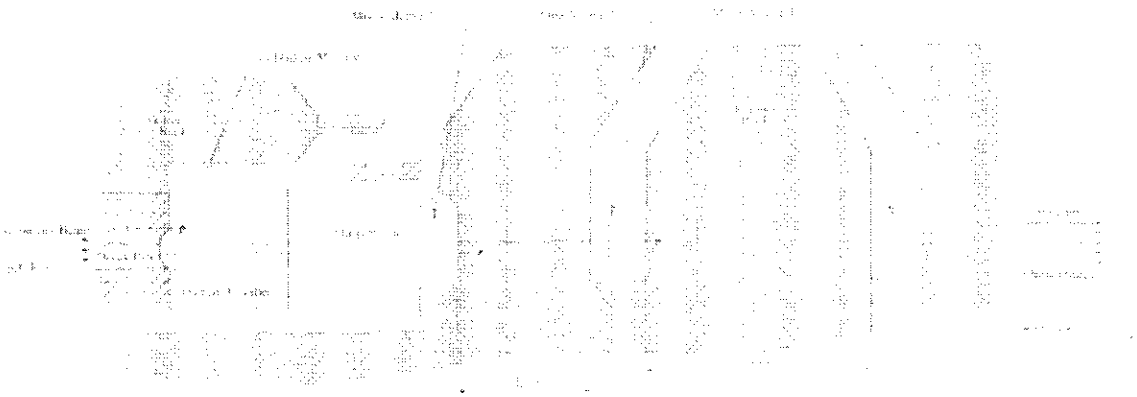

Figure 3.3: The NuMI secondary absorbers and muon monitors.

The MINERνA main detector can be thought of as two detectors: a smaller central hexagonal prism with same length but aproximately 2 m width called the Inner Detector (ID), and the surrounding volume called the Outer Detector (OD). The Inner Detector consists of: nuclear layers interleaved with scintillator planes; a region of pure scintillator planes called Active Tracker Region; the side electromagnetic calorimeter; and at the most downstream part the rest of the electromagnetic calorimeter and part of the hadronic calorimeter. The Outer Detector consists of the side hadronic calorimeter.

The active tracker region is composed exclusively of scintillating material and is the core of the MINERνA detector. The precise tracking, the low density material and fine sampling in this region guarantee difficult measurements can be performed[3]. For construction convenience and handling, the MINERνA detector is made of four types of modules: tracking, nuclear

[3]As an example the energy loss per unit length $\frac{dE}{dx}$ can be used to identify particles and reconstruct the neutrino interaction vertex when several final state charged particles are involved.

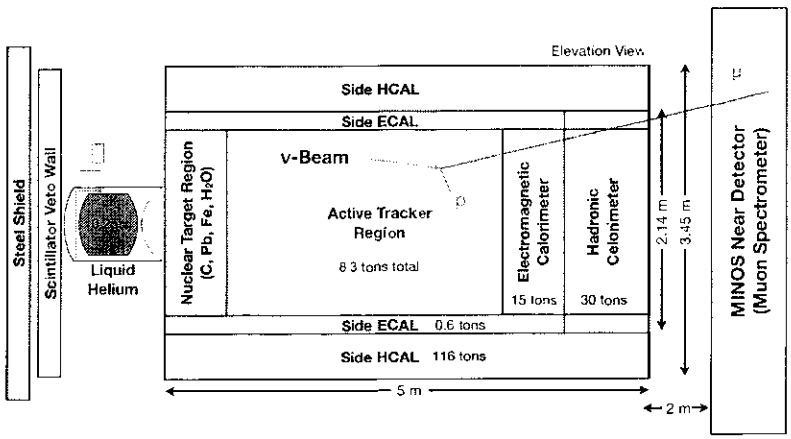

Figure 3.4: Schematic view of the MINERνA detector.

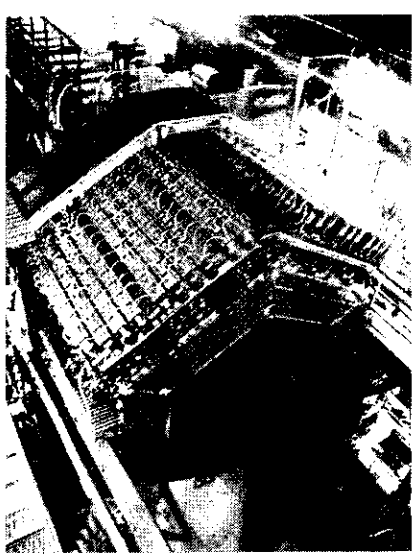

Figure 3.5: Top view of the MINERνA detector.

target, ECAL and HCAL modules. A tracking module consists of two scintillator planes and the respective Outer Detector part, which serves as a supporting structure and is made up of a frame of steel with embedded scintillators. The side electromagnetic calorimeter of the active tracker region is incorporated as a 0.2 cm thick by 15 cm wide lead "collar" between each scintillator plane as shown in figure 3.6. The active track region consists of 62 tracking modules and each scintillator plane consists of 127 scintillating strips. A scintillator plane can have one of three different orientations. The X-plane has the scintillating strips vertically positioned in order to get the x coordenate of the hit. The U- and V-planes are rotated 60

degrees clockwise and counter-wise from the X-plane respectively. Each tracking module has a X-plane and either a U- or V-plane, as shown in figure 3.7 for just two consecutive modules. In the most upstream of the detector a "veto wall" shields the detector from low energy hadrons and tags the muons produced by neutrino interactions in the rock called "rock muons". The cryogenic helium target is located between the veto wall and the main detector. The nuclear target region consists of five layers of passive targets separated by eight scintillator planes to make possible the reconstruction of the neutrino interaction vertex in the targets, and finally the downstream electromagnetic and hadronic calorimeters are made up of scintillator planes interleaved respectively with lead planes and steel planes [62].

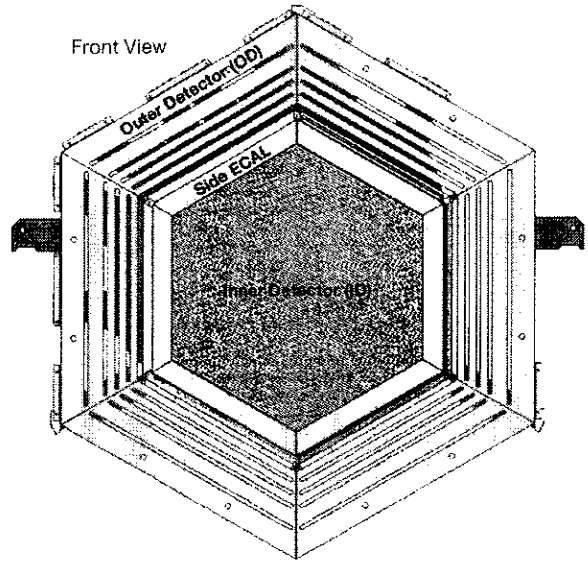

Figure 3.6: Transversal view of a MINERνA tracking module.

3.2.1 The Scintillating Strips

The scintillating strips are triangular prisms of solid scintillator (Dow Styron 663 W) doped with 2.5-diphenyloxazole (POP) (1 % per weight) and 1.4-bis (5-phenyloxazol-2-yl) benzene (POPOP) (0.03 % per weight) coated by a reflective layer of TiO_2 and traversed through the center with a green wavelength shifting (WLS) fiber (1.2 diameter, 175 ppm Y-11 doped) produced by the Kuraray corporation. The transversal lengths of the scintillating strips are shown in figure 3.8.

The scintillating strips are assembled making up a plane as is shown in figure 3.9. This configuration provides charge split between neighbor strips and improves the determination of the interaction coordinate. The combination of the three posible plane orientations provides a stereoscopic 3D image of hits (interactions) in the MINERνA detector.

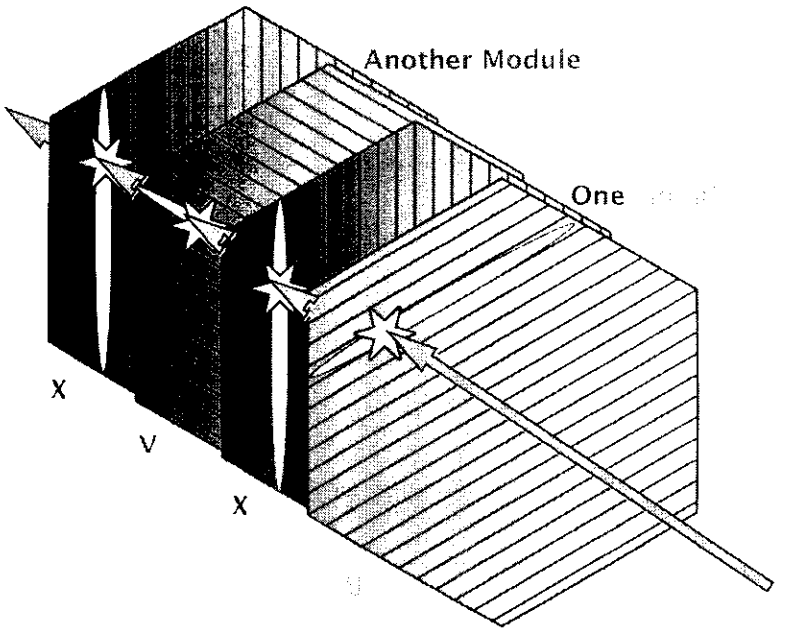

Figure 3.7: Scintillating strip orientations for consecutive modules in the MINERνA tracking region.

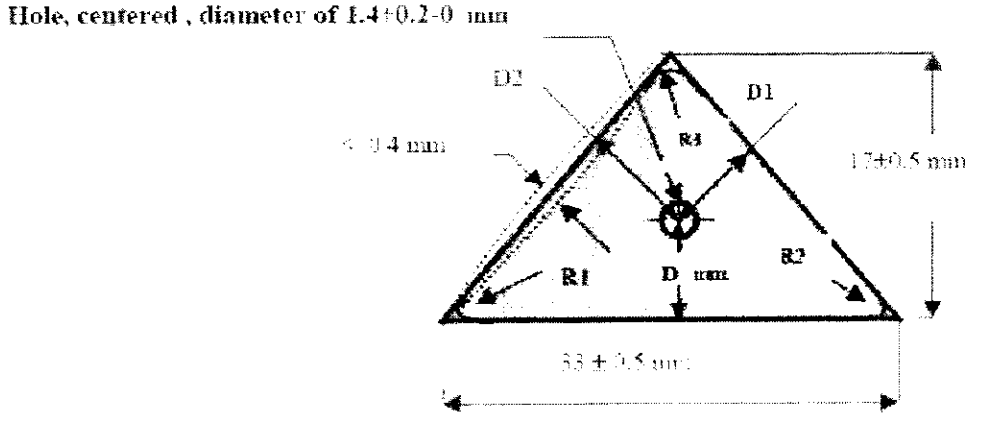

Figure 3.8: Transversal cut of the triangular scintillating prism.

3.2.2 Photodevices

The MINERνA detector uses 507 Hamamatsu Photonics H8804MOD-2 multi-anode Photomultipliers (PMTs) to amplify the scintillation light collected from the WLS (Wavelength Shifting) fibers in each scintillator strip. The PMTs are required to have a minimum quantum efficiency of 12% at 520 nm and a maximum-to-minimum gain ratio less than three. A base circuit board and the PMT are installed inside a 2.36 mm thick steel cylindrical box, keeping them protected

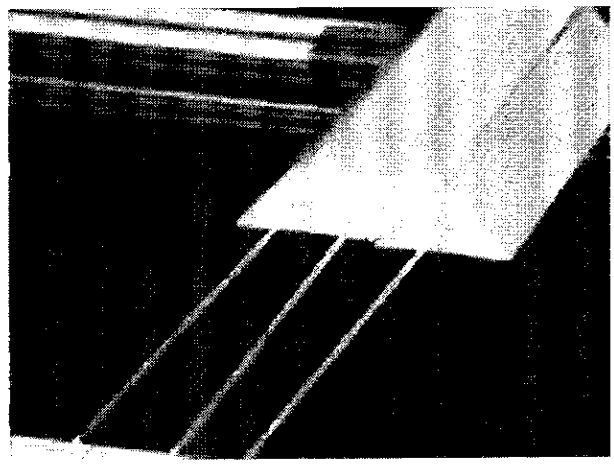

Figure 3.9: Scintillating prisms arranged to form a plane. Each prism holds an optical fiber along its full length to conduct the signal of the interaction.

from dust, ambient ligth and magnetic fields produced by MINOS near detector's magnetic coils. Each multi-anode PMT has an 8x8 array of pixels, each pixel having an effective size of 4 mm^2. Each PMT is actually 64 PMTs because it takes 64 clear fibers carrying the electrical signals from the WLS fibers of the strips as is shown in figure 3.10. These fast analog signals are fed to the Front End Boards (FEBs) attached to the optical box and located outside of it. The main functions of the FEB are to digitize timing and pulse-height signals, and communication to the VME readout controllers modules.

3.2.3 Nuclear Targets and Cryogenic Helium target

The nuclear target region located at the most upstream part of the detector is made up of five layers of passive nuclear targets in total made of Fe (998 kg), Pb (1023 kg), C (120 kg) and water. Except for the fourth and fifth layers each target is separated by four tracking modules. The figure 3.11 shows the cryogenic Helium target and the nuclear targets in the ID. There are pure material targets and mixed material targets.

The purpose of the different orientations for the materials in the mixed targets is minimization of the effect of acceptance differences for different regions in the detector. The nuclear targets are mounted in the same hexagonal steel frame (Outer Detector) as the scintillator planes. The water target do not use the OD to be mounted as is shown in figure 3.12.

The cryogenic helium target is an aluminum cryostat capable of holding approximately 2,300 L of cryogen. It consists of an inner cylinder with 152 cm inner diameter, 100 cm length, 0.635 cm wall thickness; and an external vessel cylinder of 183 cm diameter and 0.952 cm wall thick. The cryogenic helium target is planned to be removed when the MINERνA physics program

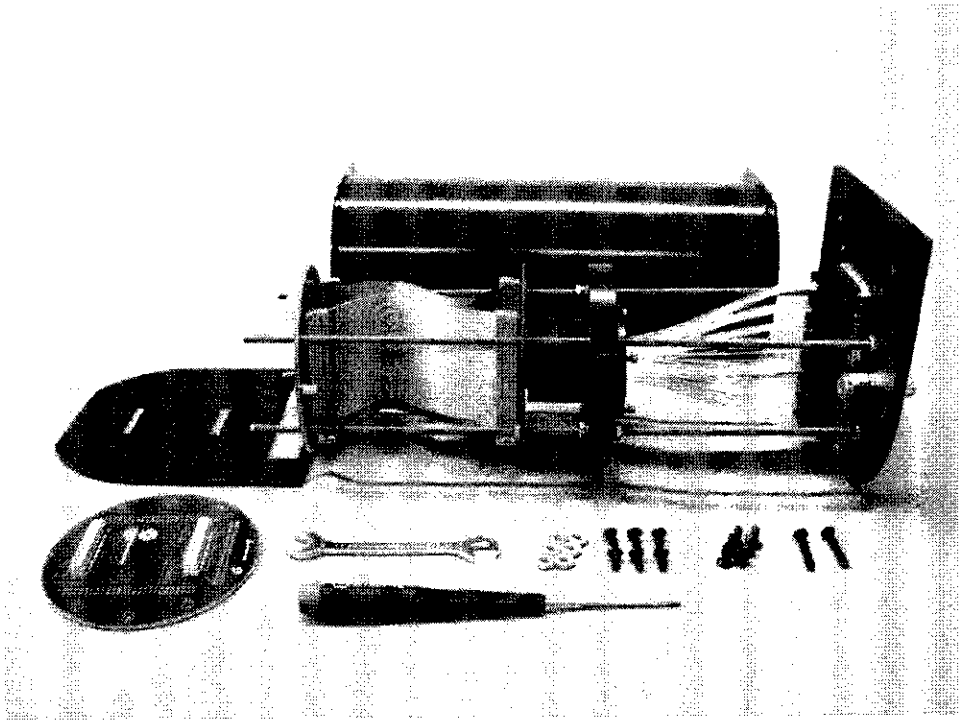

Figure 3.10: Optical box containing the Photomultiplier (small black cube) conected to the 64 clear fibers.

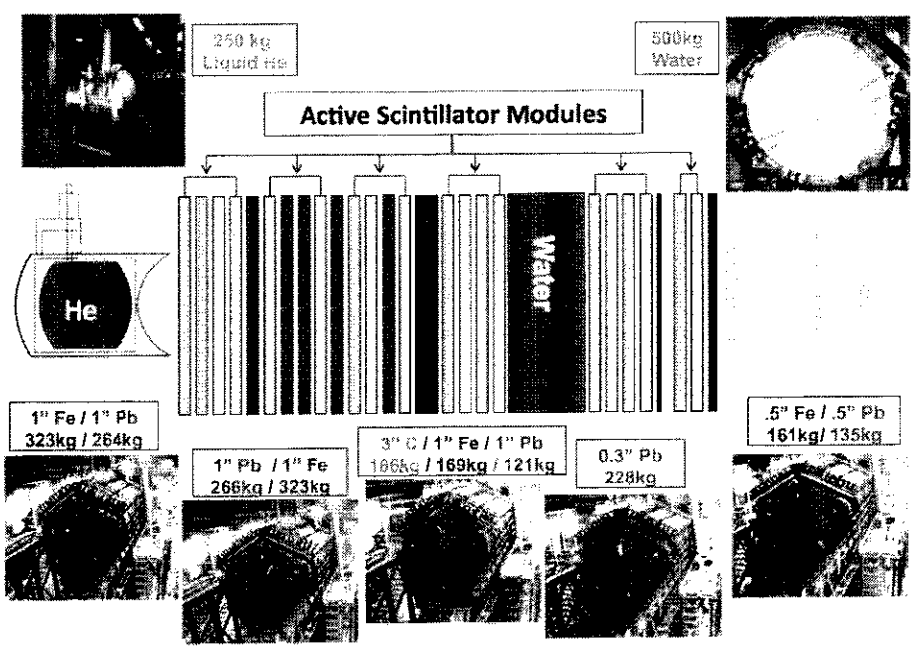

Figure 3.11: Nuclear targets.

finish in order to install the CAPTAIN detector in its place to set the CAPTAIN-MINERνA detector.

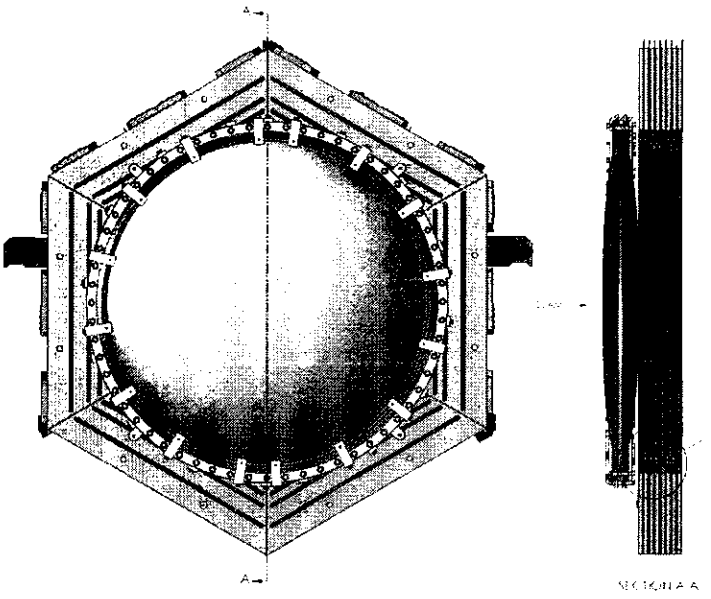

Figure 3.12: Water target

3.2.4 Electromagnetic and Hadronic calorimeters

The electromagnetic calorimeter (ECAL) is made up of ten electromagnetic modules. An ECAL module is very similar to a tracking module but instead of a Pb ring it has a Pb layer (2 mm thick) covering the hole area of each scintillating plane. This region consists of 20 layers of Pb interleaved with scintillator planes having orientations as shown in figure 3.13.

The electromagnetic calorimeter is used to decrease the shower lengths produced by charged particles in the detector. Since pair production cross section is proportional to Z^2, photons of few GeV will be detected via pair production.

The hadronic calorimeter placed at the most downstream of the detector is made up of 20 HCAL modules. Each HCAL module is made of a Fe layer (2.54 mm) and just one scintillating plane. Muons with energy up to 600 MeV and protons with energy up to 800 MeV will be stopped by the combined action of all this layers. A HCAL module is shown in figure 3.14.

3.2.5 The Outer Detector (OD)

The Outer detector (OD) is a steel hexagonal shell with inner apothem 1.168 m and outer apothem 1.727 m. All steel frames are 3.49 cm thick except for frames surrounding the thicker downstream HCAL where they are 3.81 cm thick. Each frame has four slots each holding a pair of 2.54 $\times$ 2.54 cm^2 rectangular scintillator strips for calorimetry and tracking. The total iron thickness is 43.4 cm, or 340 g/cm^2, which can stop, from ionization losses alone, up to 750 MeV protons at 90° and nearly 1 GeV protons entering at an angle of 30°.

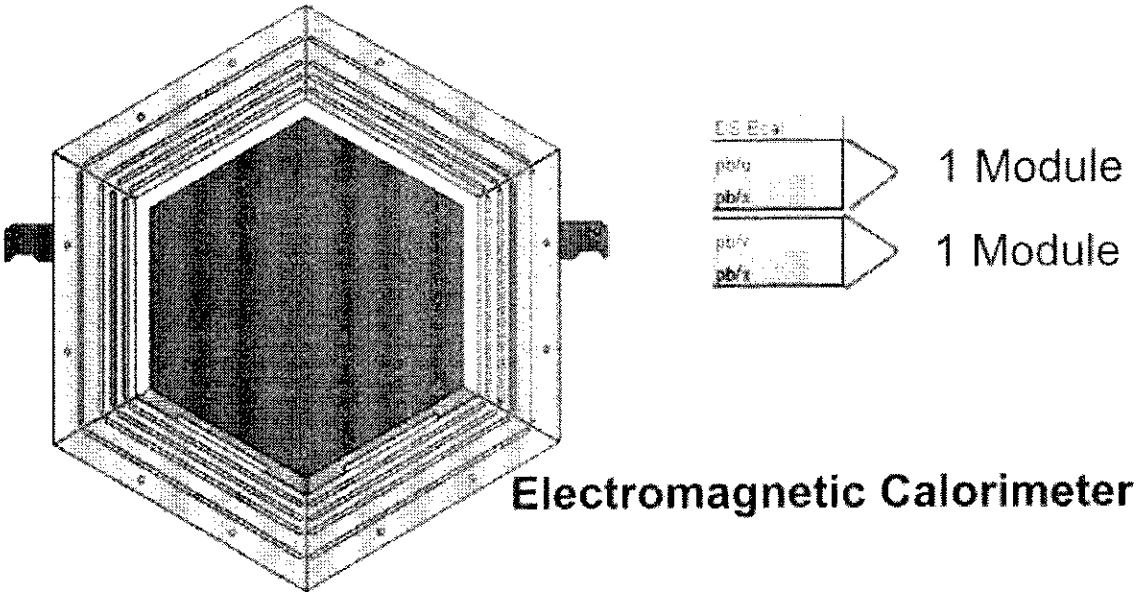

Figure 3.13: ECAL module and the orientation for two consecutive modules.

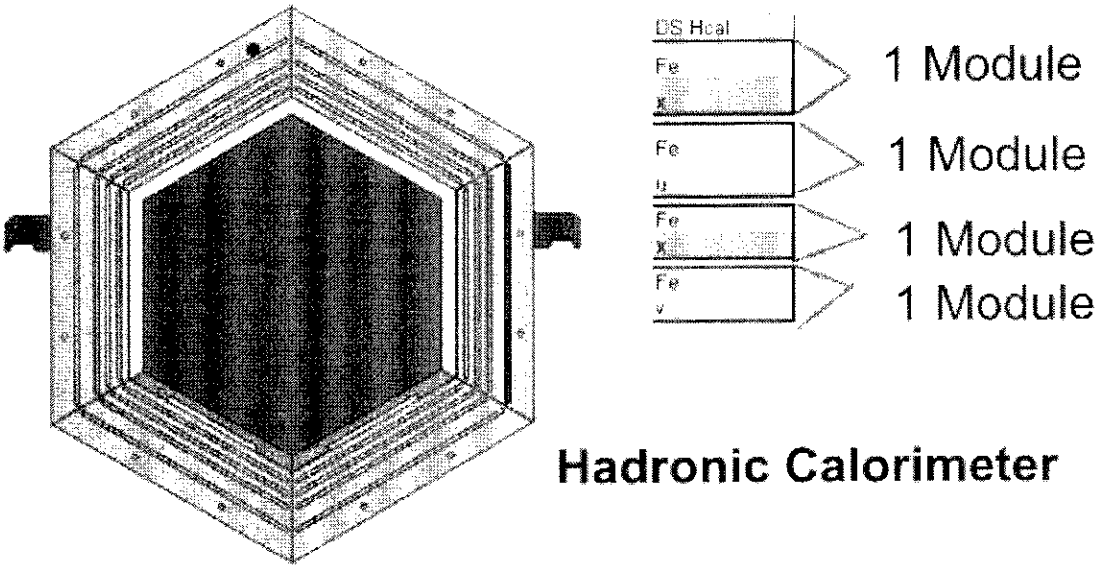

Figure 3.14: HCAL module and plane orientations for consecutive modules.

3.2.6 MINOS (Main Injector Neutrino Oscillation Search) Near Detector

MINOS is a long-baseline oscillation experiment. As an usual long-baseline type experiment it consists of two detectors separated by a long distance. The Near detector is located at

Fermilab just downstream MINERνA and the Far detector is located 450 miles away in northern Minnesota. The MINOS Near and Far detectors are made of steel and plastic scintillator [60] like the MINERνA hadronic calorimeter. One of the advantages of MINOS near detector is that it is magnetized, which makes it possible the reconstruction of the charge and momentum of the (anti)muons produced by charged current (anti)neutrino interactions. In figure 3.15 are shown two views of the MINOS near detector (ND).

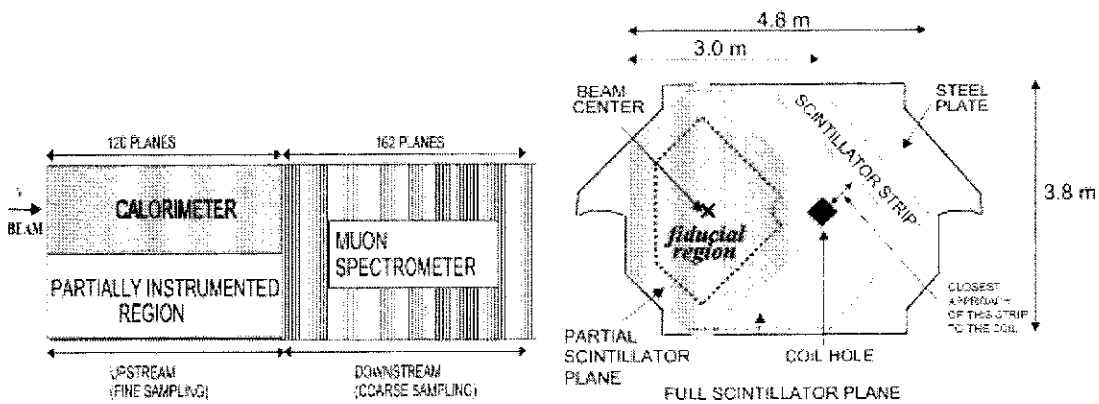

Figure 3.15: Two views of the MINOS near detector. Left: View from above. Right:View in the beam direction.[62].

Chapter 4

CAPTAIN-MINERνA Experiment

4.1 Time Projection Chamber

A Time Projection Chamber (TPC) is a particle detector that uses the ionization electrons produced by the passage of a charged particle through a sensitive substance to reconstruct the track and momentum of the particle. In general, a TPC uses a cathode and an anode plane to produce an uniform electric field inside a field cage and induction planes located just before the anode plane to detect the passage of the drifted electrons. The electrons passing through the induction planes provide a two dimensional location of the interaction and their drift time to the collector anode gives the third coordinate position. A schematic functionality of a TPC is shown in figure 4.1.

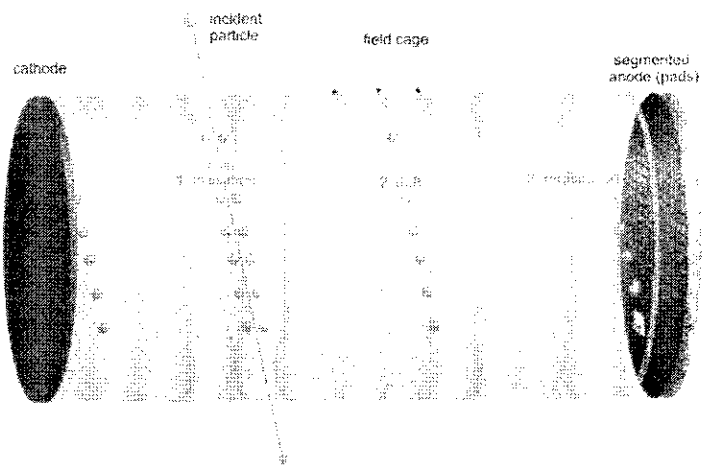

Figure 4.1: Schematic view of a TPC.

4.2 The CAPTAIN detector

Liquid Argon is advantageous as a sensitive substance for a TPC because it is dense (1.4 g/cm^3), permits electrons long drift-times thanks to its low electronegativity and high electron mobility, excellent scintillator, cheap and easy to purify [63], [64],[65]. The CAPTAIN detector is a Liquid Argon Time Projection Chamber (TPC) conformed by a portable and evacuable vacuum isolated cryostat that can hold 7700 liters of liquid Argon. A general view of CAPTAIN is shown at figure 4.2. The cryostat has side ports allowing optical access for laser calibration and a work deck mounted on the top head to provide workers safe access to the top ports of the cryostat where all instrumentation and cryogenics are made through.

Because liquid argon serves as target and detection medium for the CAPTAIN detector it must remain minimally contaminated of oxygen and water, these molecules may affect the drift of electrons. A minimum contamination of Nitrogen is also required to avoid the absorption of scintillation light. Using a design based on experiences of the MicroBooNE experiment [66], [67] and Liquid Argon Purity Demonstration (LAPD) experiment, the CAPTAIN's cryogenics system monitors and regulate the state of the liquid argon in the detector. For this purpose CAPTAIN holds a dual filter system consisting of a bed of molecular sieve (208604-5KG Type 4A) to remove moisture and another bed of activated copper material (CU-0226 S 14 X 28) to remove oxygen.

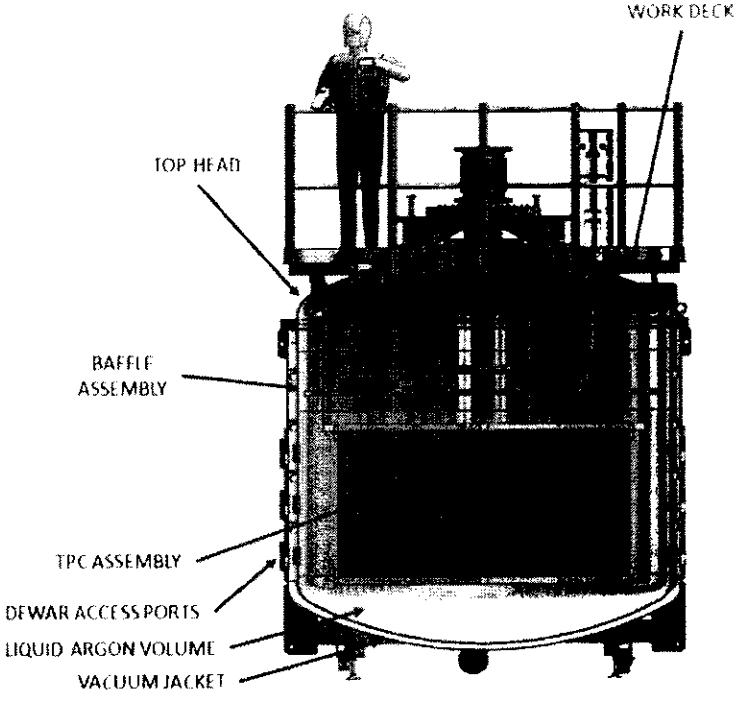

Figure 4.2: Schematic view of the CAPTAIN detector.

The CAPTAIN's Time Projection Chamber (TPC) consists of a field cage in a hexagonal shape with a mesh cathode plane on the bottom of the cage and four wire planes on the top. The construction material of the TPC is the FR4 glass fiber composite. The field cage can be seen as two modules: the drift cage module and the planes module. The planes module located at the top of the field cage consists of the grid, U, V and anode (collection) plane, as shown in figure 4.3. The U and V wires are oriented ±60 degrees relative to the anode wires. The U and V planes detect the ionized electrons by induction providing two spatial coordinates of the track and the anode plane provide the third coordinate by measuring the drift time of the electron produced by ionization. The apothem of the TPC is 100 cm and the drift length (height) is 100 cm. The field cage is double sided gold plated copper clad FR4 arranged with 5 mm wide traces separated by 1 cm. The electric field inside the cage is 500 V/cm and the electron drift velocity is 1.6 mm/μs.

The scintillation light produced in the Liquid Argon has an spectrum peak at 128 nm not energetic enough to produce secondary ionisation or excitation. The scintillation light is used as a trigger of the read-out process [68]. Detection of this light is important also to improve the energy resolution of the detector. Simulations for minimum ionizing particles (MIP) in a TPC with a field of 500 V/cm showed detection of several photoelectrons per MeV improves the energy resolution by 10-20%. This improvement is due to the anticorrelation between scintillation light and ionization electrons [69].

Unfortunately most of the photodetector window materials absorbs the liquid argon scintillation light (128 nm), so it is necessary to shift this light to visible. For this purpose a large area of the detector is covered with a thin film of tetraphenyl butadiene (TPB), the most commom of the wavelenght shifter used in liquid argon detectors. The detection of visible light is done by sixteen Hamamatsu R8520-500 photomultiplier tubes (PMT). Eight PMTs are located on top of the TPC and eight on the bottom. This configuration provides a minimum detection of 2.2 photoelectrons per MeV for a minimum ionization particle (MIP).

The calibration system consists on producing a well-defined ionization track within the liquid argon TPC in order to be able to measure the electron lifetime in-situ and determine the drift field within the TPC. Making use of the optical access windows on the sides of the detector to avoid possible dispersions by surface irregularities a frequency quadrupled Nd-YAG laser is used to produce the well-defined ionization track. This calibration method is well explained and documented in Rossi et al. [70].

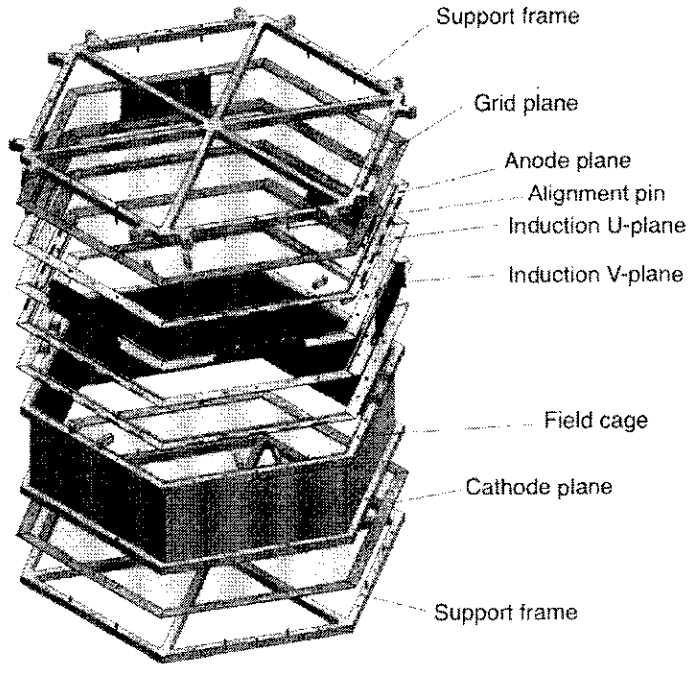

Figure 4.3: Structure of the CAPTAIN detector.

4.3 CAPTAIN-MINERνA Detector

A broad program of neutrino cross-sections measurements on a few GeV range can be pursued by installing the CAPTAIN detector upstream the MINERνA detector. The combined data of the CAPTAIN, MINERνA and MINOS could provide extremely helpfull measurements for future oscillation experiments. Comparison of cross sections on Argon (Ar) to scintillator (CH) would improve the measurements on effects of the nucleus to neutrino interactions since these cross section ratios are not affected by large flux uncertainties.

The Long Baseline Neutrino Facilty (LBNF) is being constructed at Fermilab. This facility will provide a wide-range muon neutrino energy beam for the leading-edge Deep Underground Neutrino Experiment (DUNE), a dual-site experiment for neutrino science and proton decay studies wich will be located at a baseline of 1300 km [71]. The first oscillation maximum at this baseline occurs in the neutrino energy range from 1.5 to 5 GeV, then most electron neutrinos at this range of energy are expected to be detected [72]. DUNE has proposed to use a liquid argon TPC detector and therefore measurements of neutrino-argon interactions are important for the success of the DUNE experiment. The ArgoNeuT detector, a 170 liter liquid argon TPC, published results on studies of neutrino-argon interactions in the low NuMI beam energy [73], [74], [75]. [76]. Nevertheless, these results are statistically limited. MicroBooNE [66]. [67], a 170-ton liquid Argon TPC detector will do studies of neutrino-argon interactions in the Booster Neutrino Beam (BNB) of neutrino energy peak $O(1\ GeV)$, consistent with the same

energy range for the second oscillation maximum for a baseline of 1300 km. Thus, studies made by CAPTAIN in the medium energy NuMI beamline will complement those studies made by MicroBooNE at the BNB low energy. In figure 4.4 the three fluxes provided by the Booster Neutrino Beam (BNB) for MiniBoone and MicroBooNE: Long Baseline Neutrino Facility (LBNF) for DUNE and the NuMI facility for MINERνA and MINOS are shown.

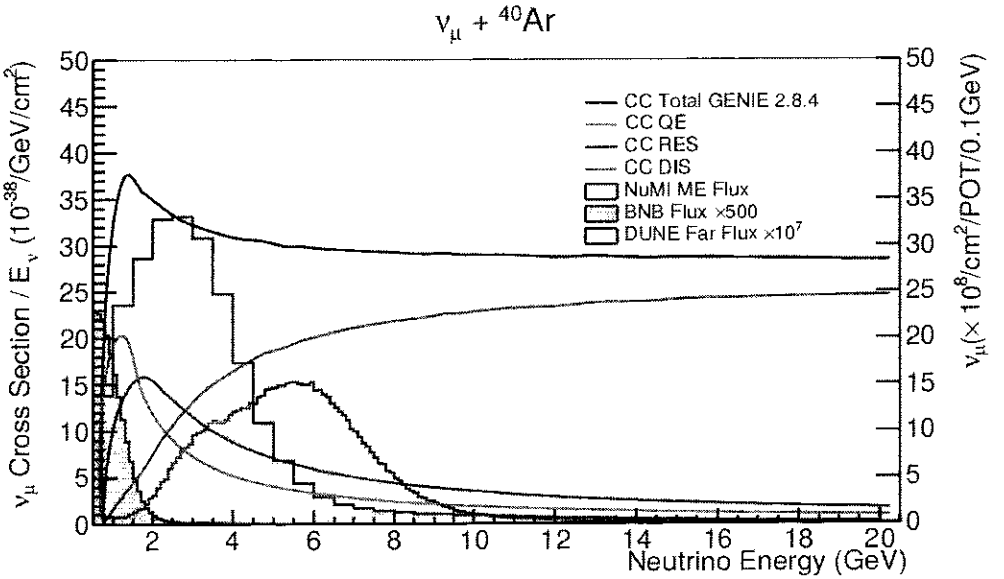

Figure 4.4: Unoscillated ν_μ DUNE far flux, BNB flux at MiniBooNE, medium-energy NuMI flux at the MINOS near hall and GENIE cross section on 40 Ar [77]

The integration of CAPTAIN to the MINERνA detector will improve the tracking and energy measurement of particles exiting CAPTAIN, most importantly muons. These will be tracked by MINERνA and/or MINOS ND providing a better estimation of the incoming neutrino energy than could be achieved by CAPTAIN detector alone. Liquid argon TPC's provide excellent energy resolution, position resolution and particle identification making posible precise reconstruction of the events.

The planned installation of CAPTAIN-MINERνA consists on replacing the MINERνA 's actual helium scryogenic target by the CAPTAIN detector as shown in figures 4.5 4.6.

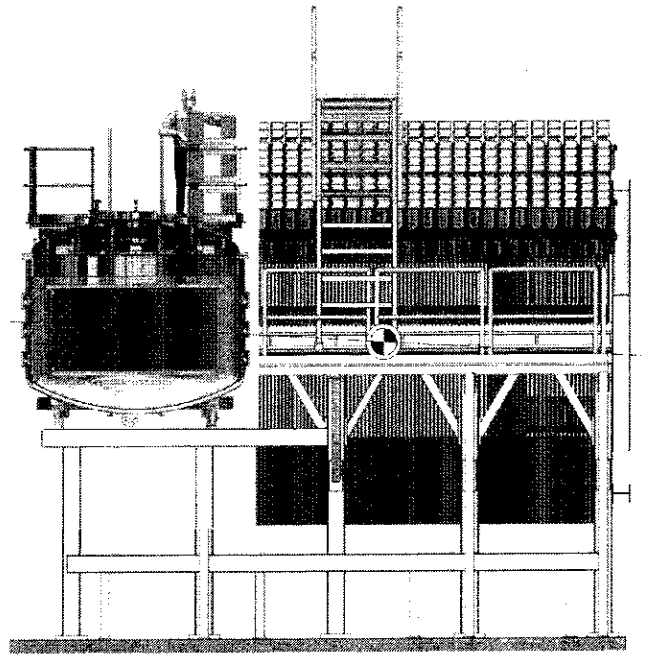

Figure 4.5: Lateral view of the CAPTAIN-MINERνA detector.

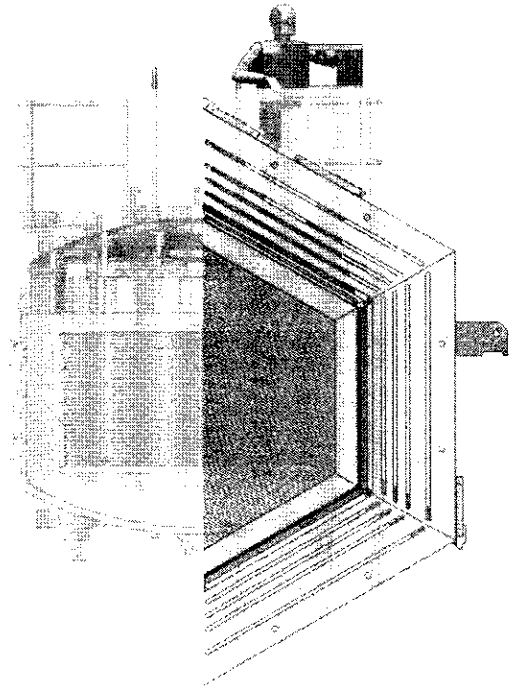

Figure 4.6: Front view showing the relative size of CAPTAIN and the MINERνA main detector.

Chapter 5

Calculation of the muon acceptance

5.1 Simulation

5.1.1 GENIE and Geant4

MINERνA uses the GENIE 2.8.4 [78] to generate events of neutrino interactions with matter. GENIE uses different cross section models for each type of interaction. The differential distribution for the model is used to get the event kinematics. GENIE has three families of models: nuclear physics, neutrino cross sections and final state interactions (FSI).

GEANT4 [79], [80] is used to simulate the passage of particles through matter. This toolkit is used by essentially all experiments and projects at Fermilab, in addition to be used in a large number of experiments in a variety of application domains, including high energy astrophysics and space science, medical physics and radiation physics. The toolkit has been designed, developed and maintained by collaborators from institutes, High Energy Particles experiments, and universities.

5.1.2 The NuMI Flux

The low probability of neutrino interaction makes it difficult the direct measurement of the energy spectrum of a neutrino beam. Actual strong interaction theory poorly models interactions in the NuMI target and a beam-line particle is expected to re-interact in any of the different components of the target. These two facts make it difficult the analytical calculation of the neutrino spectrum of the NuMI beam. Therefore MINERνA relies on a GEANT4-base simulation package named G4numi. This package considers the main geometrical details such as the NuMI target Hall, the decay pipe, absorber, etc, to simulate the neutrino beam. However the flux prediction is more sensitive to some elements than others, such as the targets and horns. g4numi uses the FTPB_BERT hadronic physics model that combines the FRITIOF Pre-

compound model [81] for processes with energies greater than 4 GeV and the Bertini cascade model [82] for energies less than 5 GeV. However it does not provide a very precise description of proton-nucleus interactions. In order to minimize these uncertainties constraints the experimental hadron production data from CERN's NA49 experiment [83] and Barton *et al* group [84] are used. Since the NA49 experiment and Barton *et al* collected data at 158 GeV/c and 100 GeV/c proton energy respectively, an energy scaling is applied based on the predictions from the FLUKA [85] hadron production simulation software.

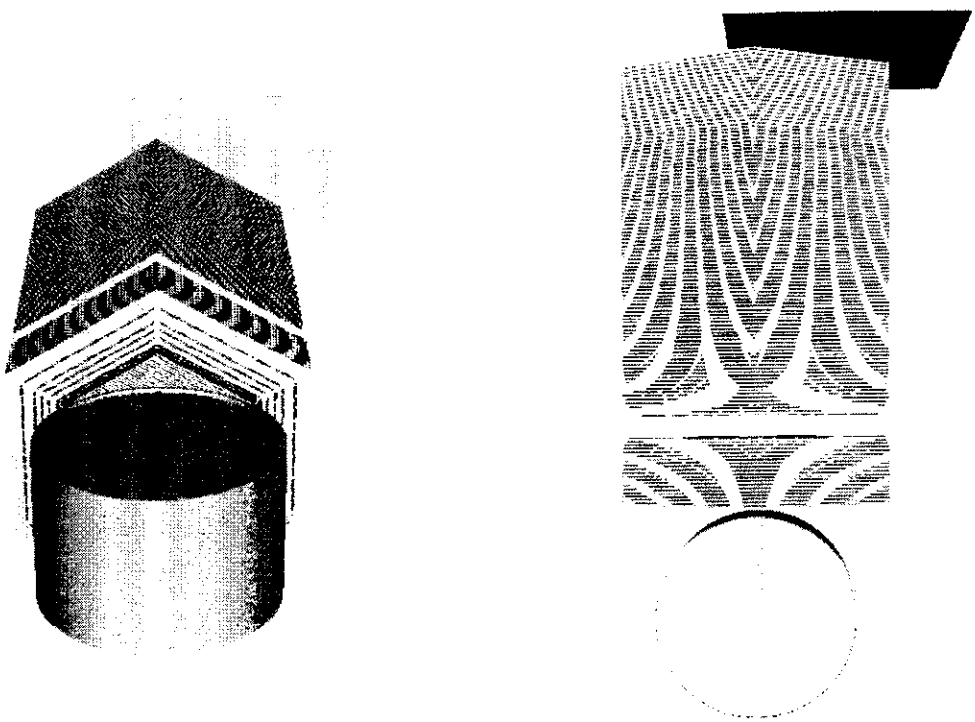

Figure 5.1: Left: Front view of the CAPTAIN-MINERνA detector. Right: View from above of the CAPTAIN-MINERνA detector.

5.1.3 CAPTAIN-MINERνA detector Geometry

The CAPTAIN-MINERνA geometry was implemented in the MINERνA experiment framework. The medium energy NuMI flux was used to generate neutrino interactions and simulate the passage of the produced particles through the geometry. The neutrino interaction events were generated by GENIE 2.8.4 and the passage of the produced particles were simulated by Geant4. The geometry was previously probed using the neutrino interactions events provided by GENIE 2.8.4 to check it was complete.

The CAPTAIN-MINERνA geometry consists of the CAPTAIN detector, the MINERνA main detector and a steel "mirror plane" as shown in figures 5.2 and 5.1. The mirror plane

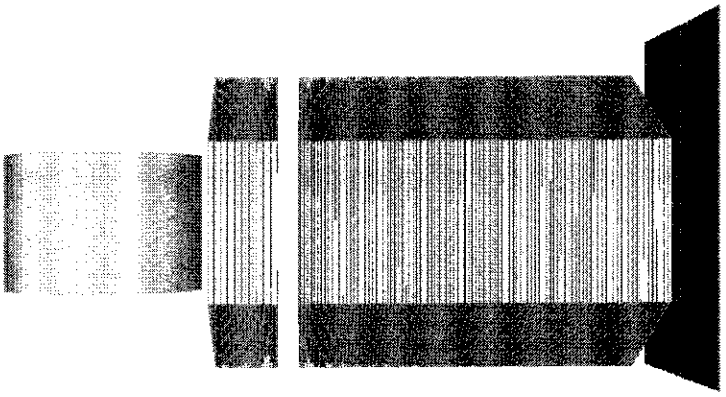

Figure 5.2: Lateral view of the CAPTAIN-MINERνA detector.

is a steel plane positioned between MINERνA and MINOS, just on the region of MINOS's return coil. This plane covers 40 of MINERνA 's PMTs providing shielding from magnetic fields produced by the coil. The veto wall, the water target and the MINOS near detector are not included in this geometry.

The CAPTAIN detector is a stainless steel cylinder of 1.8127 m height, 1.35 m radius and 44.7 mm thick wall, filled with liquid Argon (density=1.4 g/cm^3). The MINERνA main detector can be seen as a hexagonal prism of ~5.72 m length and ~3.46 m hexagon width. The nuclear target region has all the passive targets[1] as shown in figure 5.2. The tracking region, ECAL and HCAL are complete. The detector environment is air.

5.1.4 Geometry Probing

Four millions neutrino interaction events were generated in the CAPTAIN-MINERνA geometry. Figures 5.3 and 5.4 show the these GENIE events in the MINERνA coordinates from front, up and lateral views respectively. Codes were implemented to plot specific regions and/or modules of the geometry identifying the material they are made of. All these plots are presented in Appendix A. The CAPTAIN-MINERνA geometry has all the modules and targets, but the water target.

The next step is simulate the passage of particles through the detector. In the MINERνA framework GEANT4 simulation is limited by virtual planes surrounding most of the MINERνA detector. The GEANT4 simulation stops tracking particles just after they pass these planes. A rectangular virtual plane is positioned just downstream of the mirror plane positioned parallel to it and six virtual planes are extended along the lateral sides of the hexagonal MINERνA detector. These planes are identified when the end points of muons produced by the neutrino

[1] The water target is not included

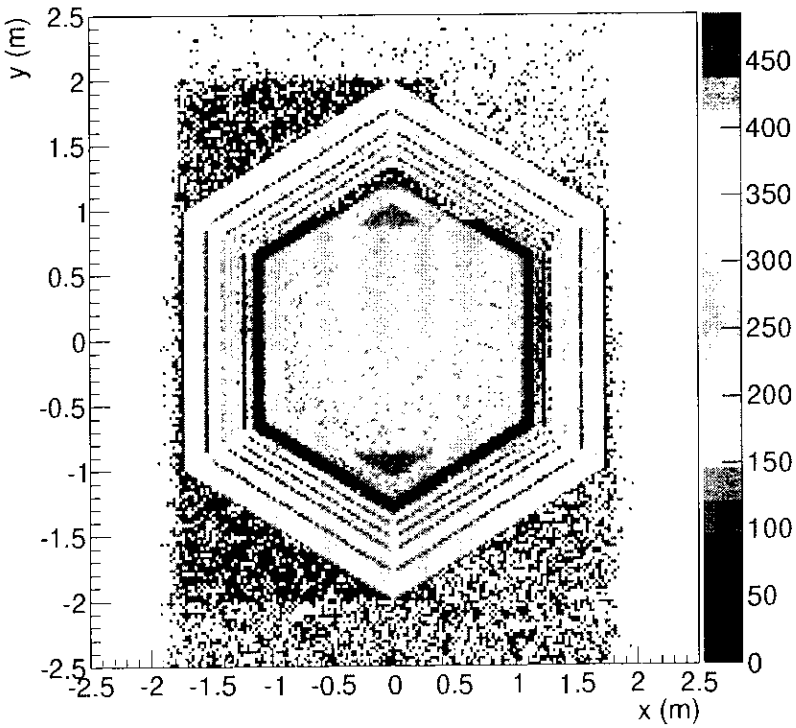

Figure 5.3: Front view plot of CAPTAIN-MINERνA detector made with GENIE events. The CAPTAIN detector and the "mirror plane" shapes can be identified. The color bar indicates density of events.

interactions are plotted as shown in figure 5.5.

The virtual planes surrounding the main detector were successfully disabled by modifying an "option file" used in the MINERνA framework. It is not possible to disable the rectangular virtual plane downstream the detector.

5.1.5 Muon acceptances

Muons from 132,589 neutrino charged current events in Argon of the CAPTAIN volume are used to obtain the muon acceptances for different regions of the CAPTAIN-MINERνA geometry. These muons are classified in five categories according to their trajectories in the detector geometry:

- muons reaching MINOS fiducial region
- muons stopping in MINERνA (stopping in any region of the MINERνA main detector)

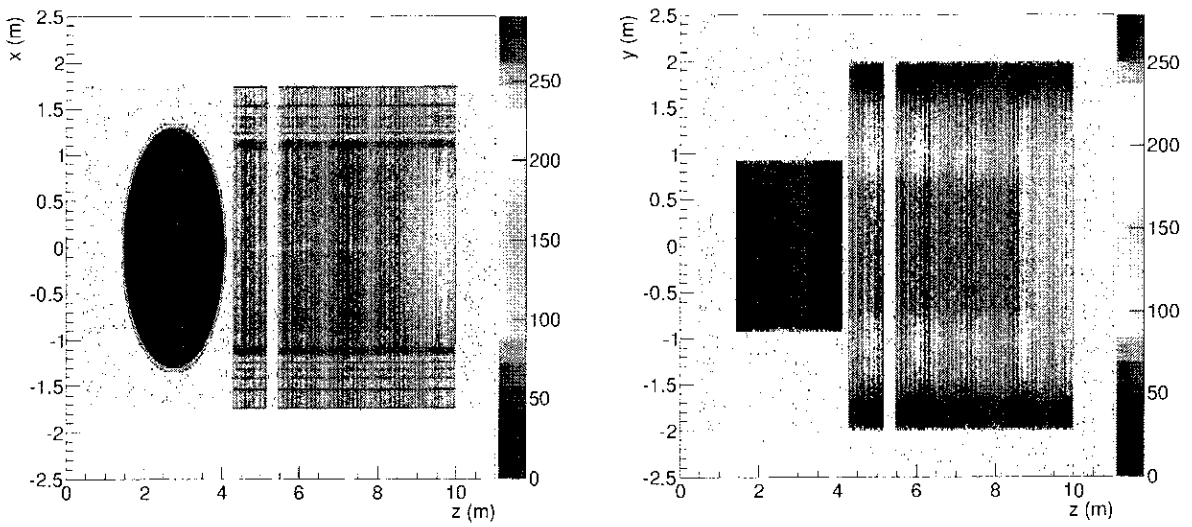

Figure 5.4: Plots of the density of events from different views. Left: View from above of the CAPTAIN-MINERνA detector. Right: Lateral view of Lateral view of the CAPTAINMINERνA detector.

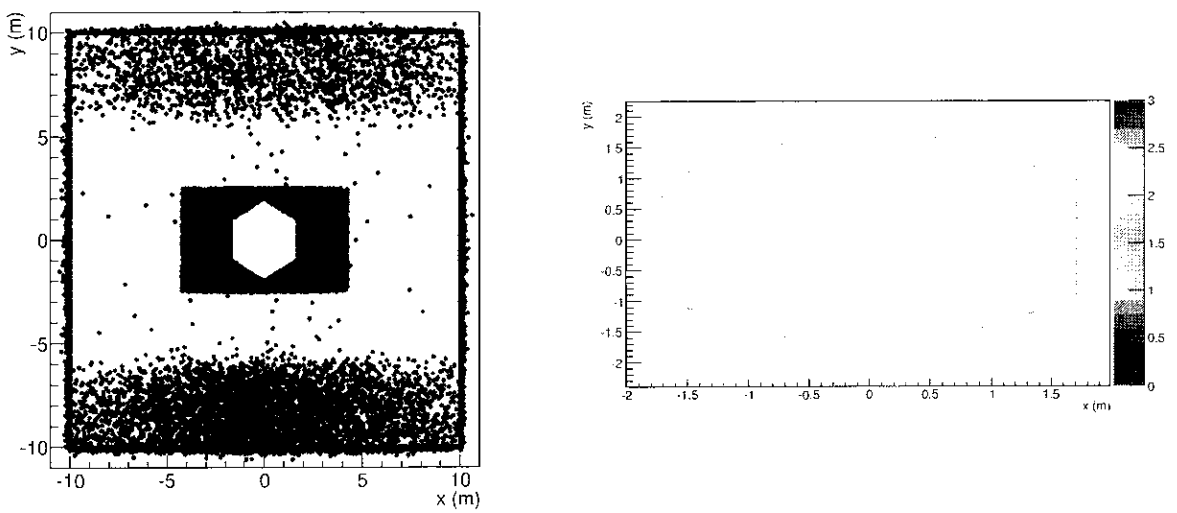

Figure 5.5: Left: Transversal view of the end points of muons produced in the CAPTAIN reaching farther the end of the MINERνA detector. End points in the area of the MINERνA detector are not plotted. The muons are stopped on the rectangular virtual plane and on the spatial limits of the simulation. Right: Transversal view of end points of muons being stopped on the planes surrounding the MINERνA main detector.

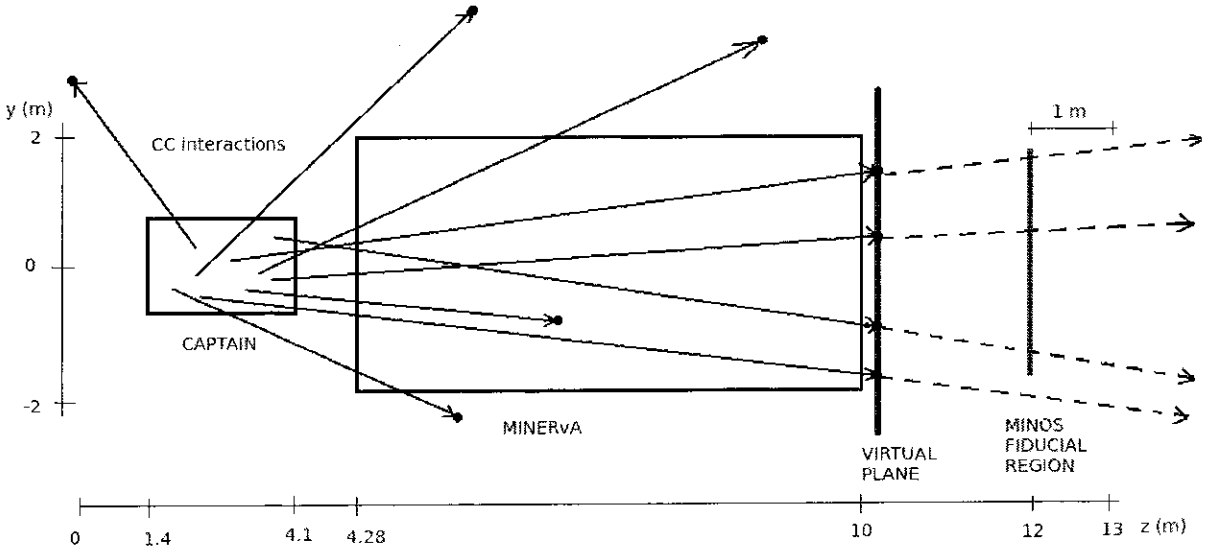

Figure 5.6: The CAPTAIN-MINERνA detector in the MINERνA framework coordinates showing the muon categories.

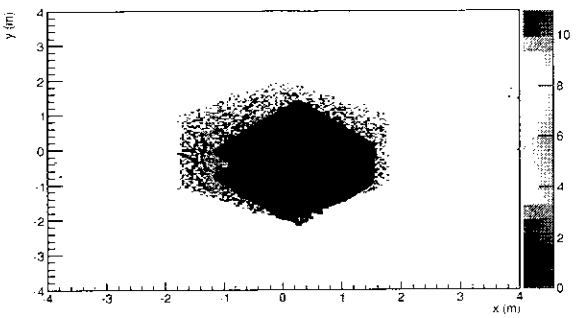

Figure 5.7: Superimposition of the Transversal Areas of the MINERνA detector and MINOS fiducial region.

- muons stopping in fiducial MINERνA (The MINERνA fiducial volume is a small hexagon prism of 0.85 m apothem and 2.95 m length (5.99<z<8.34 m in the MINERνA coordinate system) that consists of pure scintillator.)
- muons missing MINERνA
- muons crossing MINERνA (includes those muons crossing MINERνA and not reaching MINOS fiducial region)

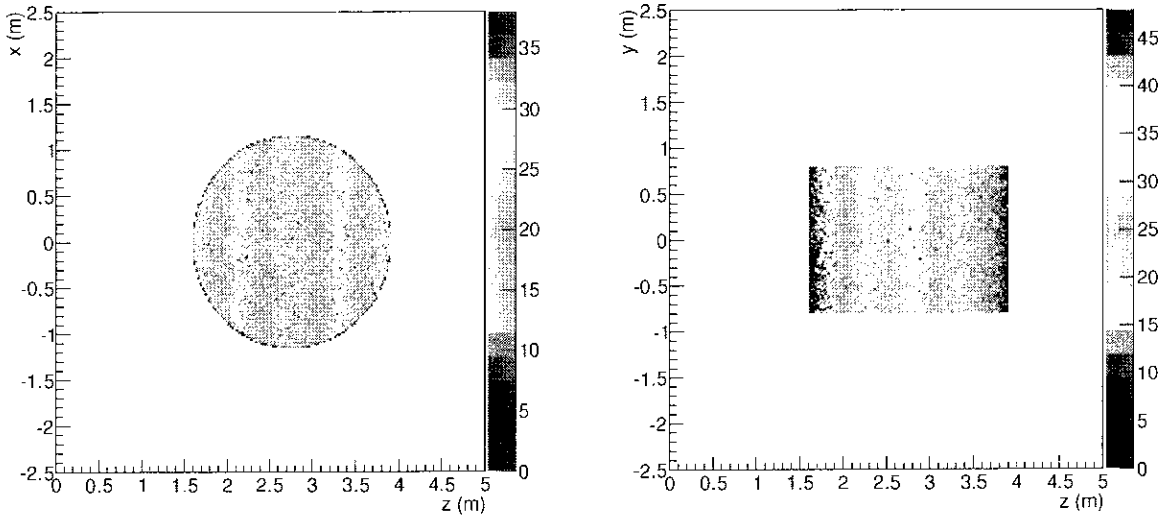

Figure 5.8: Charged Current events with Argon in the CAPTAIN fiducial volume (center=2.75; radius=1.15; -0.8<y<0.8; 1.6<z<3.9 *meters*.

The location of the geometry in the MINERνA framework coordinate system and some muon trajectories are shown in Figure 5.6. The coordinates of the geometry are extracted from Section 5.1.4 and are shown in Table 5.1.

CAPTAIN	MINERvA
height: -0.9635<y<0.9635	hexagon height: -2<y<2
widths: 1.4<z<4.1	hexagon width: -1.73<x<1.73
-0.675<x<0.675	length: 4.28<z<10

Table 5.1: MINERνA coordinates of the detector.

A three dimensional linear equation is implemented for each muon trajectory. The dimensions of the detector geometry (Table 5.1) is then used to sort every muon into the categories. Muons exiting MINERνA towards the MINOS detector are stopped in the rectangular virtual plane. In order to obtain the ones that reach the MINOS fiducial region the trajectories of muons stopped on the virtual plane are projected into the MINOS fiducial region. In addition, the projected trajectories are required to have at least one meter into the volume covered by MINOS fiducial region. The relative area sizes of the MINERνA detector and the MINOS fiducial region are plotted and shown in figure 5.7.

The charged current neutrino interactions events in Argon of the CAPTAIN fiducial volume are plotted in Figure 5.8. We will refer to CAPTAIN fiducial volume just as CAPTAIN.

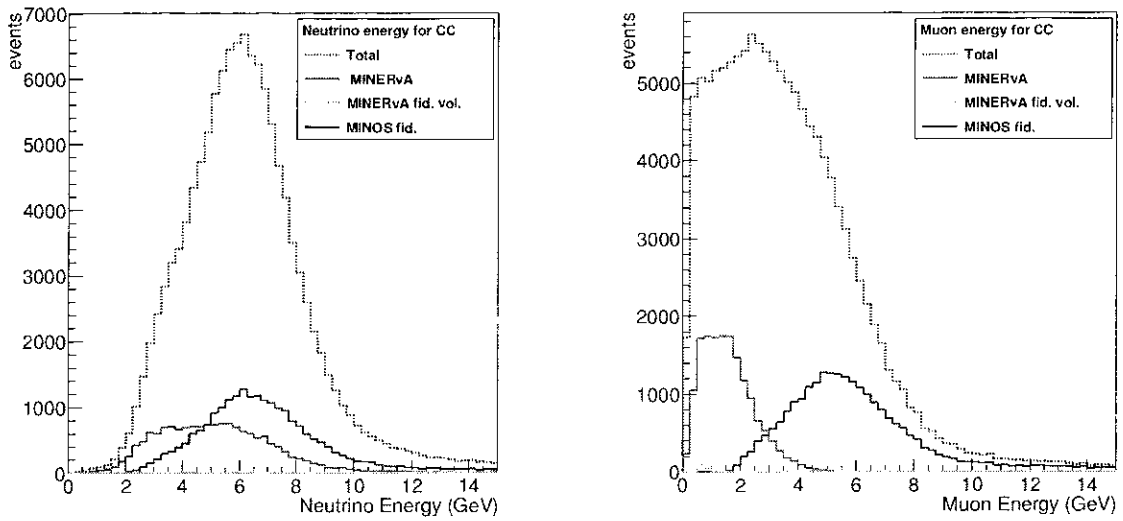

Figure 5.9: Events distributions for muons stopping in MINERνA . MINERνA fiducial volume and reaching MINOS fiducial region. Left: As a function of the neutrino energy. Right: As a function of the muon energy.

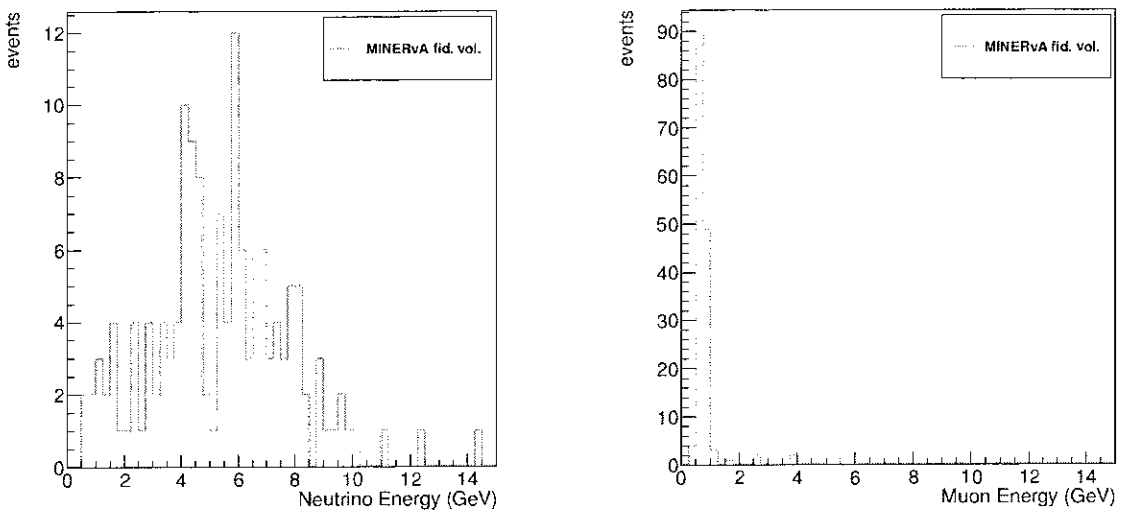

Figure 5.10: Events distributions for muons stopping in MINERνA fiducial volume. Left:As a function of the Neutrino energy. Right:As a function of the Muon energy.

Events distributions for muons stopping in MINERνA , muons stopping in fiducial MINERνA and muons reaching MINOS fiducial region, as a function of the neutrino energy and the muon energy, are shown in figure 5.9. Events distributions for muons stopping in the fiducial

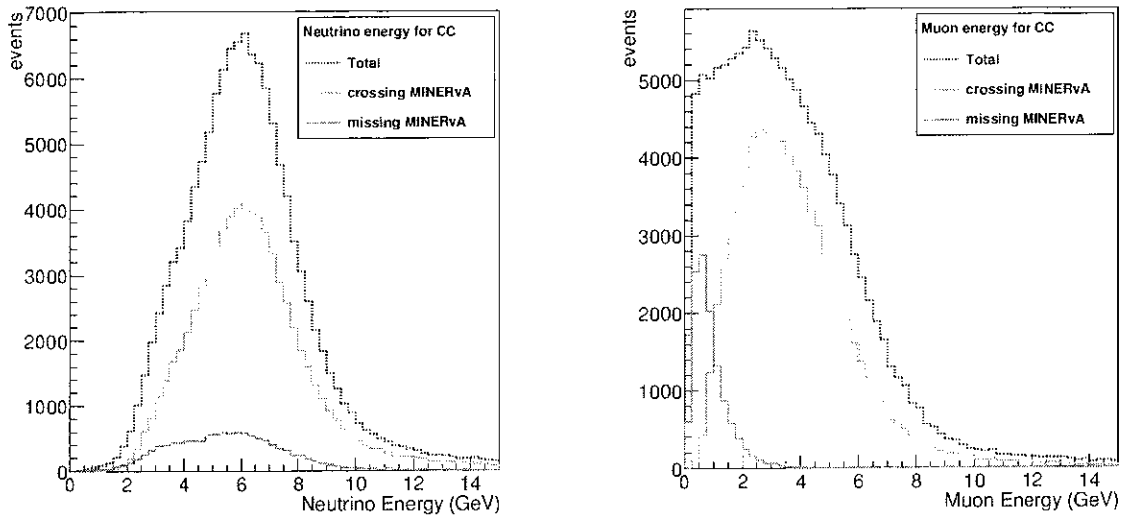

Figure 5.11: Events distributions for muons crossing and missing MINERνA . Left:As a function of the Neutrino energy. Right:As a function of the Muon energy.

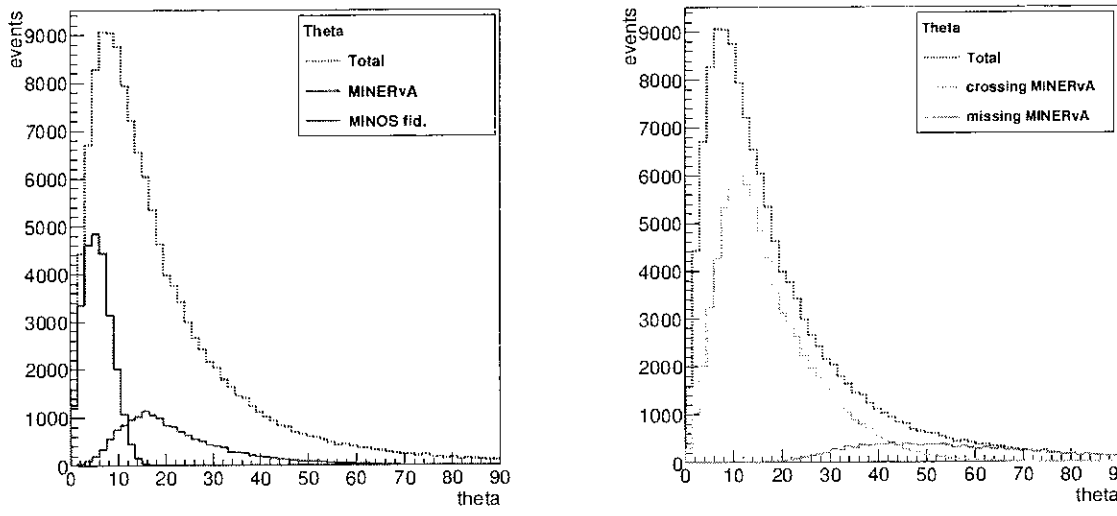

Figure 5.12: Events distributions for muons stopping in MINERνA , reaching MINOS fiducial region, crossing and missing MINERνA as a function of θ.

MINERνA are shown in an appropiate scale in Figure 5.10. Events for muons stopping in MINERνA produce more energetic hadrons than those events for muons reaching the MINOS fiducial region, as can be seen in Figure 5.9. Only the more energetic muons can go through the MINERνA detector and reach MINOS detector. The 12.92% of muons stop in MINERνA

and the 19.15% of the muons reach the MINOS fiducial region.

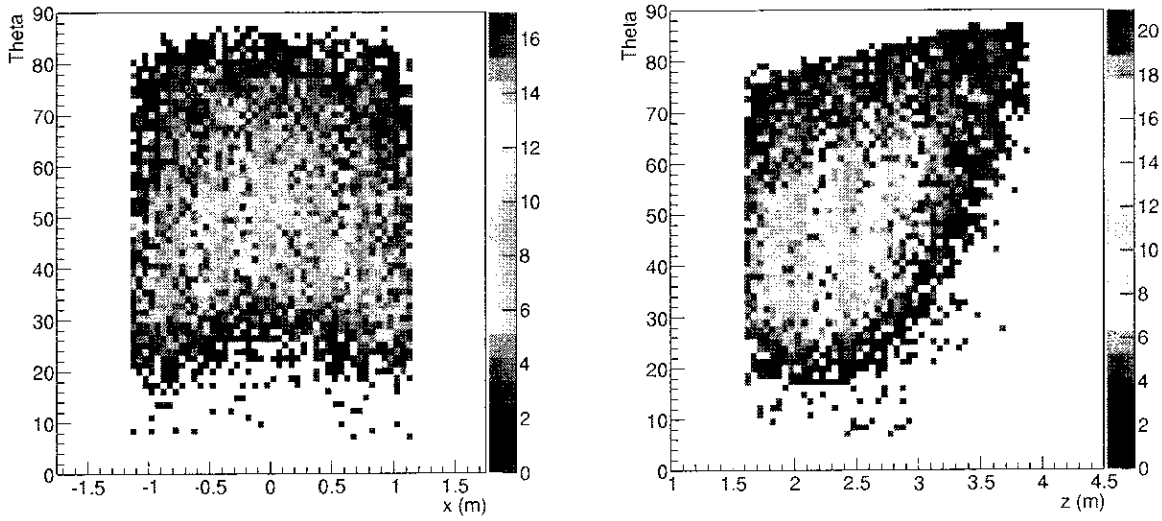

Figure 5.13: Events in the CAPTAIN volume for Muons missing MINERνA . Left:As a function of x coordenate. Right: As a function of z coordenate.

Figure 5.11 shows the events distributions for muons missing MINERνA and muons crossing MINERνA , as a function of the neutrino energy and the muon energy. Muons missing MINERνA category took into account the backward-going muons. Events for muons missing MINERνA produce more energetic hadrons than events for muons crossing MINERνA . The 10.53% of produced muons miss the MINERνA detector and 58.28% of muons cross the MINERνA detector. The muons that miss the MINERνA detector are less energetics than those muons crossing it.

Muons are produced at an angle θ with respect to the z axis of the MINERνA coordinate system. Events distributions as a function of θ for muons crossing MINERνA , missing MINERνA , stopping in MINERνA and reaching MINOS fiducial region are shown in Figure 5.12. The maximum θ angle around 18° for muons reaching MINOS agrees with previous studies [77], [86]. The wide θ distribution for muons missing MINERνA as a function of neutrino energy is reviewed in Figure 5.13 by plotting the location of these events in the CAPTAIN volume. It can be seen that events closer to the origin on the x axis have larger θ angles and events with higher z coordinate (closer to the MINERνA detector) have also larger θ angles. It follows that the wide θ angle distribution for muons missing MINERνA is due to the hexagonal shape of the MINERνA detector and the distance of the event to it.

Muon acceptance in a region of the detector is defined as the ratio between the muons reaching or stopping in this region to the total muons produced in the CAPTAIN volume.

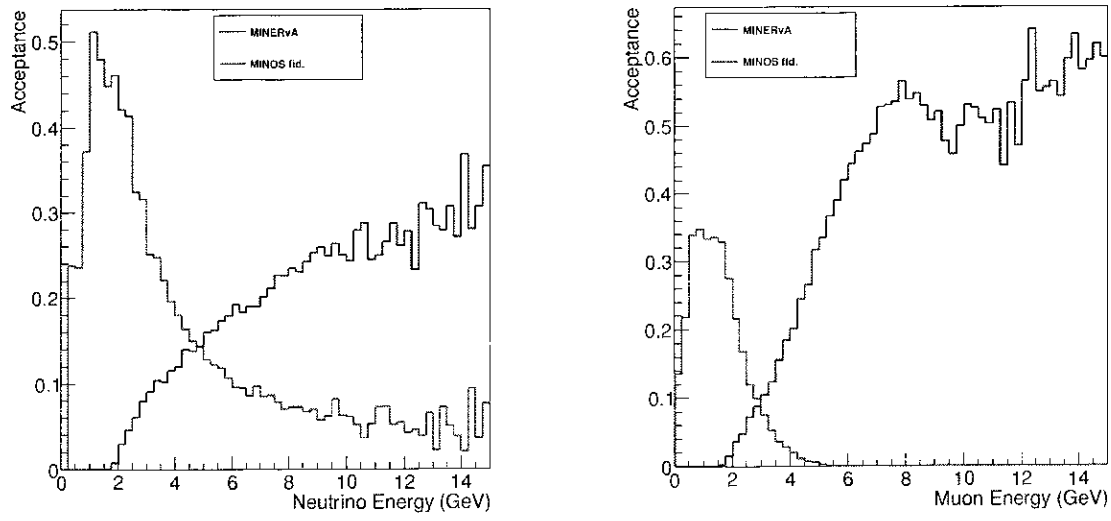

Figure 5.14: Acceptance of Muons in MINERνA and MINOS fiducial region. Left: As a function of the Neutrino energy. Right: As a function of Muon energy.

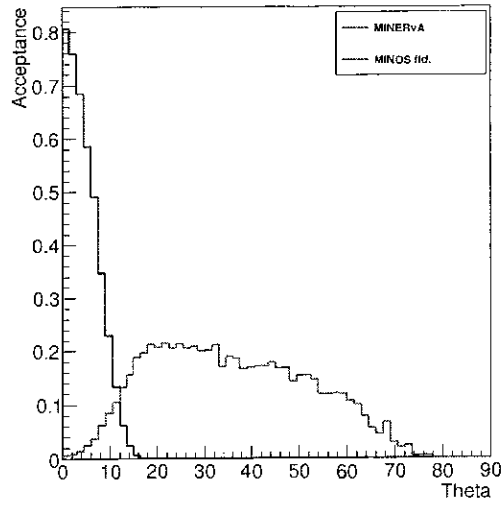

Figure 5.15: Acceptance of Muons in MINERνA and MINOS fiducial region as a function of θ.

The muon acceptances in MINERνA and the MINOS fiducial region, as a function of the neutrino and muon energy are shown in figure 5.14. As expected, higher neutrino energies are responsible for muon acceptance in the MINOS fiducial region. The Muon acceptances in MINERνA and MINOS fiducial region as a function of θ are shown in Figure 5.15. These acceptances confirm the maximum θ angle $\approx 18°$ for MINOS fiducial region and the wide

distribution for MINERrνA. A summary of the acceptances for all the muon categories are presented in Table 5.2.

Muon acceptances
MINOS→19.15%
MINERνA →12.02%
crossing→58.28%
missing→10.53%

Table 5.2: Summary of the muon acceptances.

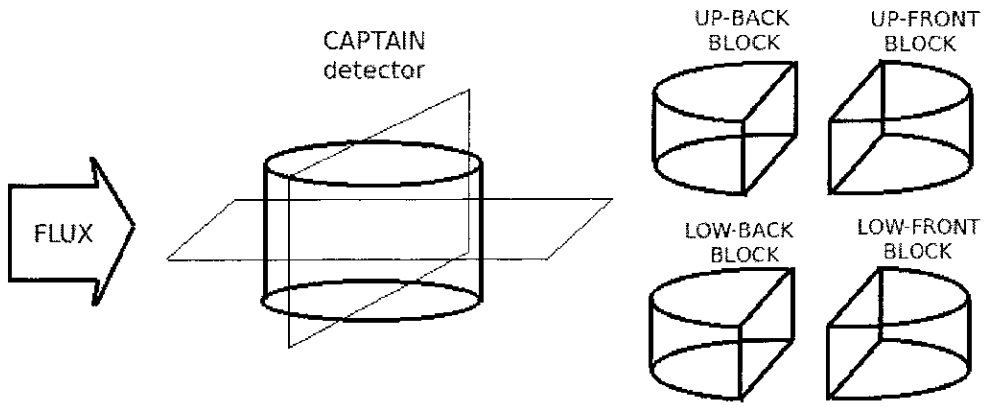

Figure 5.16: Division of CAPTAIN fiducial volume into 4 blocks. NuMI comes from the left.

Finally, CAPTAIN volume was divided in four blocks as shown in Figure 5.16. Muon acceptances in MINERνA and MINOS fiducial region as a function of the neutrino energy, muon energy and θ for all the four blocks have been obtained and are shown in Appendix C and Table 5.3 sumarizes the results.

The up-front block has most of the events and the low-back block has the fewest events. Front blocks have more events for muons stopping in MINERνA and reaching MINOS fiducial region than the back blocks. In general, each block has approximately the same number of events produced. The slight difference on the number of events observed between the up and low blocks might be consequence of the -58 *mrad* angle of the NuMI flux beam (Section 3.1) respect to the z axis on the zy plane of the MINERνA framework coordinate system.

UP-BACK	UP-FRONT
Events→ 25.51%×(Total events)	Events→ 25.68%×(Total events)
MINOS→18.41%×(up-back block events)	MINOS→21.15%×(up-front block events)
MINERνA →9.68%×(up-back block events)	MINERνA →14.44%×(up-front block events)
DOWN-BACK	DOWN-FRONT
Events→ 24.30%×(Total events)	Events→ 24.49%×(Total events)
MINOS→17.10%×(down-back block events)	MINOS→19.83%×(down-front block events)
MINERνA →9.84%×(down-back block events)	MINERνA →14.09%×(down-front block events)

Table 5.3: Acceptances in each block of CAPTAIN.

Chapter 6

Conclusions

Eight millions charged current neutrino interaction events generated by GENIE 2.8.4 were used to probe the CAPTAIN-MINERνA detector. A code was developed to visualize the composition of each module in the geometry.

The detector geometry was implemented in the MINERνA experiment framework in order to simulate the passage of the Muons produced in charged current neutrino interactions events occurring in the CAPTAIN fiducial volume and a code was developed to calculate the Muon Acceptances of the MINERνA main detector and MINOS ND.

The results can be summarized as follows

- events whose muons stop in the MINERνA main detector produce more energetic hadrons than the events whose muons reach MINOS, as shown in Figure 5.9.
- muons produced with higher energy reach MINOS ND as shown in Figure 5.9
- events whose muons miss the MINERνA main detector produce more energetic hadrons than events whose muons cross the MINERνA main detector as shown in Figure 5.11.
- muons that reaching MINOS ND are produced with a maximum angle θ of $\sim 18^{\circ}$ with respect to the z axis, in contrast to the wide distribution observed for muons that stop in the MINERνA main detector as shown in Figures 5.12 and 5.15.
- more muons reach MINOS ND than stop in the MINERνA main detector. Most of the muons cross both the MINERνA and MINOS ND and only a few miss the MINERνA main detector as shown in Table 5.2.
- muons that stop in the MINERνA main detector and and muons that reach MINOS ND are produced almost uniformly in the four sectors of the CAPTAIN detector. Muons produced in the front sectors are more likely to stop in MINERνA main detector because

these sectors are situated closer to the MINERνA detector. The observed slight difference between the production of muons in the upper and lower sectors, as shown in Table 5.3. may be due to the -58 *mrad* incidence angle of the NuMI beam into CAPTAIN.

Appendix A

Geometry probing

The plots used to check the CAPTAIN-MINERνA geometry are presented. The z coordenate values used to plot different sections of the geometry were taken from the MINERvA Wiki website [87].

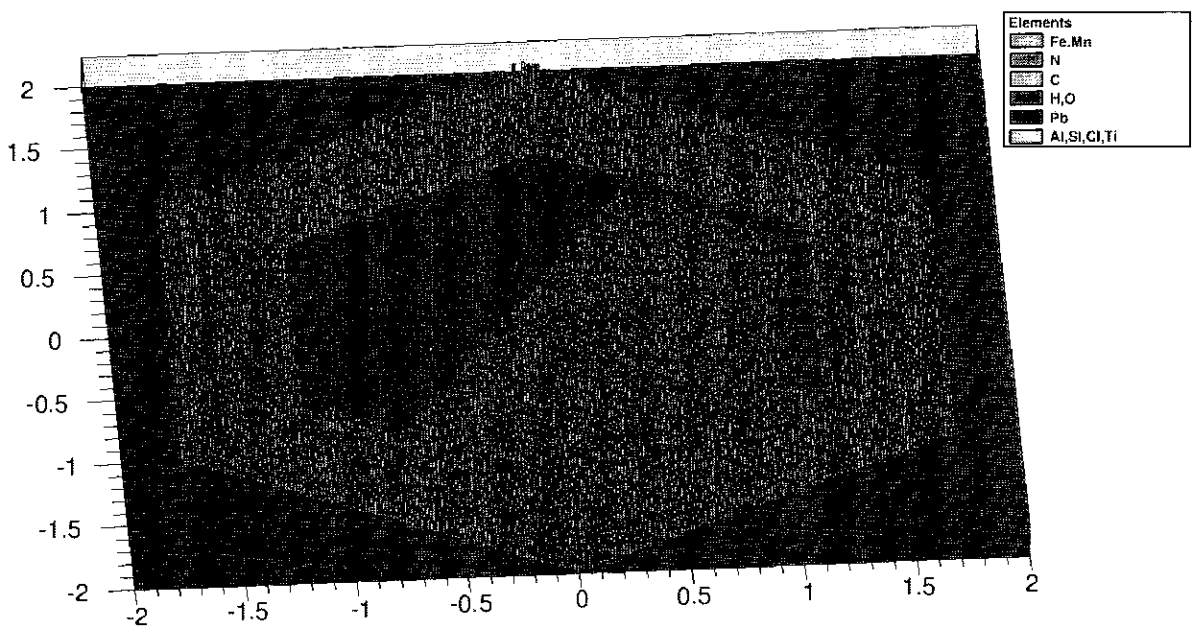

Figure A.1: First Nuclear target $4.446 < z < 4.51411$ $(meters)$

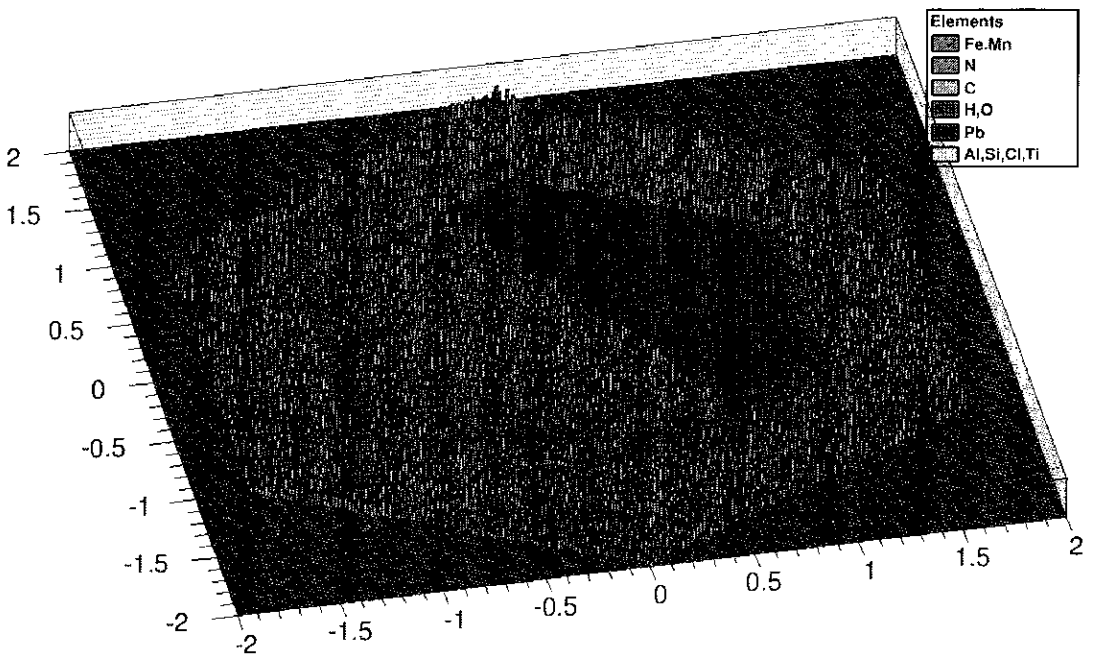

Figure A.2: Second Nuclear target $4.667 < z < 4.735$ $(meters)$

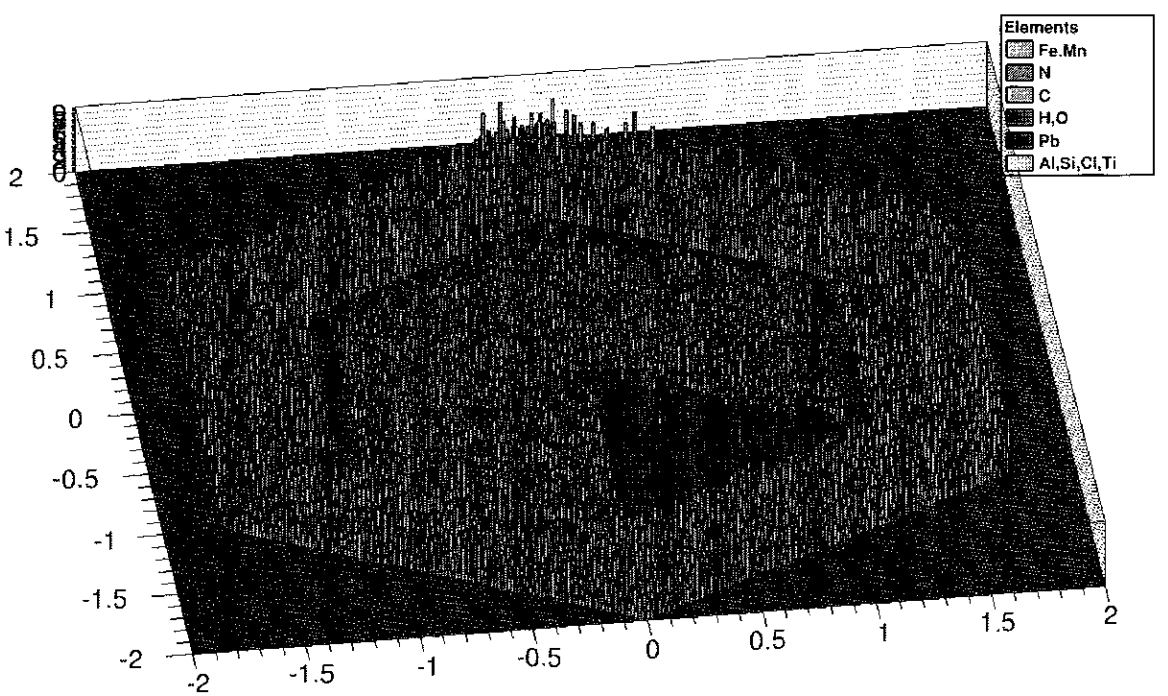

Figure A.3: Third Nuclear target $4.888 < z < 5.004$ $(meters)$

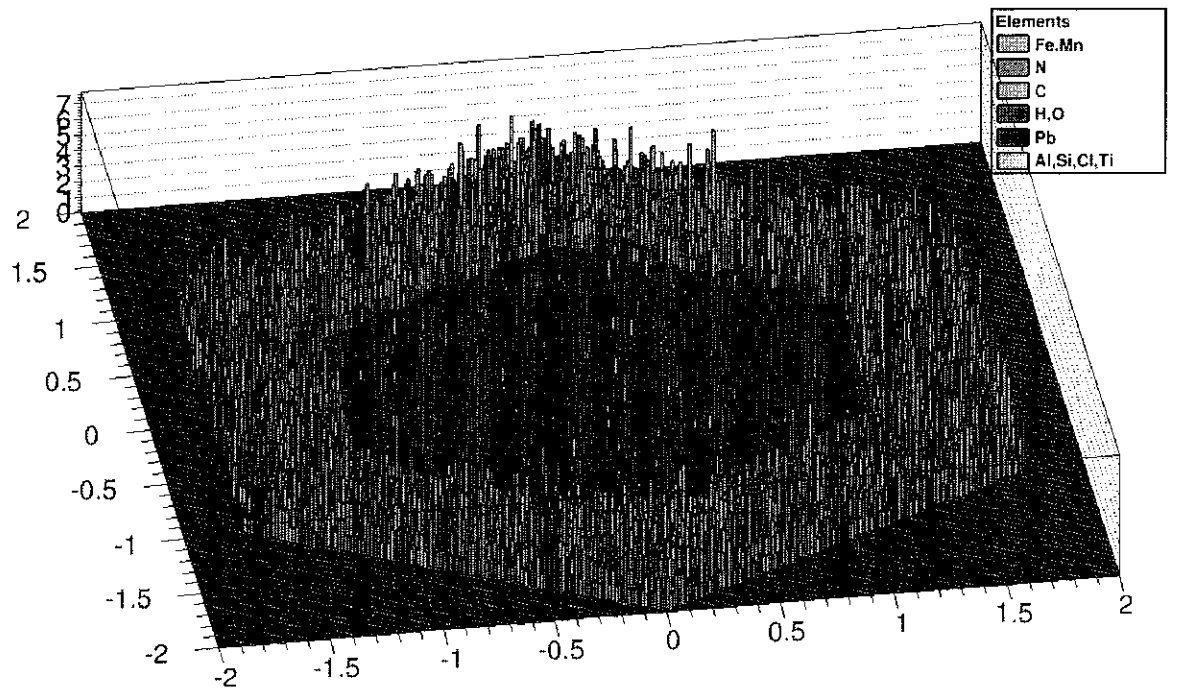

Figure A.4: Fourth Nuclear target $5.610 < z < 5.677$ $(meters)$

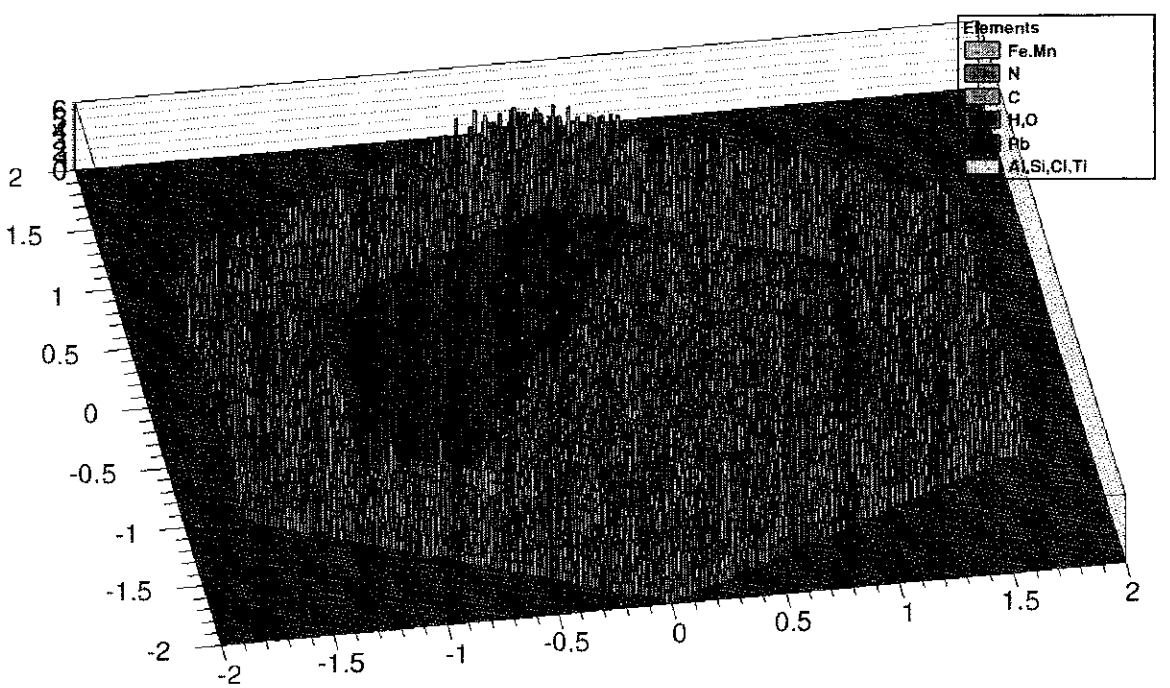

Figure A.5: Fifth Nuclear target $5.742 < z < 5.810$ $(meters)$

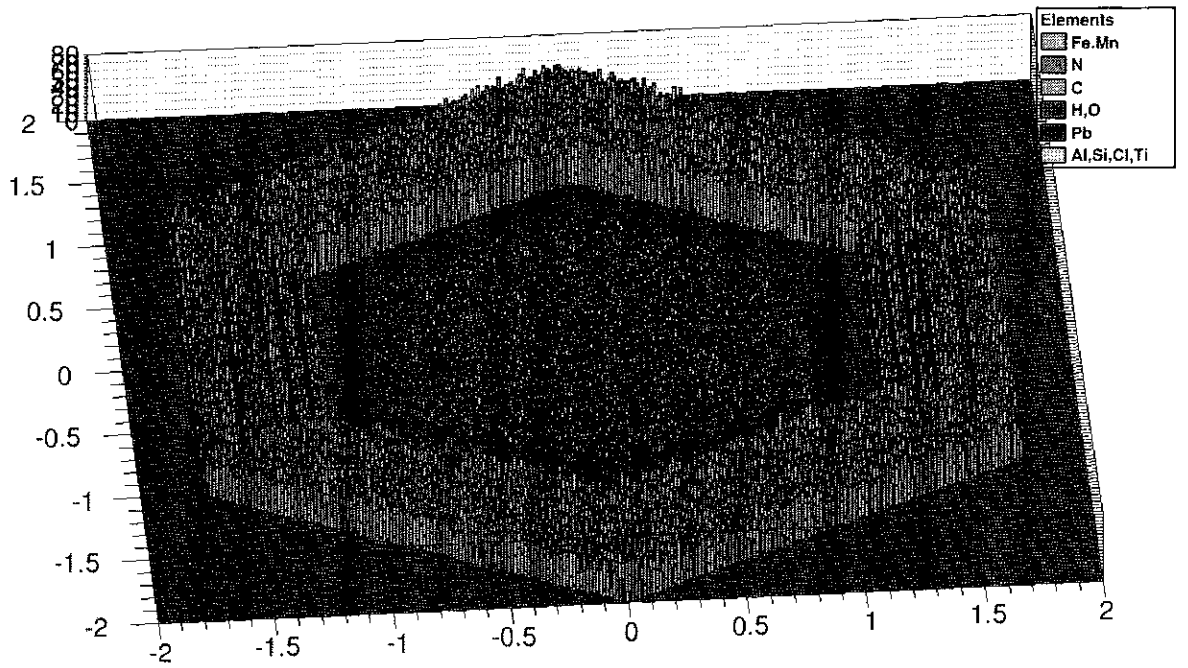

Figure A.6: MINERνA main detector $5.810 < z < 8.590$ $(meters)$

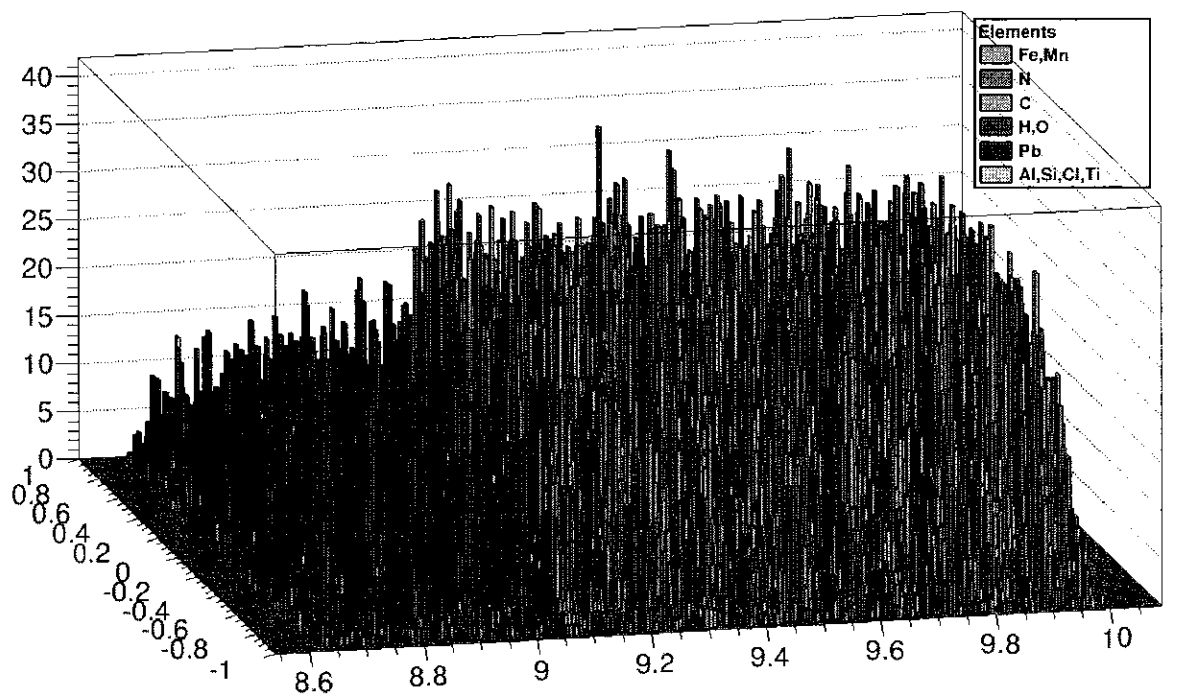

Figure A.7: Downstream Electromagnetic and Hadronic calorimeters region $8.614 < z < 10$ $(meters)$

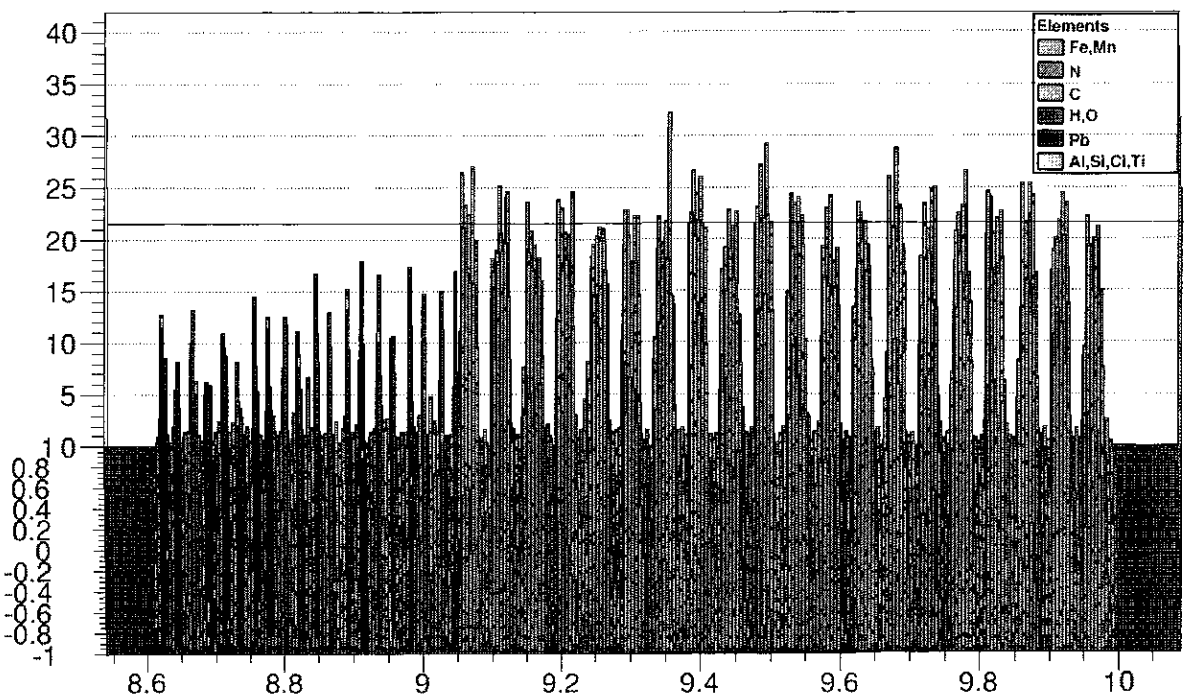

Figure A.8: Downstream Electromagnetic and Hadronic calorimeters region $8.614 < z < 10$ $(meters)$

Appendix B

Muon Acceptance code

The code developed to get the Muon accepntances is presented.

Listing B.1: Descriptive Caption Text

```
#include "iostream"
#include "TTree.h"
#include "TBranch.h"

using namespace std;


void testing()

{


        // diamater= 2.7
        // altitud= 1.9
        // default radius=1.2 , center=2.8 , -0.6<y<0.6

        bool isFiducial_Captain(double x, double y, double z)
        {
        const double radius=1.15;
        if(x*x + (z-2.75)*(z-2.75) < radius*radius & -0.8<y & y<0.8 ) return
            true;
        return false;
        }
```

```
// here, x and y is the x,y position of end of track
// w is the inner detector 'width' (2*apothem) is 2128.5mm  (DocDB
   226-v1)
// wich means absolute y length = 2.4572 and apothem = 1.06425 m
// only for track with end of track z pos > 10292.0 mm

// minerva hole volume -> (3.450/2)cos30=apothem (presentation)->
   (3.45)cos30=w=2.9877 ; begins z=4.29304 m; end z=9.9874 m (wiki
   modules)
// fiducial volume => w=2*0.85 m ; length not determined
// w=3.6


bool HexagonAccepted(double x, double y, double w)
{
double max = w/2;
double min = -w/2;
double pi=3.1415926535897;

double deltaphi = 60.0*(pi/180);
double phi = 0.0;
for (int i = 0; i < 3; ++i)
{
double xtmp = cos(phi)*x + sin(phi)*y;
phi += deltaphi;

if (xtmp < min || xtmp > max) return false;
}

 return true;

}



//For MINOS fiducial area: xm and ym is the coordinate of the track
   position
//(when the muon hit MINOS face/when it starts in MINOS). It is in
   Minerva coordinate.
//The muon  must stay in the fiducial area for 60 cm.

bool MinosAcceptedArea(double xm,double ym)
{
```

```
        bool pass_uv = false;
        double nu = (xm + ym)/sqrt(2.0); // converting to MINOS coord
        double nv = (-xm + ym)/sqrt(2.0); //converting to MINOS coord
        if( (nu > -1.340) && (nu < 1.160) &&
        (nv > -1.716) && (nv < 0.784) &&
        (xm < 1.481)){

        if(nu< -0.840 && nv< 0.284 ){
        pass_uv=true;
        }
        if(nu> -0.840 && nv> 0.284){
        pass_uv=true;
        }
        if(nu> -0.840  && nv< 0.284){
        pass_uv=true;
        }
        }
        return pass_uv;
        }


     TChain *f = new TChain("minerva","medium energy");

// With wall simulation and the 1 millons of events.
//      f->Add("/minerva/data/users/gianfred/
   mc_production_cm1_v10r8p8_complete_final_hastobe_endoftheworld/grid/
   central_value/minerva/dst/v10r8p8/00/00/00/71/
   SIM_minerva_00000071_0001_IDDDigits_DST_v10r8p4_v10r8p8.root");
//      f->Add("/minerva/data/users/gianfred/
   mc_production_cm1_v10r8p8_complete_final_hastobe_endoftheworld/grid/
   central_value/minerva/dst/v10r8p8/00/00/00/71/*.root");
//      f->Add("/minerva/data/users/gianfred/mc_production_complete_more/
   grid/central_value/minerva/dst/v10r8p8/00/00/00/81/*.root");
//      f->Add("/minerva/data/users/gianfred/mc_production_complete_more/
   grid/central_value/minerva/dst/v10r8p8/00/00/00/81/
   SIM_minerva_00000081_0001_IDDDigits_DST_v10r8p4_v10r8p8.root");
        f->Add("/minerva/data/users/gianfred/mc_production_complete_more/
           grid/central_value/minerva/dst/v10r8p8/00/00/00/81/*.root");

     double mc_traj_point_x[600][5];
     double mc_traj_point_y[600][5];
     double mc_traj_point_z[600][5];
     double mc_traj_point_E[600][5];
     double mc_traj_point_px[600][5];
```

```
double mc_traj_point_py[600][5];
double mc_traj_point_pz[600][5];
int mc_traj_pdg[600];
int mc_traj_npoints[600];
int n_mc_trajectories;

int mc_int_current[1];
int mc_int_targetZ[1];
int mc_int_FSLepton[1];
int  mc_int_channel[1];
int mc_int_FSPdg[1][30];
double mc_int_FSParticlesE[1][30];
double mc_int_vtx[1][4];
double mc_int_FSLepton4p[1][4];
double mc_int_incomingE[1];

f->SetBranchAddress("mc_int_targetZ",&mc_int_targetZ);
f->SetBranchAddress("mc_int_vtx",&mc_int_vtx);
f->SetBranchAddress("mc_int_FSLepton",&mc_int_FSLepton);
f->SetBranchAddress("mc_int_incomingE",&mc_int_incomingE);
f->SetBranchAddress("mc_int_FSLepton4p",&mc_int_FSLepton4p);
f->SetBranchAddress("mc_int_channel",&mc_int_channel);
f->SetBranchAddress("mc_int_current",&mc_int_current);

f->SetBranchAddress("mc_traj_point_px",&mc_traj_point_px);
f->SetBranchAddress("mc_traj_point_py",&mc_traj_point_py);
f->SetBranchAddress("mc_traj_point_pz",&mc_traj_point_pz);
f->SetBranchAddress("mc_traj_point_E",&mc_traj_point_E);
f->SetBranchAddress("mc_traj_point_x",&mc_traj_point_x);
f->SetBranchAddress("mc_traj_point_y",&mc_traj_point_y);
f->SetBranchAddress("mc_traj_point_z",&mc_traj_point_z);
f->SetBranchAddress("mc_traj_pdg",&mc_traj_pdg);
f->SetBranchAddress("mc_traj_npoints",&mc_traj_npoints);
f->SetBranchAddress("n_mc_trajectories",&n_mc_trajectories);



TH1F *h1 = new TH1F("h1"," VERTEX ; y (mm) ; events",100,-4,4); //end
   muons from captain and not
h1->SetXTitle("y (m)");
h1->SetYTitle("events");

 TH1F *h2 = new TH1F("h2","v energy",60,0,15); //mc_incomingE o E
 h2->SetXTitle("Neutrino Energy (GeV)");
```

```
 h2->SetYTitle("events");

 TH1F *h3 = new TH1F("h3","u energy (GeV)",60,0,15); //muon energy
 h3->SetXTitle("Muon Energy (GeV)");
 h3->SetYTitle("events");


TH1F *h4 = new TH1F("h4","thetaY",240,-180,180); //
h4->SetXTitle("thetaY");
h4->SetYTitle("events");

TH1F *h5 = new TH1F("h5","theta",60,0,90);
h5->SetXTitle("theta");
h5->SetYTitle("events");


  TH1F *h6 = new TH1F("h6"," VERTEX ; x (mm) ; events", 100,-4,4); //end
      muons from captain and not
  h6->SetXTitle("x (m)");
  h6->SetYTitle("events");


 TH1F *h7 = new TH1F("h7","ENERGY ; Neutrino Energy (GeV); events
    ",60,0,15); //mc_incomingE o E
 h7->SetXTitle("Neutrino Energy (GeV)");
 h7->SetYTitle("events");


 TH1F *h8 = new TH1F("h8","U ENERGY; Muon Energy (GeV); events",60,0,15)
    ; //muon energy
 h8->SetXTitle("Muon Energy (GeV)");
 h8->SetYTitle("events");


 TH1F *h9 = new TH1F("h9","thetaY; events",240,-180,180);
 h9->SetXTitle("thetaY");
 h9->SetYTitle("events");

TH1F *h10 = new TH1F("h10","theta",60,0,90);
h10->SetXTitle("theta");
h10->SetYTitle("events");

 TH1F *h11 = new TH1F("events muon","VERTEX MUON ; z (m); events
    ",10000,9,15); //mc_incomingE o E
```

```
h11->SetXTitle("z (m)");
h11->SetYTitle("events");


TH1F *h12 = new TH1F("h12","ENERGY ; Neutrino Energy (GeV); events
   ",60,0,15);
h12->SetXTitle("Neutrino Energy (GeV)");
h12->SetYTitle("events");


TH1F *h13 = new TH1F("h13","U ENERGY; Muon Energy (GeV); events
   ",60,0,15); //muon energy
h13->SetXTitle("Muon Energy (GeV)");
h13->SetYTitle("events");

TH1F *h131 = new TH1F("h131","U ENERGY; Muon Energy (GeV); events
   ",60,0,15); //muon energy
h131->SetXTitle("Muon Energy (GeV)");
h131->SetYTitle("events");

TH1F *h14 = new TH1F("h14","thetaY; events",240,-180,180);
h14->SetXTitle("thetaY");
h14->SetYTitle("events");


   TH1F *h15 = new TH1F("h15","events",60,0,90);
   h15->SetXTitle("theta");
   h15->SetYTitle("events");


  TH1F *h17 = new TH1F("h17","ENERGY ; Neutrino Energy (GeV); events
     ",60,0,15); //mc_incomingE o E->SetXTitle("Neutrino Energy (GeV)")
     ;
  h17->SetXTitle("Neutrino Energy (GeV)");
  h17->SetYTitle("events");


TH1F *h18 = new TH1F("h18","U ENERGY; Muon Energy (GeV); events
   ",60,0,15); //muon energy
h18->SetXTitle("Muon Energy (GeV)");
h18->SetYTitle("events");


    TH1F *h19 = new TH1F("u angle 1","thetaY; events",240,-180,180);
```

```
h19->SetXTitle("thetaY");
h19->SetYTitle("events");

TH1F *h20 = new TH1F("h20","events",60,0,90);
h20->SetXTitle("theta");
h20->SetYTitle("events");


  TH1F *hvE = new TH1F("hvE","ENERGY ; Neutrino Energy (GeV); events
     ", 60 ,0,15);
     hvE->SetXTitle("Neutrino Energy (GeV)");
     hvE->SetYTitle("events");


     TH1F *huE = new TH1F("huE","U ENERGY; Muon Energy (GeV); events
        ",60,0,15);
     huE->SetXTitle("Muon Energy (GeV)");
     huE->SetYTitle("events");


     TH1F *hbvE = new TH1F("hbvE","ENERGY ; Neutrino Energy (GeV);
        events",60,0,15);
     hbvE->SetXTitle("Energy (GeV)");
     hbvE->SetYTitle("events");


     TH1F *hbuE = new TH1F("hbuE","U ENERGY; Muon Energy (GeV);
        events",60,0,15);
     hbuE->SetXTitle("Energy (GeV)");
     hbuE->SetYTitle("events");

TH1F *hbthetaY = new TH1F("hbthetaY","events",245,-190,190);
hbthetaY->SetXTitle("thetaY");
hbthetaY->SetYTitle("events");

TH1F *hbtheta = new TH1F("hbtheta","events",60,0,90);
hbtheta->SetXTitle("theta");
hbtheta->SetYTitle("events");


TH2F *hminos = new TH2F("hminos","events",200,-4,4,200,-4,4);
hminos->SetXTitle("x (m)");
hminos->SetYTitle("y (m)");
```

```
TH2F *hmuons = new TH2F("hmuons","events",200,-4,4,200,-4,4);
hmuons->SetXTitle("x (m)");
hmuons->SetYTitle("y (m)");

TH2F *hlmzy1 = new TH2F("hlmzy1","hlmzy1",900,0,27,900,-11,11);
hlmzy1->SetXTitle("z (m)");
hlmzy1->SetYTitle("y (m)");

TH2F *hlmzx1 = new TH2F("hlmzx1","hlmzx1",900,0,27,900,-11,11);
hlmzx1->SetXTitle("z (m)");
hlmzx1->SetYTitle("x (m)");

TH2F *hfmxy1 = new TH2F("hfmxy1","hlmxy1",900,-11,11,900,-11,11);
hfmxy1->SetXTitle("x (m)");
hfmxy1->SetYTitle("y (m)");

TH2F *hlmzy2 = new TH2F("hlmzy2","hlmzy2",900,0,27,900,-11,11);
hlmzy2->SetXTitle("z (m)");
hlmzy2->SetYTitle("y (m)");

TH2F *hlmzx2 = new TH2F("hlmzx2","hlmzx2",900,0,27,900,-11,11);
hlmzx2->SetXTitle("z (m)");
hlmzx2->SetYTitle("x (m)");

TH2F *hfmxy2 = new TH2F("hfmxy2","hfmxy2",900,-11,11,900,-11,11);//
   hist front (minerva detector)
hfmxy2->SetXTitle("x (m)");
hfmxy2->SetYTitle("y (m)");


TH2F *hlmzy3 = new TH2F("hlmzy3","hlmzy3",900,0,27,900,-11,11);
hlmzy3->SetXTitle("z (m)");
hlmzy3->SetYTitle("y (m)");

TH2F *hlmzx3 = new TH2F("hlmzx3","hlmzx3",900,0,27,900,-11,11);
hlmzx3->SetXTitle("z (m)");
hlmzx3->SetYTitle("x (m)");

TH2F *hfmxy3 = new TH2F("hfmxy3","hlmxy3",900,-11,11,900,-11,11);
hfmxy3->SetXTitle("x (m)");
hfmxy3->SetYTitle("y (m)");

TH2F *hfmxy31 = new TH2F("hfmxy31","hlmxy31",900,-11,11,900,-11,11);
hfmxy31->SetXTitle("x (m)");
```

```
    hfmxy31->SetYTitle("y (m)");

    TH2F *hfmxy32 = new TH2F("hfmxy32","hlmxy32",900,-11,11,900,-11,11);
    hfmxy32->SetXTitle("x (m)");
    hfmxy32->SetYTitle("y (m)");



    TH2F *hlmzy4 = new TH2F("hlmzy4","hlmzy4",900,0,27,900,-11,11);
    hlmzy4->SetXTitle("z (m)");
    hlmzy4->SetYTitle("y (m)");

    TH2F *hlmzx4 = new TH2F("hlmzx4","hlmzx4",900,0,27,900,-11,11);
    hlmzx4->SetXTitle("z (m)");
    hlmzx4->SetYTitle("x (m)");

    TH2F *hfmxy4 = new TH2F("hfmxy4","hlmxy4",900,-11,11,900,-11,11);
    hfmxy4->SetXTitle("x (m)");
    hfmxy4->SetYTitle("y (m)");

    TH2F *hfmxy41 = new TH2F("hfmxy41","hlmxy41",900,-11,11,900,-11,11);
    hfmxy41->SetXTitle("x (m)");
    hfmxy41->SetYTitle("y (m)");


    TH2F *hfmxy42 = new TH2F("hfmxy42","hlmxy42",900,-11,11,900,-11,11);
    hfmxy42->SetXTitle("x (m)");
    hfmxy42->SetYTitle("y (m)");

    TH2F *hfmzx43 = new TH2F("hfmzx43","hfmzx43",900,0,27,900,-11,11);
    hfmzx43->SetXTitle("z (m)");
    hfmzx43->SetYTitle("x (m)");


 TH1F *h22 = new TH1F("h22","Neutrino Energy (GeV); events",60,0,15);
 h22->SetXTitle("Neutrino Energy (GeV)");
 h22->SetYTitle("events");

 TH1F *h23 = new TH1F("h23","Muon Energy (GeV); events",60,0,15);
 h23->SetXTitle("Muon Energy (GeV)");
 h23->SetYTitle("events");


TH1F *h24 = new TH1F("h24","z1 from CAPTAIN", 100,-11,25);
```

```
h24->SetXTitle("z (m)");
h24->SetYTitle("events");

 TH1F *hmtE = new TH1F("hmtE","ENERGY ; Neutrino Energy (GeV); events",
    100 ,0,15);
 hmtE->SetXTitle("Neutrino Energy (GeV)");
 hmtE->SetYTitle("events");


 TH1F *hmtuE = new TH1F("hmtuE","U ENERGY; Muon Energy (GeV); events
    ",100,0,15);
 hmtuE->SetXTitle("Muon Energy (GeV)");
 hmtuE->SetYTitle("events");

 TH1F *hfmE = new TH1F("hfmE","ENERGY ; Neutrino Energy (GeV); events
    ",60,0,15);
 hfmE->SetXTitle("Neutrino Energy (GeV)");
 hfmE->SetYTitle("events");

 TH1F *hfmuE = new TH1F("hfmuE","U ENERGY; Muon Energy (GeV); events
    ",60,0,15);
 hfmuE->SetXTitle("Muon Energy (GeV)");
 hfmuE->SetYTitle("events");

 TH1F *hfmuE1 = new TH1F("hfmuE1","U ENERGY; Muon Energy (GeV); events
    ",60,0,15);
 hfmuE1->SetXTitle("Muon Energy (GeV)");
 hfmuE1->SetYTitle("events");


TH1F *htheta = new TH1F("htheta","theta",60,0,90);
htheta->SetXTitle("theta");
htheta->SetYTitle("events");

     TH1F *hacctheta = new TH1F("hacctheta","",60,0,90);
     hacctheta->SetXTitle("theta");
     hacctheta->SetYTitle("acceptance");


TH1F *hsmmtheta = new TH1F("hsmmtheta","theta",60,0,90);
hsmmtheta->SetXTitle("theta");
hsmmtheta->SetYTitle("events");
```

```
TH1F *hsvE = new TH1F("hsvE","neutrino energies sum",60,0,15);
hsvE->SetXTitle("Neutrino Energy (GeV)");
hsvE->SetYTitle("events");

TH1F *hsuE = new TH1F("hsuE","muon energies sum",60,0,15);
hsuE->SetXTitle("Muon Energy (GeV)");
hsuE->SetYTitle("events");

 TH1F *hsmmvE = new TH1F("hsmmvE","ENERGY ; Neutrino Energy (GeV);
    events",60,0,15); //mc_incomingE o E
 hsmmvE->SetXTitle("Neutrino Energy (GeV)");
 hsmmvE->SetYTitle("events");

 TH1F *haccvE = new TH1F("haccvE","ENERGY ; Neutrino Energy (GeV);
    events",60,0,15); //mc_incomingE o E
 haccvE->SetXTitle("Neutrino Energy (GeV)");
 haccvE->SetYTitle("acceptance");



    TH1F *hstheta = new TH1F("hstheta","theta sum",60,0,90);
hstheta->SetXTitle("theta");
hstheta->SetYTitle("events");

    TH1F *hfinaluE = new TH1F("hfinaluE","final muon energy distribution
       ",60,0,15);
    hfinaluE->SetXTitle("Muon Energy (GeV)");
    hfinaluE->SetYTitle("events");

    TH1F *hbeguE = new TH1F("hbeguE","begining muon energy distribution
       ",60,0,15);
    hbeguE->SetXTitle("Muon Energy (GeV)");
    hbeguE->SetYTitle("events");


    TH2F *hfidminzx = new TH2F("hfidminzx","hfidminzx
       ",900,1,11,900,-3,3);
    hfidminzx->SetXTitle("z (m)");
    hfidminzx->SetYTitle("x (m)");

    TH2F *hfidminzy = new TH2F("hfidminzy","hfidminzy
```

```
    ",900,1,11,900,-3,3);
hfidminzy->SetXTitle("z (m)");
hfidminzy->SetYTitle("y (m)");

TH2F *hfidminxy = new TH2F("hfidminxy","hfidminxy
    ",900,-11,11,900,-11,11);
hfidminxy->SetXTitle("x (m)");
hfidminxy->SetYTitle("y (m)");

TH2F *hfidminxy1 = new TH2F("hfidminxy1","hfidminxy1
    ",900,-3,3,900,-3,3);
hfidminxy1->SetXTitle("x (m)");
hfidminxy1->SetYTitle("y (m)");

TH1F *hprobfidmin= new TH1F("hprobfidmin","hprobfidmin",60,0,15);
hprobfidmin->SetXTitle("Muon Energy (GeV)");
hprobfidmin->SetYTitle("Probability");

TH1F *hprobmin= new TH1F("hprobmin","hprobmin",60,0,15);
hprobmin->SetXTitle("Muon Energy (GeV)");
hprobmin->SetYTitle("Probability");

TH1F *hprobminos= new TH1F("hprobminos","hprobminos",60,0,15);
hprobminos->SetXTitle("Muon Energy (GeV)");
hprobminos->SetYTitle("Probability");

TH1F *haccthetaminerva=new TH1F("haccthetaminerva","haccthetaminerva
    ",60,0,90);
haccthetaminerva->SetXTitle("Theta");
haccthetaminerva->SetYTitle("Acceptance");

TH1F *haccthetaminos=new TH1F("haccthetaminos","haccthetaminos
    ",60,0,90);
haccthetaminos->SetXTitle("Theta");
haccthetaminos->SetYTitle("Acceptance");

TH1F *haccuEminerva=new TH1F("haccuEminerva","haccuEminerva
    ",60,0,15);
haccuEminerva->SetXTitle("Muon Energy (GeV)");
haccuEminerva->SetYTitle("Acceptance");

TH1F *haccuEminos=new TH1F("haccuEminos","haccuEminos",60,0,15);
haccuEminos->SetXTitle("Muon Energy (GeV)");
haccuEminos->SetYTitle("Acceptance");
```

```
TH1F *haccvEminerva=new TH1F("haccvEminerva","haccvEminerva
    ",60,0,15);
haccvEminerva->SetXTitle("Neutrino Energy (GeV)");
haccvEminerva->SetYTitle("Acceptance");

TH1F *haccvEminos=new TH1F("haccvEminos","haccvEminos",60,0,15);
haccvEminos->SetXTitle("Neutrino Energy (GeV)");
haccvEminos->SetYTitle("Acceptance");

TH2F *hcapzy = new TH2F("hcapzy","hcapzy",200,0,5,200,-2.5,2.5);
hcapzy->SetXTitle("z (m)");
hcapzy->SetYTitle("y (m)");

TH2F *hcapzx = new TH2F("hcapzx","hcapzx",200,0,5,200,-2.5,2.5);
hcapzx->SetXTitle("z (m)");
hcapzx->SetYTitle("x (m)");

TH2F *hthetacapz = new TH2F("hthetacapz","hthetacapz
    ",70,1,4.5,70,0,90);
hthetacapz->SetXTitle("z (m)");
hthetacapz->SetYTitle("Theta");

TH2F *hthetacapx = new TH2F("hthetacapx","hthetacapzx
    ",70,-1.75,1.75,70,0,90);
hthetacapx->SetXTitle("x (m)");
hthetacapx->SetYTitle("Theta");


ofstream outputFile1;
outputFile1.open("info.txt");

int w=0;
int events;

int q=0;
int allmuons;

int theminos=0;
int MINOS;

int theminerva=0;
int MINERvA;
```

```
int thefiducialminerva=0;
int FIDUCIALMINERvA;

int thecrossing=0;
int CRDSSINGMINERvA;

int themissing=0;
int MISSINGMINERvA;

int thebetween=0;
int BETWEEN;


     Int_t nentries = f->GetEntries();
     for (int i = 0; i < nentries; i++)
        {
        f->GetEntry(i);

        if (mc_int_targetZ[0]==18)
        {

        for (int j=0;j<30;++j){
                if(mc_traj_pdg[j]==13){

                int point=(mc_traj_npoints[j]-1);
                double t=180/3.1416 ;

                double px0=1e-3*mc_int_FSLepton4p[0][0];
                double py0=1e-3*mc_int_FSLepton4p[0][1];
                double pz0=1e-3*mc_int_FSLepton4p[0][2];
                double px=1e-3*mc_traj_point_px[j][0];
                double py=1e-3*mc_traj_point_py[j][0];
                double pz=1e-3*mc_traj_point_pz[j][0];

                double P=sqrt((px0*px0)+(py0*py0)+(pz0*pz0));
                double theta=t*acos(pz0/P) ;

                double uE=1e-3*mc_int_FSLepton4p[0][3];
                double E=1e-3*mc_int_incomingE[0];

                double x1=1e-3*mc_traj_point_x[j][point];
                double y1=1e-3*mc_traj_point_y[j][point];
                double z1=1e-3*mc_traj_point_z[j][point];
```

```
                double x=1e-3*mc_traj_point_x[j][0];
                double y=1e-3*mc_traj_point_y[j][0];
                double z=1e-3*mc_traj_point_z[j][0];

                double d=1e-3*mc_traj_point_E[j][point];



        if ((isFiducial_Captain(x,y,z)==true) && (mc_int_current
            [0]==1) && (px==px0) && (py==py0) && (pz==pz0))
          {

                ++w;

                hcapzy->Fill(z,y);
                hcapzx->Fill(z,x);
                hvE->Fill(E);
                huE->Fill(uE);
                h24->Fill(z1);
                htheta->Fill(theta);
        // Additional plot x range , y range and x1y1 proyection of
            the final points, and also
        // the z1 position on the hexagon shadow for z1>10.

//              if(z1>10)
//                      {

//                      hmuons->Fill(x1,y1);
//                      h1->Fill(y1);
//                      h6->Fill(x1);

//                      }

        // End muons in MINERvA ( end of MINERvA at 10.25)


                if ((HexagonAccepted(x1,y1,3.46)==true) && (4.28<z1)
                     && (z1<10) && (0<pz0)  )
                {
                ++q;
                ++theminerva;

                h2->Fill(E);
```

```
                    h3->Fill(uE);
//                  h4->Fill(thetaY);
                    h5->Fill(theta);
                    hlmzy1->Fill(z1,y1);
                    hlmzx1->Fill(z1,x1);
                    hfmxy1->Fill(x1,y1);

                    }


                // End muons in fiducial MINERvA

                    if ((HexagonAccepted(x1,y1,1.7)==true) && (5.990<z1)
                        && (z1<8.340)  && (0<pz0))
                    {

                    ++thefiducialminerva;


                    hfmE->Fill(E);
                    hfmuE->Fill(uE);
                    hfmuE1->Fill(uE);
                    hfidminzx->Fill(z1,x1);
                    hfidminzy->Fill(z1,y1);
                    hfidminxy->Fill(x1,y1);
                    hfidminxy1->Fill(x1,y1);
                    }

                // End muons between virtual plane and minerva limit


                    if ((HexagonAccepted(x1,y1,3.46)==true) && (10<z1)
                       && (z1<10.302) && (0<pz0))
                    {

                    ++q;
                    ++thecrossing;
                    ++thebetween;

                    h12->Fill(E);
                    h13->Fill(uE);
                    h15->Fill(theta);

                    }
```

```
                // End Muons reaching MINOS

                        if((HexagonAccepted(x1,y1,3.46)==true) && (10.302<z1
                           ) && (0<pz0) )
                        {
                                double zf=13 ;

                                double y4=((zf-z)*(y1-y)/(z1-z))+y;
                                double x4=((zf-z)*(x1-x)/(z1-z))+x;

//                              double y2=((zf-z1)*(b)/(c))+y1;
//                              double x2=((zf-z1)*(a)/(c))+x1;

                                hfinaluE->Fill(d);
                                hbeguE->Fill(uE);

                                //Other MINOS test  x4,y4. Line coming from
                                   MINERvA

/*                              if (MinosAcceptedArea(x4,y4) == true)
                                {
                                                h7->Fill(E);
                                                h8->Fill(uE);
                                                h9->Fill(thetaY);
                                                h10->Fill(theta);


                                }
*/
                // End Muons reaching MINOS fiducial region
                                if (MinosAcceptedArea(x4,y4) == true)
                                {

                                                ++q;
                                                ++theminos;


                                                h7->Fill(E);
                                                h8->Fill(uE);
//                                              h9->Fill(thetaY);
                                                h10->Fill(theta);
                                                h1mzy2->Fill(z1,y1);
                                                h1mzx2->Fill(z1,x1);
```

```
                                        hfmxy2->Fill(x4,y4);

                        }


                        // Some of them considered crossing

                        if (MinosAcceptedArea(x4,y4)==false)
                        {

                                ++q;
                                ++thecrossing;

                                h12->Fill(E);
                                h13->Fill(uE);
//                              h14->Fill(thetaY);
                                h15->Fill(theta);
                                hlmzy3->Fill(z1,y1);
                                hlmzx3->Fill(z1,x1);
                                hfmxy3->Fill(x1,y1);
                                hfmxy32->Fill(x4,y4);
                                h131->Fill(uE);
                        }

                        // Plotting considering the hole hexagonal
                           area

                        if(HexagonAccepted(x4,y4,3.46)==true);
                        {
                                h22->Fill(E);
                                h23->Fill(uE);

                        }

                }

        // Considering end points outside DETECTOR


                if((HexagonAccepted(x1,y1,3.46)==false) || (z1
                   <4.28))
                        {
```

```
                        double y3=((4.28-z)*(y1-y)/(z1-z))+y;
                        double x3=((4.28-z)*(x1-x)/(z1-z))+x;


        // Plotting tracks crossing MINERvA

                                        if((HexagonAccepted(x3,y3
                                            ,3.46)==true) && (z1
                                            >4.28) && (0<pz0) )
                                                {

                                                ++q;
                                                ++thecrossing;

                                                h12->Fill(E);
                                                h13->Fill(uE);
//                                              h14->Fill(thetaY);
                                                h15->Fill(theta);
                                                hlmzy3->Fill(z1,y1);
                                                hlmzx3->Fill(z1,x1);
                                                hfmxy3->Fill(x1,y1);
                                                hfmxy31->Fill(x1,y1)
                                                    ;
                                                }

        // Plotting tracks missing MINERvA

                                        if((HexagonAccepted(x3,y3
                                            ,3.46)==false) && (z1
                                            >4.28) && (0<pz0))

                                                {

                                                ++q;
                                                ++themissing;

                                                h17->Fill(E);
                                                h18->Fill(uE);
//                                              h19->Fill(thetaY);
                                                h20->Fill(theta);
                                                hlmzy4->Fill(z1,y1);
                                                hlmzx4->Fill(z1,x1);
                                                hfmxy4->Fill(x1,y1);
                                                hfmxy42->Fill(x1,y1)
```

```
                                                    ;

                                                hthetacapx->Fill(x,
                                                    theta);
                                                hthetacapz->Fill(z,
                                                    theta);

                                                }

            // Plotting tracks missing MINERvA
            // attention to pz0 condition

                                        if((0<pz0) && (z1<4.28))

                                                {
                                                ++q;
                                                ++themissing;

                                                h17->Fill(E);
                                                h18->Fill(uE);
//                                              h19->Fill(thetaY);
                                                h20->Fill(theta);
                                                hlmzy4->Fill(z1,y1);
                                                hlmzx4->Fill(z1,x1);
                                                hfmxy4->Fill(x1,y1);
                                                hfmxy41->Fill(x1,y1)
                                                    ;
                                                hfmzx43->Fill(z1,y1)
                                                    ;
                                                }


            // Plotting tracks going backward


                                        if(pz0<0)

                                                {

                                                ++q;
                                                ++themissing;

                                                hbvE->Fill(E);
                                                hbuE->Fill(uE);
```

```
//                                                          hbthetaY->Fill(
    thetaY);
                                                            hbtheta->Fill(theta)
                                                                ;


                                                            }
                                    }


                            }


                            }



                    }

                    }

                    events=w;
                    allmuons=q;
                    MINOS=theminos;
                    MINERvA=theminerva;
                    FIDUCIALMINERvA=thefiducialminerva;
                    CROSSINGMINERvA=thecrossing;
                    MISSINGMINERvA=themissing;
                    BETWEEN=thebetween;

                    }

                    cout<<"TOTAL_EVENTS="<<events;
                    cout<<"TOTAL_SUM_CATEGORIES="<<allmuons;
                    cout<<"MINOS="<<theminos;
                    cout<<"MINERvA="<<theminerva;
                    cout<<"CROSSING_MINERvA="<<thecrossing;
                    cout<<"MISSING_MINERvA="<<themissing;
                    cout<<"BETWEEN_END_&_VIRTUAL="<<thebetween;
                    cout<<"FIDUCIAL_MINERvA="<<thefiducialminerva;

                    outputFile1<<"TOTAL_EVENTS="<<events;
                    outputFile1<<"TOTAL_SUM_CATEGORIES="<<allmuons;
                    outputFile1<<"MINOS="<<theminos;
```

```
outputFile1<<"MINERvA="<<theminerva;
outputFile1<<"CROSSING_MINERvA="<<thecrossing;
outputFile1<<"MISSING_MINERvA="<<themissing;
outputFile1<<"BETWEEN_END_&_VIRTUAL="<<thebetween;
outputFile1<<"FIDUCIAL_MINERvA="<<thefiducialminerva;

outputFile1.close();

hsvE->Add(h2,1);
hsvE->Add(h7,1);
hsvE->Add(h12,1);
hsvE->Add(h17,1);
hsvE->Add(hbvE,1);

hsuE->Add(h3,1);
hsuE->Add(h8,1);
hsuE->Add(h13,1);
hsuE->Add(h18,1);
hsuE->Add(hbuE,1);


// all (60,0,90)

hstheta->Add(h5,1);     // MINERvA
hstheta->Add(h10,1);    // MINOS fiducial region
hstheta->Add(h15,1);    // crossing MINERvA
hstheta->Add(h20,1);    // missing MINERvA
hstheta->Add(hbtheta,1);  // back

hsmmvE->Add(h2,1);
hsmmvE->Add(h7,1); //muons ending MINERvA(hole)+MINOS(
   fiducial)

hsmmtheta->Add(h5,h10,1.0,1.0); // muons ending in MINERvA(
   hole) + MINOS(fiducial)

// acceptance theta MINERvA and MINOS

haccthetaminerva->Divide(h5,hstheta,1,1);

haccthetaminos->Divide(h10,hstheta,1,1);

//acceptance uE MINERvA and MINOS
```

```
haccuEminerva->Divide(h3,hsuE,1,1);


haccuEminos->Divide(h8,hsuE,1,1);


//acceptance vE MINERvA and MINOS

haccvEminerva->Divide(h2,hsvE,1,1);

haccvEminos->Divide(h7,hsvE,1,1);



hacctheta->Divide(hsmmtheta,hstheta,1,1);


haccvE->Divide(hsmmvE,hsvE,1,1);


hprobfidmin->Divide(hfmuE,hsuE,1,1);
hprobmin->Divide(h3,hsuE,1,1);
hprobminos->Divide(h8,hsuE,1,1);


TCanvas *c1 = new TCanvas ("c1","first canvas",1200,1200);
c1->cd();

hsvE->SetLineStyle(2);
hsvE->SetLineColor(1);
hsvE->SetLineWidth(4);
hsvE->SetTitleOffset(1.6,"y");
hsvE->Draw();
h2->SetLineColor(2);
h2->SetLineWidth(4);
h2->Draw("same");
h7->SetLineColor(4);
h7->SetLineWidth(4);
h7->Draw("same");
//              h22->SetLineColor(3);
//              h22->Draw("same");
hfmE->SetLineColor(8);
hfmE->SetLineWidth(4);
hfmE->Draw("same");
```

```
TLegend *leg1 = new TLegend
   (0.5235562,0.7002762,0.8427052,0.9005525,NULL,"brNDC");
leg1->SetFillStyle(0);
leg1->SetTextSize(0.025);
leg1->SetHeader("Neutrino energy for CC");
 leg1->AddEntry("hsvE","Total","lf");
 leg1->AddEntry("h2"," MINERvA","l");
 leg1->AddEntry("hfmE","MINERvA fid. vol.","l");
 leg1->AddEntry("h7","MINOS fid. vol.","l");
//  leg1->AddEntry("h22","MINOS (hexagonal region)","l");
 leg1->Draw();
c1->Print("vE_1.png");


TCanvas *c2 = new TCanvas ("c2","second canvas",1200,1200);
c2->cd();
hsvE->SetLineStyle(2);
hsvE->SetLineColor(1);
hsvE->SetLineWidth(4);
hsvE->SetTitleOffset(1.6,"y");
hsvE->Draw();
h12->SetLineColor(8);
h12->SetLineWidth(4);
h12->Draw("same");
h17->SetLineColor(46);
h17->SetLineWidth(4);
h17->Draw("same");
TLegend *leg2 = new TLegend
   (0.5235562,0.7002762,0.8427052,0.9005525,NULL,"brNDC");
leg2->SetFillStyle(0);
leg2->SetTextSize(0.025);
leg2->SetHeader("Neutrino energy for CC");
 leg2->AddEntry("hsvE","Total","lf");
 leg2->AddEntry("h12","crossing MINERvA","l");
 leg2->AddEntry("h17","missing MINERvA","l");
 leg2->Draw();
c2->Print("vE_2.png");


TCanvas *c3 = new TCanvas ("c3","third canvas",1200,1200);
c3->cd();
hsuE->SetLineStyle(2);
hsuE->SetLineColor(1);
hsuE->SetLineWidth(4);
```

```
                hsuE->SetTitleDffset(1.6,"y");
                hsuE->Draw();
                h3->SetLineColor(2);
                h3->SetLineWidth(4);
                h3->Draw("same");
                h8->SetLineColor(4);
                h8->SetLineWidth(4);
                h8->Draw("same");
//              h23->SetLineColor(3);
//              h23->Draw("same");
                hfmuE->SetLineColor(8);
                hfmuE->SetLineWidth(4);
                hfmuE->Draw("same");
                TLegend *leg3 = new TLegend
                   (0.5235562,0.7002762,0.8427052,0.9005525,NULL,"brNDC");
                leg3->SetFillStyle(0);
                leg3->SetTextSize(0.025);
                leg3->SetHeader("Muon energy for CC");
                 leg3->AddEntry("hsuE","Total","lf");
                 leg3->AddEntry("h3","MINERvA","lf");
                leg3->AddEntry("hfmuE","MINERvA fid. vol.","l");
                leg3->AddEntry("h8","MINDS fid. vol.","l");
//               leg3->AddEntry("h23","MINOS (hexagonal region)","l");
                 leg3->Draw();
                c3->Print("uE_1.png");


                TCanvas *c4 = new TCanvas ("c4","fourth canvas",1200,1200);
                c4->cd();
                hsuE->SetLineStyle(2);
                hsuE->SetLineColor(1);
                hsuE->SetLineWidth(4);
                hsuE->SetTitleDffset(1.6,"y");
                hsuE->Draw();
                h13->SetLineColor(8);
                h13->SetLineWidth(4);
                h13->Draw("same");
                h18->SetLineColor(46);
                h18->SetLineWidth(4);
                h18->Draw("same");
                TLegend *leg4 = new TLegend
                   (0.5235562,0.7002762,0.8427052,0.9005525,NULL,"brNDC");
                leg4->SetFillStyle(0);
                leg4->SetTextSize(0.025);
```

```
                leg4->SetHeader("Muon energy for CC");
                 leg4->AddEntry("hsuE","Total","lf");
                 leg4->AddEntry("h13","crossing MINERvA","l");
                 leg4->AddEntry("h18","missing MINERvA","l");
                 leg4->Draw();
                c4->Print("uE_2.png");

                TCanvas *c5=new TCanvas ("c5","fifth canvas",1200,1200);
                c5->cd();
                hbuE->SetLineColor(2);
                hbuE->SetTitleOffset(1.6,"y");
                hbuE->Draw();
                hbvE->SetLineColor(1);
                hbvE->Draw("same");
                TLegend *leg5 = new TLegend
                   (0.5235562,0.7002762,0.8427052,0.9005525,NULL,"brNDC");
                leg5->SetFillStyle(0);
                leg5->SetHeader("Backwards Muons");
                 leg5->AddEntry("hbvE","Neutrino Energy in CAPTAIN" ,"l");
                 leg5->AddEntry("hbuE","Muon Energy","l");
                 leg5->Draw();
                c5->Print("back_uEvE.png");


/*              TCanvas *c6=new TCanvas ("c6","MINOS fiducial region
   ",1200,1200);
                hmuons->Draw("colz");
                hminos->Draw("same");
                c6->Print("minos_fiducial_region.png");


                TCanvas *c8=new TCanvas ("c8","y muons",1200,1200);
                h1->Draw();
                c8->Print("y_muons.png");


                TCanvas *c9=new TCanvas ("c9","x muons",1200,1200);
                h6->Draw();
                c9->Print("x_muons.png");
*/

                TCanvas *c11=new TCanvas ("c11","MINERvA MINOS theta Y
                   ",1200,1200);
                c11->cd();
```

```
h9->SetLineColor(3);
h9->Draw();
h4->SetLineColor(2);
h4->Draw("same");
TLegend *leg6 = new TLegend
   (0.5235562,0.7002762,0.8427052,0.9005525,NULL,"brNDC");
leg6->SetFillStyle(0);
leg6->SetHeader("Theta Y angle");
 leg6->AddEntry("h4","MINERvA","lf");
 leg6->AddEntry("h9","MINOS","l");
 leg6->Draw();
c11->Print("thetaY_MINERvA_MINOS.png");


TCanvas *c12=new TCanvas ("c12","crossing missing theta Y
   ",1200,1200);
c12->cd();
h14->SetLineColor(2);
h14->Draw();
h19->SetLineColor(3);
h19->Draw("same");
TLegend *leg7 = new TLegend
   (0.5235562,0.7002762,0.8427052,0.9005525,NULL,"brNDC");
leg7->SetFillStyle(0);
leg7->SetHeader("Theta Y angle");
 leg7->AddEntry("h14","crossing MINERvA","lf");
 leg7->AddEntry("h19","missing MINERvA","lf");
 leg7->Draw();
c12->Print("thetaY_crossing_missing.png");


TCanvas *c13=new TCanvas ("c13","MINERvA MINOS theta
   ",1200,1200);
c13->cd();
hstheta->SetLineStyle(2);
hstheta->SetLineColor(1);
hstheta->SetLineWidth(4);
hstheta->SetTitleOffset(1.6,"y");
hstheta->Draw();
h5->SetLineColor(2);
h5->SetLineWidth(4);
h5->Draw("same");
h10->SetLineColor(4);
h10->SetLineWidth(4);
```

```
h10->Draw("same");
TLegend *leg8 = new TLegend
   (0.5235562,0.7002762,0.8427052,0.9005525,NULL,"brNDC");
leg8->SetFillStyle(0);
leg8->SetHeader("Theta");
leg8->AddEntry("hstheta","Total","lf");
leg8->AddEntry("h5","MINERvA","l");
 leg8->AddEntry("h10","MINOS fid. vol.","l");
 leg8->Draw();
c13->Print("theta_MINERvA_MINOS.png");



TCanvas *c14=new TCanvas ("c14","crossing missing theta
   ",1200,1200);
c14->cd();
hstheta->SetLineStyle(2);
hstheta->SetLineColor(1);
hstheta->SetLineWidth(4);
hstheta->SetTitleOffset(1.6,"y");
hstheta->Draw();
h15->SetLineColor(8);
h15->SetLineWidth(4);
h15->Draw("same");
h20->SetLineColor(46);
h20->SetLineWidth(4);
h20->Draw("same");
TLegend *leg9 = new TLegend
   (0.5235562,0.7002762,0.8427052,0.9005525,NULL,"brNDC");
leg9->SetFillStyle(0);
leg9->SetHeader("Theta");
leg9->AddEntry("hstheta","Total","lf");
leg9->AddEntry("h15","crossing MINERvA","l");
 leg9->AddEntry("h20","missing MINERvA","l");
 leg9->Draw();
c14->Print("theta_crossing_missing.png");


TCanvas *c15=new TCanvas ("c15","backward thetaY and theta
   ",1200,1200);
c15->cd();
hbtheta->SetLineColor(3);
hbtheta->SetTitleOffset(1.6,"y");
hbtheta->Draw();
```

```
                hbthetaY->SetLineColor(2);
                hbthetaY->Draw("same");
                TLegend *leg10 = new TLegend(0.2,0.7002762,0.5,0.9005525,
                   NULL,"brNDC");
                leg10->SetFillStyle(0);
                leg10->SetHeader("Theta");
                leg10->AddEntry("hbthetaY","backward Theta Y","l");
                 leg10->AddEntry("hbtheta","backward Theta","l");
                 leg10->Draw();
                c15->Print("thetaY_theta_backward.png");


/*
                TCanvas *c16=new TCanvas ("c16","Z1 from CAPTAIN",1200,1200)
                   ;
                h24->Draw();
                c16->Print("z1_from_CAPTAIN.png");
*/

                TCanvas *c17=new TCanvas ("c17","Comparing energies
                   ",1200,1200);
                c17->cd();
                hvE->SetLineColor(1);
                hvE->SetLineWidth(4);
                hvE->SetTitleOffset(1.6,"y");
                hvE->Draw("same");
                hsvE->SetLineStyle(2);
                hsvE->SetLineColor(1);
                hsvE->SetLineWidth(4);
                hsvE->Draw("same");
                TLegend *leg11 = new TLegend
                   (0.5235562,0.8002762,0.8427052,0.9005525,NULL,"brNDC");
                leg11->SetFillStyle(0);
                 leg11->SetHeader("Neutrino Energy");
                 leg11->AddEntry("hvE","Total interactiones in CAPTAIN","lf
                    ");
                 leg11->AddEntry("hsvE","All muons categories","l");
//               leg11->AddEntry("hsvE","MINERvA + MINOS + crossing +
   missing + backward","l");
                 leg11->Draw();
                c17->Print("comparing_energies.png");


                TCanvas *c18=new TCanvas ("c18","acceptancce theta
```

```
    ",1200,1200);
c18->cd();
hacctheta->SetTitleOffset(1.6,"y");
hacctheta->Draw();
c18->Print("acc_theta.png");

TCanvas *c19=new TCanvas ("c19","total vs real Theta
    ",1200,1200);
c19->cd();
htheta->SetLineColor(1);
htheta->SetTitleOffset(1.6,"y");
htheta->Draw();
hstheta->SetLineStyle(2);
hstheta->SetLineColor(1);
hstheta->Draw("same");
TLegend *leg12 = new TLegend
    (0.5235562,0.7002762,0.8427052,0.9005525,NULL,"brNDC");
leg12->SetFillStyle(0);
 leg12->SetHeader("Theta comparison");
 leg12->AddEntry("htheta","real theta","lf");
 leg12->AddEntry("hstheta","MINERvA + MINOS + crossing +
     missing + backward","l");
 leg12->Draw();
c19->Print("total_real_theta.png");


TCanvas *c20=new TCanvas ("c20","MINERvA+MINOS theta and
    real theta ",1200,1200);
c20->cd();
hstheta->SetLineStyle(2);
hstheta->SetLineColor(1);
hstheta->Draw();
hsmmtheta->SetLineColor(1);
hsmmtheta->Draw("same");
TLegend *leg13 = new TLegend
    (0.5235562,0.7002762,0.8427052,0.9005525,NULL,"brNDC");
leg13->SetFillStyle(0);
 leg13->SetHeader("theta comparison");
 leg13->AddEntry("hstheta","Total","lf");
 leg13->AddEntry("hsmmtheta","MINERvA + MINOS ","l");
 leg13->Draw();
c20->Print("MINERvA_MINOS_total_theta.png");

TCanvas *c21 = new TCanvas ("c21","end muons MINERvA zy
```

```
    ",1200,1200);
c21->cd();
hlmzy1->Draw();
c21->Print("end_muons_MINERvA_zy.png");

TCanvas *c22 =new TCanvas ("c22","end muons MINERvA zx
    ",1200,1200);
c22->cd();
hlmzx1->Draw();
c22->Print("end_muons_MINERvA_zx.png");

TCanvas *c23 =new TCanvas ("c23","end muons MINERvA xy
    ",1200,1200);
c23->cd();
hfmxy1->Draw();
c23->Print("end_muons_MINERvA_xy.png");

TCanvas *c24 =new TCanvas ("c24","energy muon virtual plane
    ",1200,1200);
hbeguE->SetLineWidth(4);
hbeguE->SetTitleOffset(1.6,"y");
hbeguE->Draw();
hfinaluE->SetLineStyle(2);
hfinaluE->SetLineWidth(4);
hfinaluE->Draw("same");
TLegend *leg14 = new TLegend
    (0.5235562,0.8002762,0.8427052,0.9005525,NULL,"brNDC");
leg14->SetFillStyle(0);
 leg14->SetHeader("Muon energy lost");
 leg14->AddEntry("hbeguE","CAPTAIN","lf");
 leg14->AddEntry("hfinaluE","plane downstream MINERvA","lf")
     ;
 leg14->Draw();
c24->Print("energy_muon_virtual_plane.png");

TCanvas *c241 =new TCanvas ("c241","muon energy comparison:
    all muons on vp,matched and not matched ",1200,1200);
hbeguE->SetLineColor(4);
hbeguE->SetLineWidth(4);
hbeguE->SetTitleOffset(1.6,"y");
hbeguE->Draw();
h131->SetLineColor(46);
h131->SetLineWidth(4);
h131->Draw("same");
```

```
h8->SetLineColor(1);
h8->SetLineWidth(4);
h8->Draw("same");
TLegend *leg141 = new TLegend
   (0.5235562,0.7502762,0.8427052,0.9005525,NULL,"brNDC");
leg141->SetFillStyle(0);
leg141->SetTextSize(0.023);
leg141->SetHeader("Exiting muons at downstream");
 leg141->AddEntry("hbeguE","Total","lf");
 leg141->AddEntry("h131","missing fiducial region","lf");
leg141->AddEntry("h8","reaching fiducial region","lf");
 leg141->Draw();
c241->Print("energy_muon_notmatched_matched_comparison.png")
   ;


TCanvas *c25 = new TCanvas ("c25","end muons MINOS zy
   ",1200,1200);
c25->cd();
hlmzy2->Draw();
c25->Print("end_muons_MINOS_zy.png");

TCanvas *c26 = new TCanvas ("c26","end muons MINOS zx
   ",1200,1200);
c26->cd();
hlmzx2->Draw();
c26->Print("end_muons_MINOS_zx.png");

TCanvas *c27 =new TCanvas ("c27","end muons MINOS xy
   ",1200,1200);
c27->cd();
hfmxy2->Draw();
c27->Print("end_muons_MINOS_xy.png");


TCanvas *c28 = new TCanvas ("c28","end muons crossing zy
   ",1200,1200);
c28->cd();
hlmzy3->Draw();
c28->Print("end_muons_crossing_zy.png");

TCanvas *c29 = new TCanvas ("c29","end muons crossing zx
   ",1200,1200);
c29->cd();
```

```
hlmzx3->Draw();
c29->Print("end_muons_crossing_zx.png");

TCanvas *c30 = new TCanvas ("c30","end muons crossing xy
   ",1200,1200);
c30->cd();
hfmxy3->Draw();
c30->Print("end_muons_crossing_xy.png");

TCanvas *c301 = new TCanvas ("c301","end muons crossing xy 1
    ",1200,1200);
c301->cd();
hfmxy31->Draw();
c301->Print("end_muons_crossing_xy_1.png");


TCanvas *c302 = new TCanvas ("c302","end muons crossing xy
   2",1200,1200);
c302->cd();
hfmxy32->Draw();
c302->Print("end_muons_crossing_xy_2.png");

TCanvas *c31 = new TCanvas ("c31","end muons missing zy
   ",1200,1200);
c31->cd();
hlmzy4->Draw();
c31->Print("end_muons_missing_zy.png");

TCanvas *c32 = new TCanvas ("c32","end muons missing zx
   ",1200,1200);
c32->cd();
hlmzx4->Draw();
c32->Print("end_muons_missing_zx.png");

TCanvas *c33 = new TCanvas ("c33","end muons missing xy
   ",1200,1200);
c33->cd();
hfmxy4->Draw();
c33->Print("end_muons_missing_xy.png");

TCanvas *c331 = new TCanvas ("c331","end muons missing xy z
   <4.28",1200,1200);
c331->cd();
hfmxy41->Draw();
```

```
c331->Print("end_muons_missing_xy_1.png");


TCanvas *c332 = new TCanvas ("c332","end muons missing xy z
   >4.28",1200,1200);
c332->cd();
hfmxy42->Draw();
c332->Print("end_muons_missing_xy_2.png");

TCanvas *c333 = new TCanvas ("c333","end muons missing zx z
   <4.28",1200,1200);
c333->cd();
hfmzx43->Draw();
c333->Print("end_muons_missing_xy_3.png");


TCanvas *c34=new TCanvas ("c34","acceptance vE",1200,1200);
c34->cd();
haccvE->Draw();
c34->Print("acc_vE.png");

TCanvas *c35=new TCanvas ("c35","fiducial volume zx
   ",1200,1200);
c35->cd();
hfidminzx->Draw();
c35->Print("fidminzx.png");

TCanvas *c36=new TCanvas ("c36","fiducial volume zy
   ",1200,1200);
c36->cd();
hfidminzy->Draw();
c36->Print("fidminzy.png");

TCanvas *c37=new TCanvas ("c37","fiducial volume xy
   ",1200,1200);
c37->cd();
hfidminxy->Draw();
c37->Print("fidminxy.png");

TCanvas *c38=new TCanvas ("c38","fiducial volume xy1
   ",1200,1200);
c38->cd();
hfidminxy1->Draw();
c38->Print("fidminxy1.png");
```

```
TCanvas *c39=new TCanvas ("c39","fiducial minerva log scale
   muon energy",1200, 1200);
c39->cd();
c39->SetLogy();
hfmuE1->SetLineColor(6);
hfmuE1->Draw();
c39->Print("uE_logscale.png");

TCanvas *c40=new TCanvas ("c40","minerva and minos muon
   probability",1200,1200);
hprobminos->SetLineColor(4);
hprobminos->Draw();
hprobmin->SetLineColor(2);
hprobmin->Draw("same");
TLegend *leg15 = new TLegend(0.2,0.7,0.38,0.9,NULL,"brNDC");
leg15->SetFillStyle(0);
 leg15->SetHeader("Muon Probabilities");
 leg15->AddEntry("hprobmin","MINERvA","l");
 leg15->AddEntry("hprobminos","MINOS","l");
leg15->Draw();
c40->Print("probabilities.png");

TCanvas *c41=new TCanvas ("c41","fiducial volume muon
   probability",1200, 1200);
c41->cd();
hprobfidmin->SetLineColor(6);
hprobfidmin->Draw();
c41->Print("probfidmin.png");

TCanvas *c42=new TCanvas ("c42","fiducial minerva log scale
   v energy",1200,1200);
c42->cd();
c42->SetLogy();
hfmE->SetLineColor(6);
hfmE->Draw();
c42->Print("vE_logscale.png");

TCanvas *c43=new TCanvas ("c43","fiducial minerva normal
   scale muon energy",1200, 1200);
c43->cd();
hfmuE1->SetLineColor(8);
hfmuE1->SetLineWidth(4);
hfmuE1->SetTitleOffset(1.6,"y");
```

```
hfmuE1->Draw();
TLegend *leg8 = new TLegend(0.57,0.795,0.8427052,0.9005525,
   NULL,"brNDC");
leg8->SetFillStyle(0);
leg8->SetTextSize(0.025);
leg8->AddEntry("hfmuE1","MINERvA fid. vol.","l");
 leg8->Draw();
c43->Print("uE_normalscale.png");

TCanvas *c44=new TCanvas ("c44","fiducial minerva normal
   scale v energy",1200,1200);
c44->cd();
hfmE->SetLineColor(8);
hfmE->SetLineWidth(4);
hfmE->SetTitleOffset(1.6,"y");
hfmE->Draw();
TLegend *leg8 = new TLegend(0.57,0.795,0.8427052,0.9005525,
   NULL,"brNDC");
leg8->SetFillStyle(0);
leg8->SetTextSize(0.025);
leg8->AddEntry("hfmE","MINERvA fid. vol.","l");
 leg8->Draw();
c44->Print("vE_normalscale.png");
/*
TCanvas *c45=new TCanvas ("c45","acceptance theta minerva
   ",1200,1200);
c45->cd();
haccthetaminerva->Draw();
c45->Print("accthetaminerva.png");

TCanvas *c46=new TCanvas ("c46","acceptance theta minos
   ",1200,1200);
c46->cd();
haccthetaminos->Draw();
c46->Print("accthetaminos.png");
*/
TCanvas *c45=new TCanvas ("c45","acceptance theta minerva
   and minos",1200,1200);
c45->cd();
haccthetaminos->SetTitleOffset(1.2,"y");
haccthetaminos->SetLineColor(4);
haccthetaminos->SetLineWidth(4);
haccthetaminos->Draw();
haccthetaminerva->SetLineColor(2);
```

```
haccthetaminerva->SetLineWidth(4);
haccthetaminerva->Draw("same");
TLegend *leg8 = new TLegend(0.6,0.795,0.8427052,0.9005525,
   NULL,"brNDC");
leg8->SetFillStyle(0);
//leg8->SetHeader("Theta");
leg8->AddEntry("haccthetaminerva","MINERvA","l");
 leg8->AddEntry("haccthetaminos","MINOS fid. vol.","l");
 leg8->Draw();
c45->Print("acctheta_minerva_minos.png");

TCanvas *c46=new TCanvas ("c46","acceptance uE minerva and
   minos",1200,1200);
c46->cd();
haccuEminos->SetTitleOffset(1.2,"y");
haccuEminos->SetLineColor(4);
haccuEminos->SetLineWidth(4);
haccuEminos->Draw();
haccuEminerva->SetLineColor(2);
haccuEminerva->SetLineWidth(4);
haccuEminerva->Draw("same");
TLegend *leg8 = new TLegend(0.2,0.795,0.4427052,0.9005525,
   NULL,"brNDC");
leg8->SetFillStyle(0);
leg8->SetHeader("Muon Energy");
leg8->AddEntry("haccuEminerva","MINERvA","l");
 leg8->AddEntry("haccuEminos","MINOS fid. vol. ","l");
 leg8->Draw();
c46->Print("accuE_minerva_minos.png");


TCanvas *c47=new TCanvas ("c47","acceptance uE minerva
   ",1200,1200);
c47->cd();
haccuEminerva->Draw();
c47->Print("accuEminerva.png");

TCanvas *c48=new TCanvas ("c48","acceptance uE minos
   ",1200,1200);
c48->cd();
haccuEminos->Draw();
c48->Print("accuEminos.png");
```

```
TCanvas *c47=new TCanvas ("c47","acceptance vE minerva and
   minos",1200,1200);
c47->cd();
haccvEminerva->SetTitleOffset(1.2,"y");
haccvEminerva->SetLineColor(2);
haccvEminerva->SetLineWidth(4);
haccvEminerva->Draw();
haccvEminos->SetLineColor(4);
haccvEminos->SetLineWidth(4);
haccvEminos->Draw("same");
TLegend *leg8 = new TLegend(0.4,0.795,0.6427052,0.9005525,
   NULL,"brNDC");
leg8->SetFillStyle(0);
leg8->SetHeader("Neutrino energy");
leg8->AddEntry("haccvEminerva","MINERvA","l");
 leg8->AddEntry("haccvEminos","MINOS fid. vol. ","l");
 leg8->Draw();
c47->Print("accvE_minerva_minos.png");

TCanvas *c49=new TCanvas ("c49","acceptance vE minerva
   ",1200,1200);
c49->cd();
haccvEminerva->Draw();
c49->Print("accvEminerva.png");

TCanvas *c50=new TCanvas ("c50","acceptance vE minos
   ",1200,1200);
c50->cd();
haccvEminos->Draw();
c50->Print("accvEminos.png");


TCanvas *c51=new TCanvas ("c51","capzy",1200,1200);
c51->cd();
hcapzy->SetTitleOffset(1.2,"y");
hcapzy->Draw("colz");
c51->Print("capzy.png");

TCanvas *c52=new TCanvas ("c52","capzx",1200,1200);
c52->cd();
hcapzx->SetTitleOffset(1.2,"y");
hcapzx->Draw("colz");
c52->Print("capzx.png");
```

```
                TCanvas *c53=new TCanvas ("c53","thetacapz",1200,1200);
                c53->cd();
                hthetacapz->SetTitleOffset(1.2,"y");
                hthetacapz->Draw("colz");
                c53->Print("thetacapz.png");

                TCanvas *c54=new TCanvas ("c54","thetacapx",1200,1200);
                c54->cd();
                hthetacapx->SetTitleOffset(1.2,"y");
                hthetacapx->Draw("colz");
                c54->Print("thetacapx.png");
}
```

Appendix C

CAPTAIN Acceptances by blocks

C.1 Acceptances as a function of the Neutrino Energy

Figure C.1: Left:Acceptance in the up-back block. Right:Acceptance in the up-front block

Figure C.2: Left:Acceptance in the Down-back block. Right:Acceptance in the Down-front block.

C.2 Acceptances as a function of the Muon Energy

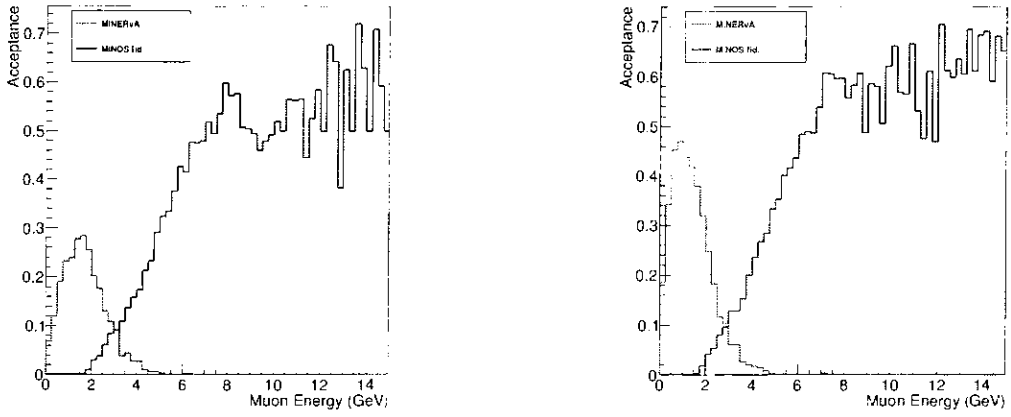

Figure C.3: Left:Acceptance in the up-back block. Right:Acceptance in the up-front block.

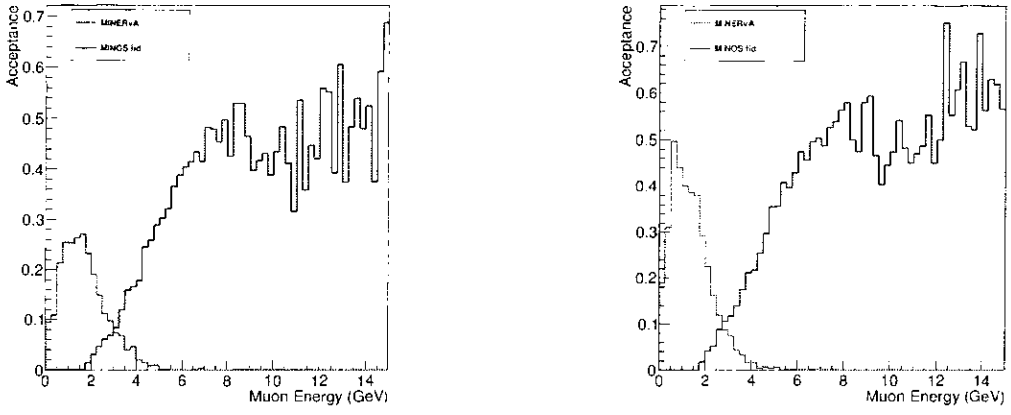

Figure C.4: Left:Acceptance in the down-back block. Right:Acceptance in the down-front block.

C.3 Acceptances as a function of the Muon Angle

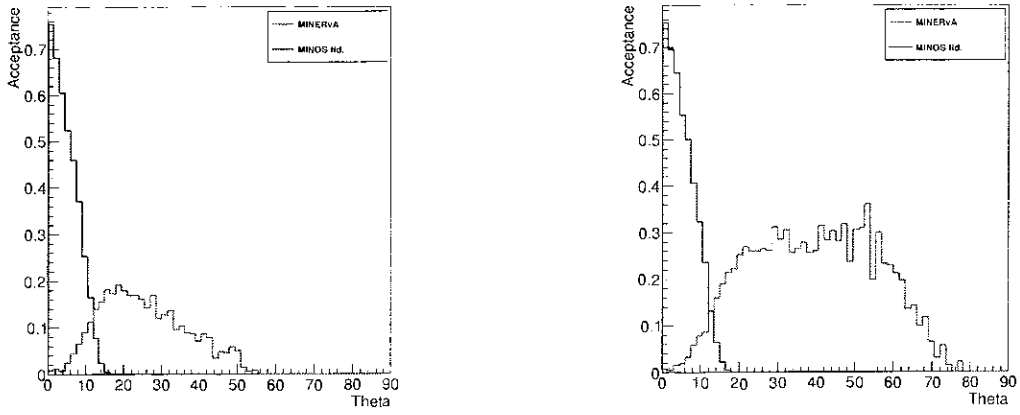

Figure C.5: Left:Acceptance in the up-back block. Right:Acceptance in the up-front block.

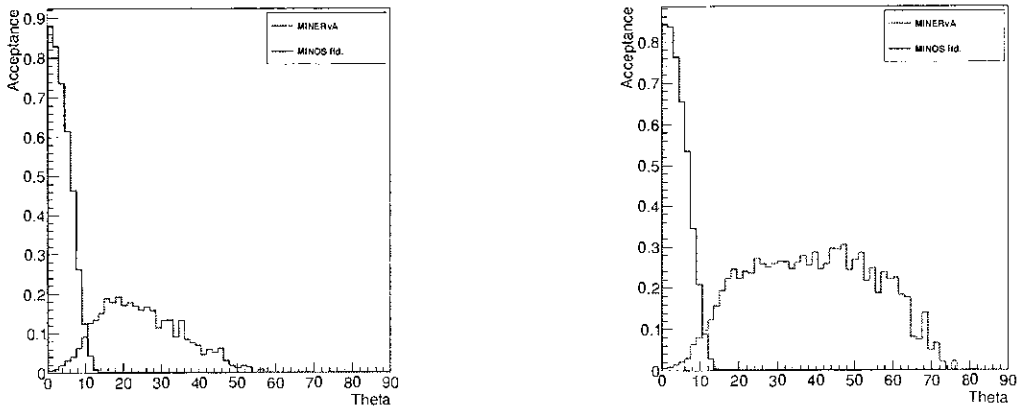

Figure C.6: Left:Acceptance in the down-back block. Right:Acceptance in the down-front block.

Bibliography

[1] Z. Maki, M. Nakagawa, and S. Sakata, Prog. Theor. Phys. 28, 870 (1962).

[2] Von Bayer, O. Hahn, L. Meitner, Phys. Zeitschrift, 12, January, 1911, p. 378.

[3] C.D. Ellis, B.A. Wooster, The average energy of desintegration of Radium E,Proc. Roy. Soc. A117(1927) 109-123.

[4] W. Pauli, Letter sent to Tubingen conference, Dec. 1930.

[5] J. Chadwick, F. (1932) Proc. Roy. Soc., A 136, 692708.

[6] Fred L. Wilson, Fermi's Theory of Beta Decay (English translation), American Journal of Physics volume 36, number 12, pagina 1150.

[7] Reines, F. and Cowan, C. L. Nov, (1953), Phys. Rev. 92(3), 830831.

[8] C. L. Cowan, F. Reines, F. B. Harrison, H. W. Kruse, A. D. McGuire, (1956), "Detection of a Free Neutrino: a Confirmation", Science Vol 124 , Number 3212.

[9] F. Reines and C.L. Cowan,(1956), "The neutrino", Nature 178 446.

[10] M. Goldhaber, L. Grodzins, and A.W. Sunyar,(1957), Helicity of neutrinos, Phys. Rev. 109 1015.

[11] R. Davis, (1955), Phys. Rev. 97, 766.

[12] R. Davis and D.S. Harmer, , Bull. Am. Phys. Soc. 4, (1959)217.

[13] C.S. Wu et al., Phys. Rev. 105 (1957)1413

[14] Danby, G., Gaillard, J.-M., Goulianos, K., Lederman, L. M., Mistry, N.,Schwartz, M., and Steinberger, J. July 1962 Physical Review Letters 9, 3644.

[15] Gargamelle Neutrino Collaboration: F.J. Hasert et al., Observation of neutrino-like interactions without muon or electron in the Gargamelle neutrino experiment, Phys. Lett. B 46 (1973)138.

[16] R. Davis.D.S. Harmer, and K.C. Hoffman, Search for neutrinos from the sun, Phys. Rev. Lett. 20 (1968)1205.

[17] Haines, T.J., Bionta, R.M., Blewitt, G., Bratton, C.B., Casper, D., Claus, R. et al. (1986) Calculation of atmospheric neutrino-induced backgrounds in a nucleon-decay search. Phys. Rev. Lett. 57, 1986-1989.

[18] Nakahata, M., Arisaka, K., Kajita, T., Koshiba, M., Oyama, Y., Suzuki, A. et al. (1986) Atmospheric neutrino background and pion nuclear effect for KAMIOKA nucleon decay experiment. J. Phys. Soc. Jpn. 55, 3786-3805.

[19] Hirata, K.S., Kajita, T., Koshiba, M., Nakahata, M., Ohara, S., Oyama, Y. et al. (1988) Experimental study of the atmospheric neutrino flux. Phys.Lett. B 205, 416-420.

[20] V.N. Gribov and B. Pontecorvo. Phys. Lett B 28(1969)493.

[21] DONUT Collaboration (2001) Phys. Lett. B504, 218224.

[22] ALEPH Collaboration:D. Decamp et al., "Determination of the Number of Light Neutrino Species", Phys. Lett. B 231(1989)519.

[23] Delphi Collaboration:P.A. Aarnio et al.,"Measurement of the Mass and Width of the Z^0 Paricle from Multi-Hadronic Final States Produced in the $e^+ e^-$ Annihilation", Phys. Lett. B 231 (1989)539.

[24] L3 Collaboration:B. Adeva et al.,"A Determination of the Properties of the Neutral Intermediate Vector Boson Z^0", phys. Lett. B 231 (1989)509.

[25] OPAL Collaboration:M.Z. Akrawy et al.,"Measurement of the Z^0 Mass and Width with the OPAL Detector at LEP", Phys. Lett. B bf 231 (1989)530.

[26] C. Patrignani et al. (Particle Data Group), Chinese Physics C, 40, 100001 (2016).

[27] J. A. Formaggio, G. P. Zeller, (2012), From eV to EeV: Neutrino cross sections across energy scales, Rev. Mod. Phys.: Volume 84,1307 .

[28] D.Casper (2002), The NUANCE Neutrino Simulation, and the Future, arXiv:hep-ph/0208030v1.

[29] B.T. Cleveland et al. Astrophys. J 496 , 505 (1998).

[30] Bahcall J N and Pena-Garay C 2004 New J. Phys.6 63.

[31] Q. R. Ahmad et al. (SNO Collaboration), Measurement of the Rate of $\nu_e + d \rightarrow p + p + e$ Interactions Produced by ^8B Solar Neutrinos at the Sudbury Neutrino Observatory. Phys. Rev. Lett. 87, 071301 (2001).

[32] Q. R. Ahmad et al. (SNO Collaboration), Direct Evidence for Neutrino Flavor Transformation from Neutral-Current Interactions in the Sudbury Neutrino Observatory. Phys. Rev. Lett. 89, 011301 (2002).

[33] J. Hosaka et al., Solar neutrino measurements in Super-Kamiokande-I. Phys. Rev., D73, 112001 (2006), hep-ex/0508053.

[34] J. N. Bahcall, A. M. Serenelli and S. Basu, New solar opacities, abundances, helioseismology, and neutrino fluxes. Astrophys. J., 621, L85L88 (2005).

[35] K. Eguchi et al.(2003) (KamLAND Collaboration) First Results from KamLAND: Evidence for Reactor Anti-Neut rino Disappearance , Phys. Rev. Lett. 90, 021802.

[36] Abe et al. (The KamLAND Collaboration)2008(), Precision Measurement of Neutrino Oscillation Parameters with KamLANDS., Phys. Rev. Lett. 100, 221803.

[37] Apollonio, M. et al. Limits on neutrino oscillations from the CHOOZ experiment. Phys. Lett. B 466, 415430 (1999).

[38] Boehm, F. et al. Search for neutrino oscillations at the Palo Verde nuclear reactors. Phys. Rev. Lett. 84, 37643767 (2000).

[39] Abe, Y. et al. Indication of reactor electron-antineutrino disappearance in the Double Chooz experiment. Phys. Rev. Lett. 108, 131801 (2012).

[40] Abe, Y. et al. Background-independent measurement of θ_{13} in Double Chooz. Phys. Lett. B 735, 5156 (2014).

[41] Ahn, J. K. et al. Observation of reactor electron antineutrino disappearance in the RENO experiment. Phys. Rev. Lett. 108, 191802 (2012).

[42] An, F. P. et al. Observation of electron-antineutrino disappearance at Daya Bay. Phys. Rev. Lett. 108, 171803 (2012).

[43] An, F. P. et al. Spectral measurement of electron antineutrino oscillation amplitude and frequency at Daya Bay. Phys. Rev. Lett. 112, 061801 (2014). Determination of the mixing angle h 13 and observation of the associated oscillations at the Daya-Bay reactor experiment.

[44] T. K. Gaisser, M. Honda. (2002). Flux of Atmospheric Neutrinos, arXiv:hep-hp/0203272v2.

[45] Y. Fukuda et al. (Super-Kamiokande Collaboration) (1998). Evidence for Oscillation of Atmospheric Neutrinos, Phys. Rev. Lett. 81, 1562

[46] T. Kafka, talk presented at 5th International Workshop on Topics in Astroparticle and Underground Physics (TAUP 97), Gran Sasso, Italy, 7-11 Sep 1997. hep-ph/9712281; E. Peterson, talk presented at The XVIIIth International Conference on Neutrino Physics and Astrophysics (NEUTRINO98), Takayama, Japan, 4-9 June, 1998; H. Gallagher, parallel session talk presented at The 29th International Conference on High-Energy Physics (ICHEP 98), 23-29 Jul 1998, Vancouver, Canada.

[47] Allison, W.W.M., Alner, G.J., Ayres, D.S., Barr, G., Barrett, W.L., Bode, C. et al.(Soudan-2 collaboration) (1999) The atmospheric neutrino flavor ratio from a 3.9 fiducial kiloton-year exposure of Soudan 2. Phys. Lett. B 449, 137-144.

[48] Ambrosio, M., Antolini, R., Aramo, C., Auriemma, G., Baldini, A., Barbarino, G.C. et al. (MACRO collaboration) (1998) Measurement of the atmospheric neutrino-induced upgoing muon flux using MACRO. Phys. Lett. B 434, 451-457.

[49] Ambrosio, M., Antolini, R., Auriemma, G., Bakari, D., Baldini, A., Barbarino, G.C. et al.(MACRO collaboration) (2000) Low energy atmospheric muon neutrinos in MACRO. Phys. Lett. B 478, 5-13.

[50] K. Abe, N. Abgrall, H. Aihara et al., The T2K experiment, Nuclear Instruments and Methods in Physics Research, Section A, vol. 659, no. 1, pp. 106135, 2011.

[51] M. H. Ahn, E. Aliu, S. Andringa et al., Measurement of neutrino oscillation by the K2K experiment, Physical Review D, vol. 74, no. 7, Article ID 072003, 39 pages, 2006.

[52] I. Ambats et al., (MINOS Collaboration). The MINOS Detectors Technical Design Report,1998.

[53] D. Ayres et al., Letter of Intent to build an Off-axis Detector to study ν_μ to ν_e oscillations with the NuMI Neutrino Beam. http://arxiv.org/abs/hep-ex/0210005.

[54] D. Ayres et al., NOvA: Proposal to build a 30 kiloton off-axis detector to study $\nu_\mu \rightarrow \nu_e$ oscillations in the NuMI beamline, 2004.

[55] D. Ayres et al., The NOvA Technical Design Report FERMILAB-DESIGN-2007-01, 2007.

[56] J. Hylen et al., NuMI Technical Design Handbook, Internal NuMI report (2003).

[57] R. M. Zwaska, Accelerator Systems and Instrumentation for the NuMI Neutrino Beam, PhD thesis University of Texas at Austin, 2005.

[58] G. Arturo Fiorentini Aguirre (2013). Measurement of ν_{mu} Induced Charged-Current Quasi-Elastic Cross Sections on Polystyrene at $E_{\nu_{mu}}$ 2 – 10. Ph.D. Theses. Centro Brasileiro de Pesquisas Fisicas (CBPF), Rio de Janeiro - Brazil.

[59] S. Kopp, The NuMI Neutrino Beam at Fermilab. Department of Physics-University of Texas, Austin, TX 78712, U.S.A.

[60] D.G. Michael et al. (MINOS collaboration), (2008), The Magnetized steel and scintillator calorimeters of the MINOS experiment. Nucl. Inst. and Meth., Phys. Res. Sect. A. 596:190228.

[61] Richard Gran (2007). The MINERνA Neutrino Interaction Experiment. arXiv:0711.3029.

[62] L. Aliaga et. al.: Design, Calibration, and Performance of the MINERvA Detector: Nucl.Inst.Meth. A473 (2014) 130: arxiv:1305.5199.

[63] C. Rubbia (1977), The Liquid-Argon Time Projection Chamber: A New Concept for Neutrino Detectors, CERN, EP Internal Report 77-8.

[64] Piotr Poski, Dorota Stefan, Robert Sulej, Krzysztof Zaremba, Image Segmentation in Liquid Argon Time Projection Chamber Detector

[65] http://www2.warwick.ac.uk/fac/sci/physics/research/epp/exp/detrd/lar/doc/larseminarv6.pdf

[66] H. Chen et al. [MicroBooNE Collaboration]. FERMILAB-PROPOSAL-0974.

[67] L. Camilleri [MicroBooNE Collaboration]. Nucl. Phys. Proc. Suppl. 237-238, 181 (2013).

[68] Qiuguang Liu, The CAPTAIN Liquid Argon Neutrino Experiment. Physics Procedia 61 (2015) 483-487.

[69] E. Conti et al., Phys. Rev. B 68(2003) 054201

[70] B. Rossi et al. JINST 4(2009)P07011

[71] LOI presented to Fermilab PAC, http://www.fnal.gov/directorate/program planning/Jan2015Public/LOI- LBNF.pdf

[72] C. Adams et al. (LBNE Collaboration). arXiv:1307.7335 hep-ex.

[73] C. Anderson et al. (ArgoNeuT Collaboration). Phys. Rev. Lett. 108, 161802 (2012).

[74] R. Acciarri et al. (ArgoNeuT Collaboration), Phys. Rev. D89, 112003 (2014).

[75] R. Acciarri et al. (ArgoNeuT Collaboration), Phys. Rev. D90, 012008 (2014).

[76] R. Acciarri et al. (ArgoNeuT Collaboration), arXiv:1408:0598 hep-ex.

[77] (2015),Proposal CAPTAIN-MINERA: Neutrino-Argon Scattering in a Medium-Energy Neutrino Beam

[78] Andreopoulos, C. et al, Nuclear Instruments and Methods in Physics Research A 614, 87 (2010).

[79] S. Agostinelli et al. [GEANT4 Collaboration], Nucl. Instrum. Meth. A 506, 250 (2003).

[80] J. Allison, K. Amako, J. Apostolakis, H. Araujo, P. A. Dubois, M. Asai, G. Bar- rand and R. Capra et al., IEEE Trans. Nucl. Sci. 53, 270 (2006).

[81] Geant4, Model: Ftfp, Accessed: 2016-02-11, URL http://geant4.cern.ch/support/proc_mod_catalog/models/hadronic/FTFP.html.

[82] Geant4, Model:Bertini cascade, Accessed:2016-02-11, URL http://geant4.cern.ch/suppo

[83] C. Alt et al., Eur. Phys. J. C 49, 897 (2007).

[84] D. S. Barton et al., Phys. Rev. D 27, 2580 (1983).

[85] A. Ferrari, P.R. Sala, A. Fasso, and J. Ranft. Fluka. CERN-library in: http://fluka. web. cern. ch/fluka, (2005)

[86] Aaron Higuera, CAPTAIN-MINERvA . MINERvA Document 11029-v1.

[87] https://cdcvs.fnal.gov/redmine/projects/minerva/wiki/Z_Positions_of_Planes_in_the_Full_MINERvA_Detector